INFORMATION TO USERS

This manuscript has been reproduced from the microfilm master. UMI films the text directly from the original or copy submitted. Thus, some thesis and dissertation copies are in typewriter face, while others may be from any type of computer printer.

The quality of this reproduction is dependent upon the quality of the copy submitted. Broken or indistinct print, colored or poor quality illustrations and photographs, print bleedthrough, substandard margins, and improper alignment can adversely affect reproduction.

In the unlikely event that the author did not send UMI a complete manuscript and there are missing pages, these will be noted. Also, if unauthorized copyright material had to be removed, a note will indicate the deletion.

Oversize materials (e.g., maps, drawings, charts) are reproduced by sectioning the original, beginning at the upper left-hand corner and continuing from left to right in equal sections with small overlaps. Each original is also photographed in one exposure and is included in reduced form at the back of the book.

Photographs included in the original manuscript have been reproduced xerographically in this copy. Higher quality 6" x 9" black and white photographic prints are available for any photographs or illustrations appearing in this copy for an additional charge. Contact UMI directly to order.

UMI

A Bell & Howell Information Company
300 North Zeeb Road, Ann Arbor MI 48106-1346 USA
313/761-4700 800/521-0600

A

Studies on the Effective Properties of Suspensions

by

Yongguang Wang

A Dissertation Submitted to the Graduate Faculty in
Engineering in Partial Fulfillment of the Requirements for the
Degree of Doctor of Philosophy

The City University of New York

1997

This manuscript has been read and accepted for the Graduate Faculty in Engineering in satisfaction of the dissertation requirement for the degree of Doctor of Philosophy.

8/6/97
Date

Professor Andreas Acrivos
Chairman of Examining Committee

8/6/97
Date

Dean Gerard Lowen
Executive Officer

Professor Peter Ganatos

Professor Joel Koplik

Professor Michael Loewenberg

Professor Roberto Mauri

Supervisory Committee

THE CITY UNIVERSITY OF NEW YORK

ABSTRACT

Studies on the Effective Properties of Suspensions

by

Yongguang Wang

Advisor: Professor Andreas Acrivos

Co-Advisor: Professor Roberto Mauri

Four problems concerning the average properties of dilute suspensions are studied under the conditions that all inertia, interparticle potential and Brownian motion effects are negligible; thus only hydrodynamic interactions are important, which are governed by the creeping flows equations. First, the thermocapillary migration in a well-mixed bidisperse suspension of spherical bubbles is studied and the expression for the migration velocity is given for dilute systems. Second, for a monodisperse suspension of neutrally buoyant rigid spheres undergoing simple shearing motion, the shear-induced self-diffusion coefficients of both a liquid tracer and a tagged sphere in the di-

rection perpendicular to the ambient flow are computed to leading order in particle concentration c. Then, the volumetric flux of particles in such a suspension in the direction of the ambient velocity due to a concentration gradient in the direction of the velocity gradient of the bulk flow is calculated again to leading order in c. Finally, the gradient diffusion coefficient of the particles in such a suspension in the direction of the velocity gradient of the bulk flow is computed for a monolayer of spherical particles to leading order in the particle areal fraction.

Acknowledgments

I wish to thank Professors Andreas Acrivos and Roberto Mauri for their guidance, encouragement and many contributions to this work. Professor Acrivos's dedication to excellence greatly inspired me in the study and his keen and deep insight into the subjects guided me throughout the work. Professor Mauri's valuable suggestions and generous help contributed significantly to this thesis.

This work was supported by the National Science Foundation grant CTS-9012937.

Contents

List of Tables

List of Figures

Chapter 1

Thermocapillary Migration of a Bidisperse Suspension of Bubbles

abstract

We consider the thermocapillary motion of a well-mixed suspension of non-conducting spherical bubbles of negligible viscosity in a viscous conducting liquid under conditions of vanishingly small Reynolds and Marangoni numbers. Recently, Acrivos, Jeffrey & Saville (1990) showed that when all the bubbles are of identical size, the ensemble averaged migration velocity $\overline{\mathbf{U}}_1$ of a test bubble of radius a_1 within the suspension equals $\mathbf{U}_1^{(0)}[1-\frac{3}{2}c_1+O(c_1^2)]$, where c_1 is the volume fractions of the bubbles and $\mathbf{U}_1^{(0)}$ is the thermocapillary velocity of a single bubble given by Young, Goldstein & Block (1959). Here we extend this result to a bi-disperse suspension containing bubbles of

radii a_1 and $a_2 \equiv \lambda a_1$ in which case $\overline{U}_1 = U_1^{(0)}[1 - \frac{3}{2}c_1 - S(\lambda)c_2 + ...]$, where c_1 and c_2 are the corresponding volume fraction of the two sets of bubbles. Values for $S(\lambda)$ are presented for some typical size ratios λ and asymptotic expressions for $S(\lambda)$ are derived for $\lambda \longrightarrow 0$ and for $\lambda \longrightarrow \infty$.

1. Introduction

A cloud of bubbles suspended in a viscous liquid of non-uniform temperature will move towards the hotter fluid, owing to the dependence of surface tension on temperature. In addition to its importance from a fundamental point of view, this effect has taken on a new practical significance in that, under near-weightless conditions, it offers the only technique presently available for removing unwanted gas bubbles from a liquid solution. This in turn is a crucial step in the manufacturing process of ultra high purity materials in outer space.

The thermocapillary motion of a single drop having arbitrary values of its thermal conductivity and viscosity relative to those of the ambient liquid was studied by Young, Goldstein & Block (1959) under conditions of vanishingly small Reynolds and Marangoni numbers. More recently, that study was extended to the case of two bubbles or drops by, among others, Meyyappan & Subramanian (1984) and Anderson (1985) via the direct reflection method, and by Satrape (1992) using the method of twin multipole expansions, all of whom showed that, when the surface tension is high enough to keep them spherical, two equi-sized bubbles move with the same velocity as one isolated bubble. Acrivos, Jeffrey & Saville (1990) extended this result by proving that it continues to hold for any number of equi-sized bubbles. Moreover, those authors showed that the velocity field is irrotational and that its velocity potential is uniquely related to the temperature, so that the hydrodynamic

and thermal two-body interactions exactly cancel each other.

On the other hand, when the two bubbles have different radii, the hydrodynamic and thermal effects no longer cancel each other so that the particle velocities (now different from each other) will depend on the distance between the two bubbles, their orientation relative to the direction of the applied temperature gradient and on the ratio of their radii.

In this paper we wish to calculate the average velocity of a test bubble in a dilute suspension of bubbles having a different size. The renormalization technique developed by Jeffrey (1973) is applied to this problem, extending the result of Acrivos et al. (1990), who considered monodisperse suspensions. The paper is organized as follows. After formulating the problem in §2, the mobility functions for two bubbles with arbitrary size ratio and arbitrary orientation relative to the imposed temperature gradient are obtained in §3 using the twin multipole expansion method developed by Jeffrey & Onishi (1984). These mobility functions, expanded in terms of the interparticle distance and size ratio, are then employed in §4 to find the average bubble velocity by making use of a renormalization technique described by Acrivos et al. (1990). Finally in §5, asymptotic expressions for the average bubble velocity are obtained in the limiting cases where the size ratio is either very large or very small.

2. The governing equations and a relation for a special case

A cloud of N bubbles suspended in an unbounded fluid of viscosity μ, density ρ and thermal diffusivity $\bar{\alpha}$ will move under the influence of a non-uniform ambient temperature field T_∞, due to the temperature dependence of the surface tension of the bubble-fluid interface. We assume that the surface tension of any bubble i, $\gamma_i (i = 1, 2, ..., N)$, decreases linearly with the temperature T and is large enough to keep each bubble spherical with radius a_i. We also suppose that both the Reynolds number Re and the Marangoni number Ma are small, with $Re = \rho a_i U/\mu$ and $Ma = a_i U/\bar{\alpha}$, where U denotes a characteristic velocity.

For the quasi-steady state case being considered here, the governing equation and boundary conditions for the temperature field T are given by

$$\nabla^2 T = 0, \tag{1.1}$$

$$T \longrightarrow T_\infty \quad \text{as} \quad \rho_i \longrightarrow \infty, \tag{1.2}$$

$$\mathbf{n}_i \cdot \nabla T = 0 \quad \text{on} \quad \rho_i = a_i, \tag{1.3}$$

where $\rho_i = |\boldsymbol{\rho}_i|$, with $\boldsymbol{\rho}_i$ denoting the position vector referred to the center of the i-th bubble, T_∞ is the unperturbed temperature field which also satisfies Laplace's equation, while $\mathbf{n}_i$ is a unit vector normal to the surface of the i-th bubble.

Similarly, the velocity field $\mathbf{u}$ and pressure field p satisfy

$$\nabla^2\mathbf{u} = \frac{1}{\mu}\nabla p, \tag{1.4}$$

$$\nabla\cdot\mathbf{u} = 0, \tag{1.5}$$

$$\mathbf{u}\longrightarrow\mathbf{u}_\infty \quad \text{as} \quad \rho_i \longrightarrow \infty, \tag{1.6}$$

$$\mathbf{n}_i\cdot\mathbf{u} = \mathbf{n}_i\cdot\mathbf{U}_i \quad \text{on} \quad \rho_i = a_i, \tag{1.7}$$

$$\mathbf{n}_i\cdot\boldsymbol{\sigma}\cdot(\mathbf{I}-\mathbf{n}_i\mathbf{n}_i) = (-\frac{d\gamma_i}{dT})(\mathbf{I}-\mathbf{n}_i\mathbf{n}_i)\cdot\nabla T \quad \text{on} \quad \rho_i = a_i, \tag{1.8}$$

where $\boldsymbol{\sigma}$is the stress tensor, $\mathbf{u}_\infty$ is the unperturbed velocity field which also satisfies (1.4) and (1.5), while $\mathbf{U}_i$ is the velocity of the i-th bubble. We further require that the bubbles be force-free, i.e.

$$\mathbf{F}_i = 0.$$

Note that the corresponding torque-free condition is automatically satisfied in view of the expression, given by (1.8), for the jump in shear stress along the surface of each bubble.

From (1.1) – (1.8) it is evident that, in the absence of convection, the transport of energy is independent of that of momentum. In fact, the temperature distribution can first be determined through (1.1) – (1.3), and the boundary value problem (1.4) – (1.8) can subsequently be solved to find the flow field.

The case of a single bubble suspended in an unbounded fluid in the presence of a constant ambient temperature gradient, i.e. $\nabla T_\infty = \mathbf{H}$, was first

solved by Young et al. (1959), who found that the thermocapillary velocity of an isolated bubble is given by

$$\mathbf{U}_i^{(0)} = \frac{a_i}{2\mu}(-\frac{d\gamma_i}{dT})\mathbf{H}. \tag{1.9}$$

Moreover as shown by Subramanian (1985) this expression for the thermocapillary velocity of a single bubble also applies when T_∞ is any harmonic function having singularities outside the space occupied by the bubble, provided that $\mathbf{H}$ is replaced by $(\nabla T_\infty)_o$, i.e. the ambient temperature gradient evaluated at the center of the bubble.

Consider next N bubbles whose parameters a_i and $d\gamma_i/dT$ satisfy the relations

$$a_1(-\frac{d\gamma_1}{dT}) = a_2(-\frac{d\gamma_2}{dT}) = ... = a_N(-\frac{d\gamma_N}{dT}) \equiv -2\mu b, \tag{1.10}$$

where b is a constant, so that

$$\mathbf{U}_1^{(0)} = \mathbf{U}_2^{(0)} = ... = \mathbf{U}_N^{(0)}.$$

Now, if the ambient temperature and velocity fields, T_∞ and $\mathbf{u}_\infty$ respectively, satisfy the relation

$$\mathbf{u}_\infty = b\nabla T_\infty, \tag{1.11}$$

then the flow field remains irrotational and is given by

$$\mathbf{u} = b\nabla T \quad \text{with} \quad p = 0, \tag{1.12}$$

and all the bubbles will be stationary, i.e.

$$\mathbf{U}_i = 0. \tag{1.13}$$

The relations (1.12) and (1.13) can be easily verified by direct substitution into (1.4) – (1.8) and using the conditions (1.3) and (1.10).

A physical interpretation of this result can be obtained by first considering a single bubble immersed in the ambient fields T_∞, $\mathbf{u}_\infty$ which satisfy (1.11). It can easily be verified then that the resulting flow field $\mathbf{u}' = b\nabla T'$, where T' is the new temperature profile, is that formed by a stationary bubble in an irrotational inviscid flow which also satisfies the shear stress balance equation (1.8) as well as the conditions of zero force and torque. Now another bubble is placed in the fields T' and $\mathbf{u}'$, which in turn can be viewed as the ambient fields. The same argument can be applied again except for the generations of further reflections by the presence of the first bubble, which, once again, satisfy (1.11). Finally, using the same argument repeatedly, we conclude that if any number of bubbles are placed in the fields T_∞, $\mathbf{u}_\infty$ the results (1.12) and (1.13) are valid, showing that, as in the case of an isolated bubble, the effects of the temperature and of the flow field on the velocity of the bubbles exactly balance each other. Although equation (1.10) is of course totally unphysical, the resulting analysis just described will prove useful later on in constructing the solution to our mathematical problem.

The thermocapillary velocities of N identical bubbles immersed in a quiescent ambient fluid with constant temperature gradient $\nabla T_\infty = \mathbf{H}$ can be easily obtained using (1.11) and (1.13). In fact, by superimposing the uniform flow fields $\mathbf{u}_\infty = b\mathbf{H}$ and $\mathbf{u}_\infty = -b\mathbf{H}$, we see that the former will 'balance' the

effect of the temperature gradient [cf. (1.13)], while the latter will produce a net uniform velocity. Finally, we may conclude that each bubble will move with the same constant velocity $\mathbf{U}^{(0)} = -b\mathbf{H}$ as if it were alone, in agreement with the result obtained by Acrivos et al. (1990).

Another interesting application of (1.12) and (1.13), which will be found useful when performing the analysis of §5.1, pertains to the motion of a bubble near a stress-free plane on which a fixed temperature gradient $\nabla T = \mathbf{H}$ is imposed perpendicular to the plane on the side facing the bubble. By the method of images, the plane can then be replaced by an identical second bubble placed at the position symmetric about the plane and with $\nabla T = -\mathbf{H}$ on the other side facing the second bubble, so that the stress-free condition on the plane is satisfied identically. Now, repeating the same argument as before, i.e. by superimposing the two flows $\mathbf{u}_\infty = \pm b\nabla T_\infty$ and noting that the flow $\mathbf{u}_\infty = b\nabla T_\infty$ balances the effect of the temperature gradient according to (1.11) - (1.13), we conclude that the original bubble will move with a constant velocity $-b\mathbf{H}$ as if the plane were absent.

3. The solution of the two bubble problem

In this section we shall study the motion of two bubbles in an unbounded fluid resulting from the presence of a constant ambient temperature gradient $\mathbf{H}$. The solution of this problem is required in §4 to determine the average velocity of a bubble immersed in a suspension of bubbles of a different size.

As noted earlier, the motion of two unequal-size bubbles can be determined by first solving the thermal problem to find the temperature distribution and the surface tension distribution on the surface of the bubbles, and then solving the hydrodynamic problem to find the velocity of the bubbles. This problem is greatly simplified when the two bubbles are aligned with the temperature gradient (i.e. with axisymmetric geometry), so that spherical bipolar coordinates can be used, as shown by Meyyappan et al. (1983) and by Keh & Chen (1990). For the general case of two bubbles with radii a_1 and $a_2 \equiv \lambda a_1$ and arbitrary orientation, Anderson (1985) applied the direct reflection method to determine the bubble velocities up to terms of order $O(R^{-6})$, with $R \equiv r/a_1$, where r denotes the center-to-center distance between the two bubbles, while Keh & Chen (1992, 1993) used a boundary collocation technique to find the mobility functions of two drops and two bubbles for $\lambda = \frac{1}{2}, 1$ and 2.

In this section, we shall show that higher accuracy can be reached by applying the method of twin multipole expansions, an approach that was also followed in a recent work by Satrape (1992). In both cases the solution is expanded as an infinite series whose coefficients are to be determined by satisfying the boundary conditions of the problem. But whereas in the approach adopted by Satrape the series expansion was truncated and these coefficients were determined to the desired accuracy for every value of R and λ, in what follows the coefficients of the multipole expansions will be

expanded as power series in λ/R and $1/R$ and therefore expansions will be derived for the bubble velocities in a form where their dependence on R and λ is factored out. Consequently, although our results are equivalent to those obtained by Satrape (1992), they are expressed in a more convenient form for the purpose of obtaining the ensemble averaged velocity of a test bubble in the suspension.

3.1. The general solution

Due to the linearity of the thermal and the hydrodynamic problems, the general case of arbitrary orientation of the two bubbles with respect to the ambient temperature gradient $\mathbf{H}$ is decomposed into two problems, in which the centerline $\mathbf{r}$ is parallel and perpendicular to $\mathbf{H}$, respectively; the former case is obviously axisymmetric and the latter is not.

Following Jeffrey & Onishi (1984), two sets of spherical polar coordinates $(\rho_\alpha, \theta_\alpha, \phi)$ are chosen $(\alpha = 1, 2)$ to describe the two bubble geometry.

First consider the thermal problem, which is a special case of a more general problem solved by Thovert & Acrivos (1989) involving two spheres of different sizes and equal but arbitrary heat conductivities embedded in an ambient temperature field of constant gradient.

The temperature distribution outside the bubbles is expanded, for the parallel case $(m = 0)$ and the perpendicular case $(m = 1)$ respectively, as

$$T_m = (-1)^{m(\alpha+1)} H \rho_\alpha Y_{m1}(\theta_\alpha, \phi) + H \sum_{n=m}^{\infty} [\, g_{mn}^{(\alpha)} \left(\frac{a_\alpha}{\rho_\alpha} \right)^{n+1} Y_{mn}(\theta_\alpha, \phi)$$

$$+g_{mn}^{(3-\alpha)}\left(\frac{a_{3-\alpha}}{\rho_{3-\alpha}}\right)^{n+1}Y_{mn}(\theta_{3-\alpha},\phi)\,] \quad (1.14)$$

with $H = |\mathbf{H}|$, where $Y_{mn}(\theta_\alpha,\phi)$ are spherical surface harmonics, while the coefficients $g_{mn}^{(\alpha)}$, which depend on λ and R, are to be determined from the boundary conditions. Expanding $g_{mn}^{(\alpha)}$ as a double power series in terms of $t_\alpha \equiv a_\alpha/r$,

$$g_{mn}^{(\alpha)} = (-1)^{(m+1)\alpha}a_\alpha\sum_{p=0}^{\infty}\sum_{q=0}^{\infty}G_{npq}^{m}t_\alpha^p t_{3-\alpha}^q, \quad (1.15)$$

and substituting (1.14) and (1.15) into (1.3), yields the recurrence relation:

$$G_{npq}^{m} = (-1)^{(m+1)}\left(\frac{n}{n+1}\right)\sum_{s=m}^{\infty}\binom{n+s}{n+m}G_{s,q-s-2,p-n+1}^{m} \quad (1.16)$$

with

$$G_{100}^{m} = \frac{1}{2}(-1)^{(m+1)}. \quad (1.17)$$

Equations (1.16) and (1.17) completely determine the temperature field.

We next turn to the hydrodynamic problem. The pressure and flow fields can be written as the sum of the contributions of singularities at the center of the bubbles (Jeffrey & Onishi, 1984):

$$p = p^{(\alpha)} + p^{(3-\alpha)},$$

and

$$\mathbf{u} = \mathbf{u}^{(\alpha)} + \mathbf{u}^{(3-\alpha)}, \quad (1.18)$$

where

$$p^{(\alpha)} = \mu\sum_{m=0}^{\infty}\sum_{n=m}^{\infty}\frac{1}{a_\alpha}p_{mn}^{(\alpha)}\left(\frac{a_\alpha}{\rho_\alpha}\right)^{n+1}Y_{mn}(\theta_\alpha,\phi), \quad (1.19)$$

and

$$\mathbf{u}^{(\alpha)} = \sum_{m=0}^{\infty}\sum_{n=m}^{\infty}\{\nabla\times\left[\boldsymbol{\rho}_\alpha q_{mn}^{(\alpha)}\left(\frac{a_\alpha}{\rho_\alpha}\right)^{n+1}Y_{mn}(\theta_\alpha,\phi)\right] + a_\alpha\nabla\left[v_{mn}^{(\alpha)}\left(\frac{a_\alpha}{\rho_\alpha}\right)^{n+1}Y_{mn}(\theta_\alpha,\phi)\right] - \frac{n-2}{2n(2n-1)a_\alpha}\rho_\alpha^2\nabla\left[p_{mn}^{(\alpha)}\left(\frac{a_\alpha}{\rho_\alpha}\right)^{n+1}Y_{mn}(\theta_\alpha,\phi)\right] + \frac{n+1}{n(2n-1)a_\alpha}\boldsymbol{\rho}_\alpha p_{mn}^{(\alpha)}\left(\frac{a_\alpha}{\rho_\alpha}\right)^{n+1}Y_{mn}(\theta_\alpha,\phi)\}. \tag{1.20}$$

The coefficients $p_{mn}^{(\alpha)}$, $v_{mn}^{(\alpha)}$ and $q_{mn}^{(\alpha)}$ are functions only of r and λ, and are to be determined from the boundary conditions.

To simplify the application of the boundary conditions, we follow Happel & Brenner (1991) and Jeffrey & Onishi (1984) in first constructing the following three scalar equations

$$\hat{\boldsymbol{\rho}}_\alpha\cdot\mathbf{u} = \hat{\boldsymbol{\rho}}_\alpha\cdot\mathbf{U}_\alpha = \sum_{m=0}^{\infty}\sum_{n=m}^{\infty}\chi_{mn}^{(\alpha)}Y_{mn}(\theta_\alpha,\phi), \tag{1.21}$$

$$\frac{1}{\mu}\left[{a_\alpha}^2\nabla\cdot(\boldsymbol{\sigma}\cdot\hat{\boldsymbol{\rho}}_\alpha) - \frac{\partial}{\partial\rho_\alpha}(\boldsymbol{\rho}_\alpha\cdot\boldsymbol{\sigma}\cdot\boldsymbol{\rho}_\alpha)\right] = \frac{{a_\alpha}^2}{\mu}\nabla_s\cdot\mathbf{f}_s = \sum_{m=0}^{\infty}\sum_{n=m}^{\infty}\psi_{mn}^{(\alpha)}Y_{mn}(\theta_\alpha,\phi), \tag{1.22}$$

$$\frac{a_\alpha}{\mu}\boldsymbol{\rho}_\alpha\cdot[\nabla\times(\boldsymbol{\sigma}\cdot\hat{\boldsymbol{\rho}}_\alpha)] = \frac{a_\alpha}{\mu}\boldsymbol{\rho}_\alpha\cdot(\nabla_s\times\mathbf{f}_s) = \sum_{m=0}^{\infty}\sum_{n=m}^{\infty}\omega_{mn}^{(\alpha)}Y_{mn}(\theta_\alpha,\phi), \tag{1.23}$$

where $\hat{\boldsymbol{\rho}}_\alpha = \boldsymbol{\rho}_\alpha/\rho_\alpha$, $\mathbf{f}_s = (\mathbf{I}-\hat{\boldsymbol{\rho}}_\alpha\hat{\boldsymbol{\rho}}_\alpha)\cdot(\boldsymbol{\sigma}\cdot\hat{\boldsymbol{\rho}}_\alpha)$ and $\nabla_s = (\mathbf{I}-\hat{\boldsymbol{\rho}}_\alpha\hat{\boldsymbol{\rho}}_\alpha)\cdot\nabla$, while the functions $\chi_{mn}^{(\alpha)}$, $\psi_{mn}^{(\alpha)}$ and $\omega_{mn}^{(\alpha)}$ can be obtained from the boundary conditions (1.7) and (1.8).

Next, we use the scalar equations (1.21) – (1.23) just constructed to find the relations for the coefficients $p_{mn}^{(\alpha)}$, $v_{mn}^{(\alpha)}$ and $q_{mn}^{(\alpha)}$ in (1.19) and (1.20).

Substituting (1.18) into the boundary conditions (1.21) – (1.23), expressing all the functions of $\rho_{3-\alpha}, \theta_{3-\alpha}$ and ϕ in terms of $r, \rho_\alpha, \theta_\alpha$ and ϕ by the transformation rule [see equation (2.1) in Jeffrey & Onishi, 1984] and then using the orthogonality relations of $Y_{mn}(\theta_\alpha, \phi)$ yield three relations for $p_{mn}^{(\alpha)}$, $v_{mn}^{(\alpha)}$ and $q_{mn}^{(\alpha)}$. For convenience in later computations, the first two relations are reorganized. Finally, we obtain the following three general recurrence relations for $p_{mn}^{(\alpha)}$, $v_{mn}^{(\alpha)}$ and $q_{mn}^{(\alpha)}$:

$$2(2n+1)\left\{(n+1)v_{mn}^{(\alpha)} - \frac{n}{2(2n+3)}\sum_{s=m}^{\infty}\binom{n+s}{n+m}t_\alpha^{n-1}t_{3-\alpha}^{s}p_{ms}^{(3-\alpha)}\right\} = \psi_{mn}^{(\alpha)} + 2(n^2-1)\chi_{mn}^{(\alpha)}, \quad (1.24)$$

$$2(2n+1)\left\{\frac{(n+1)}{2(2n-1)}p_{mn}^{(\alpha)} + \sum_{s=m}^{\infty}\binom{n+s}{n+m}t_\alpha^{n-1}t_{3-\alpha}^{s}\left[im(-1)^\alpha q_{ms}^{(3-\alpha)} + nv_{ms}^{(3-\alpha)}t_{3-\alpha}^2 + \left(\frac{(n^2-m^2)(sn-2s-2n+1)}{s(2s-1)(2n-1)(n+s)} - \frac{n(s-2)}{2s(2s-1)}\right)p_{ms}^{(3-\alpha)}\right]\right\} = \psi_{mn}^{(\alpha)} + 2n(n+2)\chi_{mn}^{(\alpha)} \quad (1.25)$$

$$n(n+1)(n+2)q_{mn}^{(\alpha)} + (n-1)\sum_{s=m}^{\infty}\binom{n+s}{n+m}t_\alpha^n t_{3-\alpha}^s \left[nsq_{ms}^{(3-\alpha)}t_{3-\alpha} + (-1)^{3-\alpha}\frac{m}{s}ip_{ms}^{(3-\alpha)}\right] = \omega_{mn}^{(\alpha)}. \quad (1.26)$$

The force-free condition on the bubbles yields

$$p_{01}^{(\alpha)} = p_{11}^{(\alpha)} = 0,$$

which, together with (1.24) – (1.26) completely determine the coefficients p_{mn}^{α}, $v_{mn}^{(\alpha)}$, $q_{mn}^{(\alpha)}$ and U_{α}, once $\chi_{mn}^{(\alpha)}$, $\psi_{mn}^{(\alpha)}$ and $\omega_{mn}^{(\alpha)}$ have been calculated from (1.7), (1.8), (1.21) – (1.23).

Before applying these general results to the parallel and the perpendicular cases separately, we define the mobility functions, which are the quantities of most interest.

The mobility functions $A_{\alpha\beta}$ (for the axisymmetric case) and $B_{\alpha\beta}$ (for the perpendicular case) $(\alpha, \beta = 1, 2)$ are defined through the relations

$$\mathbf{U}_{\alpha} = \mathbf{M}_{\alpha\alpha} \cdot \mathbf{U}_{\alpha}^{(0)} + \mathbf{M}_{\alpha(3-\alpha)} \cdot \mathbf{U}_{(3-\alpha)}^{(0)}, \tag{1.27}$$

for the velocities of two bubbles arbitrarily oriented relative to $\mathbf{H}$, where

$$\mathbf{M}_{\alpha\beta} = A_{\alpha\beta}(r, \lambda)\frac{\mathbf{rr}}{r^2} + B_{\alpha\beta}(r, \lambda)(\mathbf{I} - \frac{\mathbf{rr}}{r^2}). \tag{1.28}$$

In this definition, it is implicitly assumed that, in both the parallel and perpendicular cases, the velocity of each bubble is parallel to $\mathbf{H}$ as it can be easily inferred from the possible general form $\mathbf{U}_{\alpha} = [f_1(\lambda, r)\mathbf{I} + f_2(\lambda, r)\mathbf{rr}] \cdot \mathbf{H}$ and from the symmetry of the problem.

Finally, it is easy to see from the result of §2 that if $\mathbf{U}_1^{(0)} = \mathbf{U}_2^{(0)}$ then $\mathbf{U}_1 = \mathbf{U}_2 = \mathbf{U}_1^{(0)} = \mathbf{U}_2^{(0)}$. Therefore equations (1.27) and (1.28) give

$$A_{\alpha\alpha}(r, \lambda) + A_{\alpha(3-\alpha)}(r, \lambda) = 1, \tag{1.29}$$

$$B_{\alpha\alpha}(r, \lambda) + B_{\alpha(3-\alpha)}(r, \lambda) = 1. \tag{1.30}$$

It is also easy to see by interchanging the labels 1 and 2, that

$$A_{\alpha\beta}(r,\lambda) = A_{(3-\alpha)(3-\beta)}(r,\lambda^{-1}), \tag{1.31}$$

$$B_{\alpha\beta}(r,\lambda) = B_{(3-\alpha)(3-\beta)}(r,\lambda^{-1}). \tag{1.32}$$

So, our problem reduces to finding two independent scalar mobility functions, say, A_{11} and B_{11}.

3.2. Determination of $A_{\alpha\beta}$ (i.e. the parallel case)

Consider first the axisymmetric case where the ambient temperature gradient $\mathbf{H}$ is parallel to the centerline $\mathbf{r}$. Since $\mathbf{U}_1^{(0)}$ and $\mathbf{U}_2^{(0)}$ are also parallel to $\mathbf{H}$ and therefore to $\mathbf{r}$, equations (1.27) and (1.28) yield

$$U_1 = A_{11}U_1^{(0)} + A_{12}U_2^{(0)}, \tag{1.33}$$

where $A_{12} = 1 - A_{11}$ [cf. (1.29)], $U_1 = |\mathbf{U}_1|$ and similarly for $U_1^{(0)}$ and $U_2^{(0)}$. In turn, A_{11} can be determined by considering two separate cases in which the velocities of the two bubbles are either parallel or antiparallel to each other, i.e. $\mathbf{U}_1^{(0)} = \pm\mathbf{U}_2^{(0)} = \mathbf{U}_0$. Denoting by $U_+^{(1)}$ and $U_-^{(1)}$ the resulting velocities of bubble 1, we find that $A_{11} = (U_+^{(1)} + U_-^{(1)})/2U_0$ where $U^{(1)}$(the $\pm$ subscript is hereby omitted for the sake of simplicity) can be determined through equations (1.14) – (1.20), subject to the following boundary conditions [cf. equation (1.21) – (1.23)]

$$\psi_{0n}^{(\alpha)} = -6(\pm 1)^{\alpha}(n+1)\sum_{p=0}^{\infty}\sum_{q=0}^{\infty} G_{npq}^{m} t_{\alpha}^{p} t_{3-\alpha}^{q}, \equiv U_0 \sum_{p=0}^{\infty}\sum_{q=0}^{\infty} B_{npq} t_{\alpha}^{p} t_{3-\alpha}^{q}, \tag{1.34}$$

$$\chi_{0n}^{(\alpha)} = -(\mp 1)^{3-\alpha}\delta_{n1}U^{(\alpha)}, \tag{1.35}$$

$$\omega_{0n}^{(\alpha)} = 0, \tag{1.36}$$

where the $\pm$ sign refers to the parallel and anti-parallel cases, respectively.

Now, we expand $p_{0n}^{(\alpha)}$, $q_{0n}^{(\alpha)}$ and $v_{0n}^{(\alpha)}$ in (1.19) and (1.20),

$$p_{0n}^{(\alpha)} = (\mp 1)^{3-\alpha}U_0\sum_{p=0}^{\infty}\sum_{q=0}^{\infty}P_{npq}t_\alpha^p t_{3-\alpha}^q, \tag{1.37}$$

$$q_{0n}^{(\alpha)} = (\mp 1)^{3-\alpha}U_0\sum_{p=0}^{\infty}\sum_{q=0}^{\infty}Q_{npq}t_\alpha^p t_{3-\alpha}^q, \tag{1.38}$$

$$v_{0n}^{(\alpha)} = (\mp 1)^{3-\alpha}U_0\sum_{p=0}^{\infty}\sum_{q=0}^{\infty}\frac{1}{2n+1}V_{npq}t_\alpha^p t_{3-\alpha}^q, \tag{1.39}$$

where, from the force-free condition on the bubbles,

$$P_{1pq} = 0. \tag{1.40}$$

Note that in this (i.e. the axisymmetric) case, $q_{0n}^{(\alpha)}$, the coefficients of the azimuthal term in the velocity field (1.20), are identically zero on account of the symmetry of the problem. Moreover the velocities of the bubbles, defined following Jeffrey & Onishi (1984) as $\mathbf{U}_1 = U^{(1)}\mathbf{H}/H$ and $\mathbf{U}_2 = \pm U^{(2)}\mathbf{H}/H$ again can be expanded as

$$U^{(\alpha)} = (\mp 1)^{3-\alpha}U_0\sum_{p=0}^{\infty}\sum_{q=0}^{\infty}U_{pq}t_\alpha^p t_{3-\alpha}^q, \tag{1.41}$$

Substituting (1.37) - (1.41) into the general recurrence relations (1.24) - (1.26) we obtain, for $n \geq 2$,

$$P_{npq} = \frac{2(2n-1)}{n+1}\left\{-\frac{B_{npq}}{2(2n+1)} \mp \sum_{s=1}^{\infty}\binom{n+s}{n}\left[\frac{n}{2s+1}V_{s,q-s-2,p-n+1}\right.\right.$$
$$\left.\left. + \left(\frac{n^2(sn-2s-2n+1)}{s(2s-1)(2n-1)(n+s)} - \frac{n(s-2)}{2s(2s-1)}\right)P_{s,q-s,p-n+1}\right]\right\}, \tag{1.42}$$

$$V_{npq} = \frac{2n+1}{n+1}\left\{-\frac{B_{npq}}{2(2n+1)} \pm \frac{n}{2(2n+3)}\sum_{s=1}^{\infty}\binom{n+s}{n}P_{s,q-s,p-n+1}\right\}, \quad (1.43)$$

and for $n = 1$,

$$U_{pq} = \frac{1}{6}B_{1pq} + \left\{P_{1pq} \pm \sum_{s=1}^{\infty}\binom{1+s}{1}\left[\frac{1}{2s+1}V_{s,q-s-2,p} + \frac{1-s}{2s(2s-1)}P_{s,q-s,p}\right]\right\}. \quad (1.44)$$

Finally, the values of $U_+^{(1)}$ and $U_-^{(1)}$ can be evaluated through (1.41) - (1.44). In agreement with the analysis preceding equation (1.13), we find that $U_+^{(1)} = U_0$ and on substituting the value of $U_-^{(1)}$ into $A_{11} = (1+U_-^{(1)}/U_0)/2$ we find that

$$A_{11} = \frac{1}{2} + \frac{1}{2}\sum_{k=0}^{\infty}\sum_{q=0}^{k}U^-_{(k-q)q}\frac{a_1^{k-q}a_2^p}{r^k} = \sum_{k=0}^{\infty}\frac{A_{11}^{(k)}(\lambda)}{R^k}, \quad (1.45)$$

with $R = r/a_1$, where

$$A_{11}^{(k)}(\lambda) = \frac{1}{2}\delta_{k1} + \frac{1}{2}\sum_{q=0}^{k}U^-_{(k-q)q}\lambda^q. \quad (1.46)$$

Here U^-_{pq} is given by equation (1.44) for the anti-parallel case. The first few terms of (1.45) are

$$A_{11}(R,\lambda) = 1 - \frac{\lambda^3}{R^3} - 2\frac{\lambda^3}{R^6} - 3\frac{\lambda^5}{R^8} - 4\frac{\lambda^6}{R^9} - 4\frac{\lambda^7}{R^{10}} - \frac{9\lambda^6+6\lambda^8}{R^{11}} - \frac{8\lambda^6+5\lambda^9}{R^{12}} + O(\frac{1}{R^{13}}). \quad (1.47)$$

This extends Anderson's (1985) result which consists of the first three terms of (1.47).

Some typical numerical values of $A_{11}(R,\lambda)$ obtained by summing the series (1.45) up to terms of order $O(1/R^{120})$, are given in Table 1.1.

R-1 -λ	$\lambda = 1/20$	$\lambda = 1/10$	$\lambda = 1/2$	$\lambda = 1$	$\lambda = 2$	$\lambda = 10$	$\lambda = 20$
0.00	0.99962	0.99734	0.89534	0.71979	0.49589	0.16307	0.09714
0.01	0.99967	0.99770	0.90606	0.74049	0.51759	0.16822	0.09930
0.05	0.99976	0.99834	0.92943	0.79161	0.57960	0.18719	0.10764
0.10	0.99981	0.99871	0.94385	0.82645	0.62842	0.20791	0.11744
0.50	0.99995	0.99964	0.97971	0.92262	0.78802	0.31893	0.18058
1.00	0.99998	0.99987	0.99088	0.95932	0.86696	0.41065	0.24150
2.00	1.00000	0.99996	0.99694	0.98382	0.93447	0.54142	0.33982

Table 1.1: The function $A_{11}(R, \lambda)$ obtained by summing the series (1.45) to terms $O(1/R^{120})$, $R = r/a_1, \lambda = a_2/a_1$.

3.3. Determination of $B_{\alpha\beta}$ (i.e. the perpendicular case)

When **H** is perpendicular to the centerline **r**, equation (1.27) yields

$$U_1 = B_{11}U_1^{(0)} + B_{12}U_2^{(0)}, \tag{1.48}$$

where $B_{12} = 1 - B_{11}$ [cf. (1.30)].

Next we proceed as in the previous case, with $m = 1$ replacing $m = 0$ in equations (1.34) - (1.40). Substituting (1.37) - (1.41) into the general recurrence relations (1.24) - (1.26) yields, for $n \geq 2$,

$$P_{npq} = \frac{2(2n-1)}{n+1}\left\{-\frac{B_{npq}}{2(2n+1)} \mp \sum_{s=1}^{\infty}\binom{n+s}{n+1}\left[Q_{s,q-s-1,p-n+1}\right.\right.$$
$$+\frac{n}{2s+1}V_{s,q-s-2,p-n+1} + \left(\frac{(n^2-1)(sn-2s-2n+1)}{s(2s-1)(2n-1)(n+s)}\right.$$
$$\left.\left.\left.-\frac{n(s-2)}{2s(2s-1)}\right)P_{s,q-s,p-n+1}\right]\right\}, \tag{1.49}$$

$$V_{npq} = \frac{2n+1}{n+1}\left\{-\frac{B_{npq}}{2(2n+1)} \pm \frac{n}{2(2n+3)}\sum_{s=1}^{\infty}\binom{n+s}{n+1}P_{s,q-s,p-n11}\right\}, \quad (1.50)$$

$$Q_{npq} = \pm\frac{n-1}{n(n+1)(n+2)(n+3)}\sum_{s=1}^{\infty}\binom{n+s}{n+1}\left[nsQ_{s,q-s-1,p-n} + \frac{1}{s}P_{s,q-s,p-n}\right] \quad (1.51)$$

and for $n = 1$,

$$U_{pq} = \frac{1}{6}B_{1pq} + \left\{P_{1pq} \pm \sum_{s=1}^{\infty}\binom{1+s}{2}\left[\frac{1}{2s+1}V_{s,q-s-2,p-n+1} + \frac{2-s}{2s(2s-1)}P_{s,q-s,p}\right]\right\}. \quad (1.52)$$

Finally, the bubble velocity U_α is evaluated by substituting (1.52) into (1.41). For the case $U_1^{(0)} = U_2^{(0)}$, we find $U_1 = U_2 = U_0$, in agreement with (1.13), and combining the results of the two cases $U_1^{(0)} = \pm U_2^{(0)}$, we obtain

$$B_{11} = \frac{1}{2} + \frac{1}{2}\sum_{k=0}^{\infty}\sum_{q=0}^{k}U^{-}_{(k-q)q}\frac{a_1^{k-q}a_2^{p}}{r^k} = \sum_{k=0}^{\infty}\frac{B_{11}^{(k)}(\lambda)}{R^k}, \quad (1.53)$$

where

$$B_{11}^{(k)}(\lambda) = \frac{1}{2}\delta_{k1} + \frac{1}{2}\sum_{q=0}^{k}U^{-}_{(k-q)q}\lambda^q. \quad (1.54)$$

The first few terms of (1.53) are

$$B_{11}(R,\lambda) = 1 + \frac{\lambda^3}{2R^3} + \frac{\lambda^3}{4R^6} + \frac{\lambda^5}{4R^8} + \frac{\lambda^6}{8R^9} + \frac{\lambda^7}{4R^{10}} + \frac{4\lambda^6+\lambda^8}{8R^{11}} + \frac{\lambda^6+4\lambda^9}{16R^{12}} + O(\frac{1}{R^{13}}). \quad (1.55)$$

Again this generalizes Anderson's (1985) result which consists of the first three terms of (1.55) .

Some typical numerical values of $B_{11}(R,\lambda)$ obtained by summing the series (1.53) up to terms of order $O(1/R^{120})$, are given in Table 1.2. Also we note that our numerical values for the velocity of the bubbles and those given by Satrape (1992) were found to agree to five significant figures.

R-1 -λ	$\lambda = 1/20$	$\lambda = 1/10$	$\lambda = 1/2$	$\lambda = 1$	$\lambda = 2$	$\lambda = 10$	$\lambda = 20$
0.00	1.00008	1.00055	1.02281	1.07038	1.15643	1.37727	1.43240
0.01	1.00008	1.00052	1.02214	1.06900	1.15459	1.37620	1.43177
0.05	1.00007	1.00044	1.01989	1.06408	1.14768	1.37201	1.42929
0.10	1.00005	1.00038	1.01766	1.05884	1.13986	1.36688	1.42621
0.50	1.00002	1.00014	1.00835	1.03332	1.09521	1.32943	1.40272
1.00	1.00001	1.00006	1.00413	1.01892	1.06321	1.28973	1.37581
2.00	1.00000	1.00002	1.00148	1.00788	1.03216	1.22774	1.32883

Table 1.2: The function $B_{11}(R,\lambda)$ obtained by summing the series (1.53) to terms $O(1/R^{120})$, $R = r/a_1, \lambda = a_2/a_1$.

4. The Average Velocity of a Bubble

Acrivos et al. (1990) calculated the ensemble averaged bubble velocity in a monodispersed suspension of bubbles. In this section, we extend the calculation to bi-dispersed dilute suspensions by determining the average velocity of bubble 1 in a space-filling suspension of bubbles 2.

As was pointed out by Acrivos et al. (1990), such a calculation requires the application of a renormalization procedure which takes into account the following two constraints: (1) that the ensemble averaged velocity at any point in the suspension is zero and (2) that the corresponding ensemble

averaged temperature gradient equals the imposed temperature gradient $\mathbf{H}$. In terms of ensemble averages, these constraints for a dilute suspension of bubbles 2 are

$$\int \mathbf{u}P(\mathbf{r})d\mathbf{r} = 0 \quad \text{and} \quad \int(\nabla T - \mathbf{H})P(\mathbf{r})d\mathbf{r} = 0, \tag{1.56}$$

where $P(\mathbf{r})$ is the unconditional probability that the center of a single bubble 2 is at $\mathbf{r}$, while $\mathbf{u} = \mathbf{u}(\mathbf{r})$ and $\nabla T = \nabla T(\mathbf{r})$ are, respectively, the velocity and the temperature gradient at the origin, when a single bubble 2 is present with its center at $\mathbf{r}$. Here, we have used the assumption that the suspension is so dilute that the probability of two bubbles 2 being at distance $r \sim O(a_1 + a_2)$ from the origin is of $O(c_2^2)$ and can therefore be neglected, where c_2 is the volume fraction occupied by bubbles 2.

Next, consider the average velocity of a test bubble 1 with its center at the origin,

$$\overline{\mathbf{U}}_1 = \mathbf{U}_1^{(0)} + \int(\mathbf{U}_1 - \mathbf{U}_1^{(0)})P(\mathbf{r}|\mathbf{0})d\mathbf{r}, \tag{1.57}$$

where $\mathbf{U}_1 = \mathbf{U}_1(\mathbf{0}|\mathbf{r})$ is the velocity of a bubble 1 at the origin in the presence of a single bubble 2 with its center at $\mathbf{r}$ and $P(\mathbf{r}|\mathbf{0})$ is the conditional probability of having a single bubble 2 at $\mathbf{r}$ given that a bubble 1 is at the origin.

All the integrals in (1.56) and (1.57) are non-convergent, with the divergent terms representing the zeroth-order reflections of the velocity and temperature fields, i.e. the velocity of bubble 1 at the origin induced by the velocity and temperature disturbance of a single bubble 2 at $\mathbf{r}$. Therefore,

as shown by Acrivos et al. (1990), these identical divergent terms can be subtracted from each other, and $\overline{\mathbf{U}}_1$ can be determined by evaluating the remaining higher-order terms representing higher-order reflections.

Thus we arrive at:

$$\overline{\mathbf{U}}_1 = \mathbf{U}_1^{(0)} + \int \mathbf{u}(\mathbf{r})[P(\mathbf{r}|0) - P(\mathbf{r})]d\mathbf{r}$$
$$+ \frac{\mathbf{U}_1^{(0)}}{H} \int (\nabla T - \mathbf{H})[P(\mathbf{r}|0) - P(\mathbf{r})]d\mathbf{r} + \int \mathbf{W}(\mathbf{r})P(\mathbf{r}|\mathbf{0})d\mathbf{r}, \qquad (1.58)$$

where $\mathbf{W}(\mathbf{r})$, defined by

$$\mathbf{U}_1 = \mathbf{U}_1^{(0)} + \mathbf{u} + \frac{\mathbf{U}_1^{(0)}}{H}(\nabla T - \mathbf{H}) + \mathbf{W}, \qquad (1.59)$$

is obtained from equation (1.27) by retaining only the terms of order higher than $O(1/R^3)$ in (1.47) and (1.55).

For well-mixed suspensions of bubbles 2, the probability and conditional probability functions are given by (Jeffrey, 1973)

$$P(\mathbf{r}) = \frac{c_2}{\frac{4}{3}\pi a_2^3} \qquad (1.60)$$

and

$$P(\mathbf{r}|0) = 0 \quad \text{for} \quad r < a_1 + a_2$$
$$P(\mathbf{r}|0) = P(\mathbf{r}) = \frac{c_2}{\frac{4}{3}\pi a_2^3} \quad \text{for} \quad r \geq a_1 + a_2, \qquad (1.61)$$

where we have assumed that, in the presence of the test bubble 1, the distribution of bubbles 2 is still uniform outside the exclusion layer $r = a_1 + a_2$.

Substituting the probability distributions (1.60) and (1.61) into the first two integrals in (1.58) yields

$$\overline{\mathbf{U}}_1 = \mathbf{U}_1^{(0)} - c_2\mathbf{U}_2^{(0)} - \frac{1}{2}c_2\mathbf{U}_1^{(0)} + c_2\int_{r\geq a_1+a_2}\mathbf{W}(\mathbf{r})\frac{d\mathbf{r}}{\frac{4}{3}\pi a_2^3}. \tag{1.62}$$

Now, since in any physically relevant situation the surface tensions of bubbles 1 and 2 have the same temperature dependence, i.e. $d\gamma_1/dT = d\gamma_2/dT$, so that $\mathbf{U}_2^{(0)} = \lambda\mathbf{U}_1^{(0)}$, (1.62) reduces to

$$\overline{\mathbf{U}}_1 = \mathbf{U}_1^{(0)}\left\{1 - \frac{3}{2}c_1 - S(\lambda)c_2 + ...\right\}, \tag{1.63}$$

where the dependence of $\overline{\mathbf{U}}_1$ on c_1 was already given by Acrivos et al.(1990). In the above, terms of $O(c_1^2)$, $O(c_2^2)$, $O(c_1c_2)$ and higher have been neglected since the analysis is restricted to dilute suspensions. Also

$$S(\lambda) \equiv (\lambda + \frac{1}{2}) + I(\lambda), \tag{1.64}$$

with

$$I(\lambda) = \frac{\lambda - 1}{\lambda^3}\int_{1+\lambda}^{\infty}(A_{11} + 2B_{11} - 3)\,R^2dR. \tag{1.65}$$

On substituting (1.45) and (1.53) into (1.64) and (1.65) we then obtain

$$S(\lambda) = (\lambda + \frac{1}{2}) + (\lambda - 1)\frac{(1+\lambda)^3}{\lambda^3}\sum_{n=6}^{\infty}\frac{A_{11}^{(n)} + 2B_{11}^{(n)}}{(n-3)(1+\lambda)^n} \tag{1.66}$$

where $A_{11}^{(n)}$ and $B_{11}^{(n)}$ are given by (1.46) and

The function $S(\lambda)$ is tabulated in Table 1.3 and is plotted in Fig.1.1 together with its asymptotic expressions to be derived below for $\lambda \longrightarrow \infty$

(1.54).

λ	$I(\lambda)$	From (1.83)	From (1.75)
1/64	0.4766	0.4755	
1/32	0.4545	0.4509	
1/16	0.4119	0.4019	
1/8	0.3413	0.3038	
1/4	0.2365	0.1075	
1/2	0.1112	−0.2850	−1.6800
1	0.0000	−1.0700	−0.8400
2	−0.0628	−2.6400	−0.4200
4	−0.0743		−0.2100
8	−0.0585		−0.1050
16	−0.0380		−0.0525
32	−0.0222		−0.0263
64	−0.0130		−0.0131

Table 1.3: Values of the function $I(\lambda)$, defined by (1.64), computed by summing the series in (1.66) to terms $O(1/R^{120})$ and then extrapolating the result, as well as the corresponding asymptotic expressions for $\lambda << 1$ and $\lambda >> 1$ as obtained from equations (1.83) and (1.75), respectively.

and $\lambda \longrightarrow 0$, respectively. Also shown in Table 1.3 are tabulated values of the function which is obtained from (1.66) by retaining only the first term of the infinite series. Clearly, as pointed out by one of the referees, the expression given above provides a very good approximation for $S(\lambda)$ over the whole range of λ. We note that the values given by Keh & Chen (1993) for $S(\frac{1}{2})$ and $S(\frac{1}{2})$ are 1.013 and 2.438, respectively, of which the former appears to be somewhat inaccurate.

It is worth remarking that the first two terms in (1.64) for $S(\lambda)$ merely reflect the presence of the renormalization constraints. Specifically, since

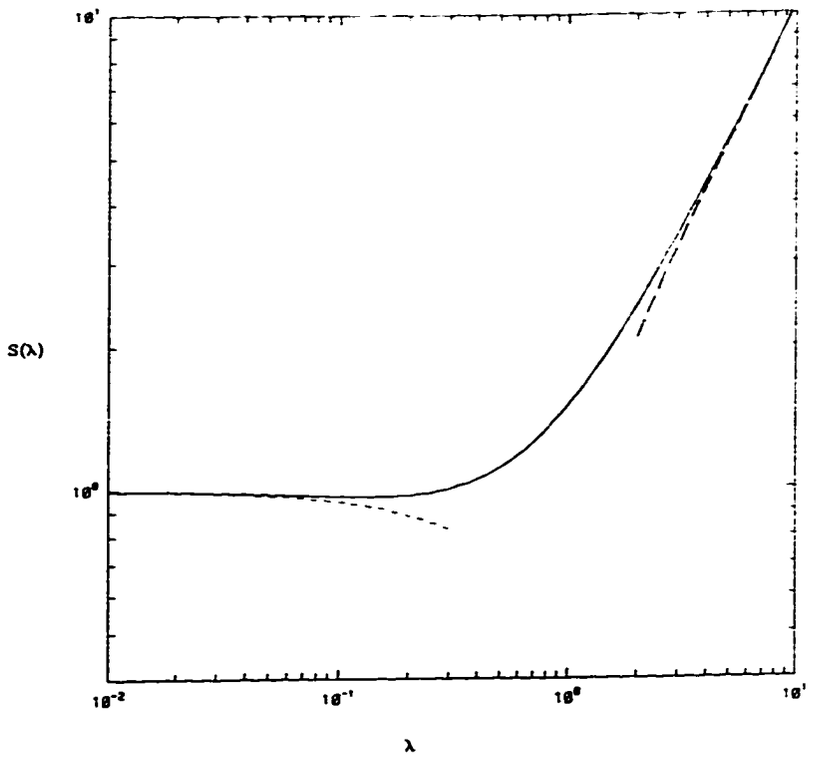

Figure 1.1: The function $I(\lambda)$, defined by (1.64), with the solid line representing the computed results by summing the series in (1.66), while the dashed lines on the left and right sides are based on the asymptotic expressions (1.83), for $\lambda \longrightarrow 0$ and (1.75), for $\lambda \longrightarrow \infty$, respectively.

the motion of the bubbles in the suspension in the direction of $\mathbf{H}$ must be accompanied by a corresponding mean back flux of fluid so that the constraint of zero mean flux at each point in the suspension is satisfied, a single bubble 1 in the fluid is then carried by the back flow with velocity $-(c_1\mathbf{U}_1^{(0)} + c_2\mathbf{U}_2^{(0)})$. This generates the leading term in (1.64). Similarly, the constraint on the mean temperature gradient at each point in the suspension requires that the average temperature gradient in the fluid be $(1 - \frac{1}{2}c_1 - \frac{1}{2}c_2)\mathbf{H}$ since the

temperature gradient inside an isolated bubble is $\frac{3}{2}\mathbf{H}$ (Jeffrey, 1973). In turn, this change in the average temperature gradient in the fluid is responsible for the second term in $S(\lambda)$. Clearly, in view of the results in Table 1.3, the sum of the two renormalization constraints provides an excellent estimate for $S(\lambda)$ when $\lambda > 1/2$.

5. Asymptotic expressions for $S(\lambda)$ for the cases $\lambda \gg 1$ and $\lambda \ll 1$

Although the series expression (1.66) can be used to evaluate $S(\lambda)$ for all values of λ, its usefulness is limited since it converges very slowly when the two bubbles have drastically different sizes. In fact, when $\lambda \longrightarrow 0$ or $\lambda \longrightarrow \infty$ the thermal and hydrodynamic interactions are confined to a small region near the small bubble, and our method describing these interactions in terms of singularities at the center of the large bubble is ineffective. So, it is desirable to find asymptotic expressions for $S(\lambda)$ when $\lambda \gg 1$ and $\lambda \ll 1$. A similar problem was studied by Chang & Acrivos (1986) for the case of heat conduction from a heated sphere to a matrix containing passive spheres of a different conductivity.

5.1. Asymptotic expression for $S(\lambda)$ when $\lambda \gg 1$

When $\lambda \gg 1$, the small test bubble 1 is immersed in a suspension of large bubbles 2. To find the average velocity of the test bubble $\overline{\mathbf{U}}_1$ from (1.63)

- (1.65), we need to find the pair of mobility functions A_{11} and B_{11} which, according to (1.33) and (1.48), are the velocities of bubble 1 when the center-line is parallel and perpendicular to the temperature gradient, respectively, divided by $U_1^{(0)}$ and when, in addition, $\mathbf{U}_2^{(0)}$ =0, that is when bubble 2 is passive. [1]

When the two bubbles are far from each other, i.e. when $R \gg \lambda$, the expressions (1.45) and (1.53) yield the outer expansions:

$$A_{11} = 1 - \frac{\lambda^3}{R^3} - 2\frac{\lambda^3}{R^6} + O(\frac{\lambda^5}{R^8}) \quad l \geq O(\lambda), \quad \lambda \longrightarrow \infty, \tag{1.67}$$

$$B_{11} = 1 + \frac{\lambda^3}{2R^3} + \frac{\lambda^3}{4R^6} + O(\frac{\lambda^5}{R^8}) \quad l \geq O(\lambda), \quad \lambda \longrightarrow \infty, \tag{1.68}$$

where $l \equiv R - \lambda$.

Next, let us consider the case where the small bubble 1 is close to the large passive bubble 2, i.e. when $l \sim O(1)$. First, we estimate the order of magnitude of the velocity of the large passive bubble. According to Faxen's law (Rallison 1978), it equals the velocity at its center induced by the singularities at the center of the small active bubble. Since the latter is force-free, the induced velocity must decay at least as fast as $O(a_1^2/r^2)$, which contributes to A_{11} and B_{11} an $O(1/\lambda^2)$ correction. But, since we wish to determine $S(\lambda)$ only up to $O(1/\lambda)$, equations (1.63) - (1.65) show that the motion of the large bubble has only a smaller order effect on $S(\lambda)$ so that the large bubble can be viewed as being stationary to this order of approximation.

[1] A passive bubble is here defined as having its surface tension independent of temperature, i.e. $d\gamma/dT = 0$.

Next, let us determine the inner expansions for A_{11}, i.e. the velocity of a small active bubble near a large passive one in the axisymmetric case, where the centerline is parallel to the temperature gradient. The temperature distribution in the absence of bubble 1 is (Acrivos et al., 1990):

$$T'_\infty = \left[1 + \frac{a_2^3}{2\rho_2^3}\right] \mathbf{H} \cdot \boldsymbol{\rho}_2.$$

Now, the presence of the small bubble 1 induces a temperature disturbance T' such that $\partial(T' + T'_\infty)/\partial\rho_1 = 0$ is satisfied on the surface of the small bubble. Expanding T'_∞ about the center of the small bubble, this boundary condition becomes

$$\frac{\partial T'}{\partial \rho_1} = -\frac{\partial}{\partial \rho_1}\left[\frac{3l}{\lambda}\mathbf{H}\cdot\boldsymbol{\rho}_1 - \frac{3}{4a_1\lambda}\frac{\mathbf{H}\cdot\mathbf{r}}{r}(3\frac{\mathbf{HH}}{H^2} - \mathbf{I}) : \boldsymbol{\rho}_1\boldsymbol{\rho}_1 + O(\frac{1}{\lambda^2})\right] \text{ at } \rho_1 = a_1, \tag{1.69}$$

while the boundary condition on the surface of the large bubble is still $\partial T'/\partial\rho_2 = 0$ at $\rho_2 = a_2$ since $\partial T'_\infty/\partial\rho_2 = 0$.

Next we examine the effect of each term in the above expansion separately, noting that, within the inner region $1 \leq l < O(\lambda)$, the large bubble can be replaced, as far as its first order effects on the small bubble are concerned, with a non-conducting, stress-free planar wall.

The first term in the bracket of the right-hand-side of (1.69) corresponds to the case when a non-conducting bubble has been placed near a plane on which the temperature gradient perpendicular to it has been set equal to $3lH/\lambda$. But as shown in §2, the velocity of the bubble is then the same as

that of an isolated bubble in a linearly varying ambient temperature field, hence

$$\mathbf{U}_1 = \frac{3l}{\lambda}\mathbf{U}_1^{(0)}.$$

On the other hand, the velocity corresponding to the second term on the right-hand-side of (1.69) can be obtained using the procedure of §3. Specifically, by the method of images, the plane can be replaced by an image bubble so that both the temperature and the velocity fields are symmetric about the plane thereby satisfying identically the non-conducting and stress-free boundary conditions on the plane. The problem then becomes that of determining the motion of two identical non-conducting bubbles in an ambient temperature field T_∞, which is

$$T_\infty = -\frac{3}{4a_1\lambda}\frac{\mathbf{H}\cdot\mathbf{r}}{r}(3\frac{\mathbf{HH}}{H^2} - \mathbf{I}) : \boldsymbol{\rho}_1\boldsymbol{\rho}_1 \quad \text{at} \quad \rho_1 = a_1,$$

on the side of the original bubble and symmetrically on the side of the image bubble. In turn, the velocities of the two bubbles are calculated by applying the technique of §3 to the solution of the above problem, which gives for the velocity of bubble 1

$$\mathbf{U}_1 = \mathbf{U}_1^{(0)}\left\{\frac{1}{\lambda}\sum_{n=2}^{\infty}\frac{C_n}{l^n}\right\}, \tag{1.70}$$

where the C_n's, with $C_2 = -\frac{3}{4}, C_3 = C_4 = 0, C_5 = -\frac{3}{16}, C_6 = 0, C_7 = -\frac{9}{64}, \ldots$ are constants found by solving the two bubble problem.

Finally, combining the contributions from the two terms, we obtain:

$$A_{11} = \frac{3l}{\lambda} + \frac{1}{\lambda}\sum_{n=2}^{\infty}\frac{C_n}{l^n} + O(\frac{1}{\lambda^2}) \quad 1 \le l < O(\lambda), \quad \lambda \longrightarrow \infty. \tag{1.71}$$

We next apply the same method to determine the inner expansion for B_{11}, i.e. the velocity of a small active bubble near a large passive one when $\mathbf{H}$ is perpendicular to the centerline of the two bubbles.

Expanding T'_∞ about the center of bubble 1, the boundary condition on the small bubble can be written as:

$$\frac{\partial T'}{\partial \rho_1} = -\frac{\partial}{\partial \rho_1}\left[(\frac{3}{2} - \frac{3l}{2\lambda})\mathbf{H}\cdot\boldsymbol{\rho}_1 + \frac{3}{4a_1\lambda}(\frac{\mathbf{Hr}+\mathbf{rH}}{Hr}) : \boldsymbol{\rho}_1\boldsymbol{\rho}_1 + O(\frac{1}{\lambda^2})\right] \text{at} \rho_1 = a_1. \tag{1.72}$$

The first term corresponds to the case where a bubble is placed near a non-conducting, stress-free wall with a constant temperature gradient parallel to the plane in the direction of $\mathbf{H}$. Once again, in view of the result of §2, the velocity of the bubble remains unchanged by the presence of the plane, i.e.

$$\mathbf{U}_1 = \left[\frac{3}{2} - \frac{3l}{2\lambda}\right]\mathbf{U}_1^{(0)}.$$

The velocity corresponding to the second term can be found by a similar method as that used in the axisymmetric case to find (1.70). The result is

$$\mathbf{U}_1 = \mathbf{U}_1^{(0)}\left\{\frac{1}{\lambda}\sum_{n=7}^{\infty}\frac{C'_n}{l^n}\right\}, \tag{1.73}$$

with $C'_7 = \frac{9}{1024}$,...

Finally, we obtain

$$B_{11} = (\frac{3}{2} - \frac{3l}{2\lambda}) + \frac{1}{\lambda}\sum_{n=7}^{\infty}\frac{C'_n}{l^n} + O(\frac{1}{\lambda^2}) \quad 1 \le l < O(\lambda),\ \lambda \longrightarrow \infty, \tag{1.74}$$

We now substitute the inner and outer asymptotic expansions for A_{11} and B_{11} into (1.65) to determine the asymptotic expression for $S(\lambda)$. To this end,

we divide the interval of integration into an inner region $\lambda+1 \leq R \leq \lambda+O(\lambda)$ and an outer region $\lambda + O(\lambda) \leq R \leq \infty$, and note that within each domain we have a locally valid asymptotic expression for A_{11} and B_{11}.

By substituting (1.67) and (1.68) into (1.65) we find that, in the outer region, $I_{out} = O(1/\lambda^2)$, i.e. the contribution of the outer region to $S(\lambda)$ is negligible to this order of approximation.

On the other hand, in the inner region, substituting (1.71) and (1.74) into (1.65), and noting that R is basically equal to λ in this region, we obtain

$$I_{in} = \frac{1}{\lambda}\sum_{n=2}^{\infty}\frac{C_n + C_n'}{n-1} + O(\frac{\ln\lambda}{\lambda^2}) = -\frac{0.84}{\lambda} + O(\frac{\ln\lambda}{\lambda^2}).$$

Here, since the sum containing the first k terms was found to be essentially linear in $1/k$ for $k > 20$, the summation was determined by evaluating its first 30 terms and extrapolating the result.

Finally, by combining the results for the two regions, we obtain the following asymptotic result:

$$S(\lambda) = \lambda + \frac{1}{2} - \frac{0.84}{\lambda} + O(\frac{\ln\lambda}{\lambda^2}), \quad \lambda \longrightarrow \infty. \tag{1.75}$$

Clearly, in view of (1.63), a bubble of type 1 could move *against* the temperature gradient for sufficiently large values of λ even if c_2 is small.

5.2. Asymptotic expression for $S(\lambda)$ when $\lambda \ll 1$

We finally consider the other limiting case, i.e. $\lambda = a_2/a_1 \ll 1$, and find the average velocity of a large test bubble 1 immersed in a suspension

of small bubbles 2. It turns out however, that it is easier to determine the velocity of a large passive bubble in the presence of a small active one, i.e. A_{12} and B_{12} for the parallel and perpendicular cases, respectively.

When the two bubbles are far from each other, i.e. when $R \gg 1$, the expressions (1.45) and (1.53) yield the outer expansions:

$$A_{12} = \frac{\lambda^3}{R^3} + 2\frac{\lambda^3}{R^6} + O(\lambda^6) \quad R - 1 \geq O(1), \ \lambda \longrightarrow 0, \tag{1.76}$$

$$B_{12} = -\frac{\lambda^3}{2R^3} - \frac{\lambda^3}{4R^6} + O(\lambda^6) \quad R - 1 \geq O(1), \ \lambda \longrightarrow 0 \tag{1.77}$$

Next we derive the inner expansions for A_{12} and B_{12} when the small bubble 2 is close to the large bubble 1, i.e. when $\bar{l} \sim O(1)$, where $\bar{l} \equiv (R-1)/\lambda$. To begin with, we note that the velocity of a large passive bubble immersed in the flow field generated by a small active one can be determined using Faxen's law, in terms of the strength of the singularities at the center O_2 of the small bubble by evaluating the velocity they induce at the center of the large bubble, $\rho_2 = a_1 R$.

But, once again, since, up to leading order, the strengths of the singularities at O_2 are affected only if $\bar{l} \sim O(1)$, these can be determined by replacing the passive bubble by a non-conducting, stress-free planar wall.

We start by considering the axisymmetric case. The strengths of the singularities at O_2 can be evaluated by expanding the boundary conditions

of the temperature field on the surface of the small bubble,

$$\frac{\partial T'}{\partial \rho_2} = -\frac{\partial}{\partial \rho_2}\left[3\lambda \bar{l}\mathbf{H}\cdot\boldsymbol{\rho}_1 - \frac{3\lambda}{4a_2}\frac{\mathbf{H}\cdot\mathbf{r}}{r}(3\frac{\mathbf{HH}}{H^2} - \mathbf{I}) : \boldsymbol{\rho}_2\boldsymbol{\rho}_2 + O(\lambda^4)\right] \text{ at } \rho_2 = a_2. \tag{1.78}$$

The first term in the expansion corresponds to the constant-gradient case. Applying the method of images as in §5.1 we see that, in this case, the flow field is irrotational and decays as $O(\lambda a_2^3/\rho_2^3)$ thereby contributing to the velocity of bubble 1, or to A_{12} an $O(\lambda^4)$-term and to $S(\lambda)$ an $O(\lambda^2)$-term, which is negligible to this order of approximation.

The second term in the temperature expansion is a quadratic distribution. The leading term of the flow field induced by bubble 2 is an $O(\lambda a_2^2/\rho_2^2)$ stresslet term (Anderson, 1985), which contributes to to A_{12} an $O(\lambda^4)$-term and to $S(\lambda)$ an $O(\lambda)$-term, while the contributions from higher order singularities at the center of bubble 2 [cf. (1.20)] are of smaller order and thus negligible. The strength of the stresslet at the center of the small bubble or $p_{01}^{(2)}$ can be found as an intermediate result in deriving (1.70). Finally, substitution of $p_{01}^{(2)}$ into (1.20), yields $\mathbf{U}_1$ and then A_{12},

$$A_{12} = 3\lambda^3 + \lambda^3 \sum_{n=3}^{\infty} \frac{D_n}{\bar{l}^n} + O(\lambda^4) \quad \bar{l} \sim O(1), \quad \lambda \longrightarrow 0, \tag{1.79}$$

where D_n are constants that can be found using the intermediate result in §5.1 with the first few of them being $D_3 = \frac{3}{4}, D_4 = D_5 = 0, D_6 = \frac{3}{16}, D_7 = 0, D_8 = \frac{27}{256}, \ldots$.

Now let us turn to the perpendicular case, where the temperature expansion is

$$\frac{\partial T'}{\partial \rho_2} = -\frac{\partial}{\partial \rho_2}\left[(\frac{3}{2} - \frac{3\bar{l}\lambda}{2})\mathbf{H}\cdot\boldsymbol{\rho}_2 + \frac{3\lambda}{4a_2}(\frac{\mathbf{Hr}+\mathbf{rH}}{H\tau}) : \boldsymbol{\rho}_2\boldsymbol{\rho}_2 + O(\lambda^2)\right]. \quad (1.80)$$

Once again, the case corresponding to the constant gradient term can be treated by the method of images and the flow field is found to be irrotational. This decays as $O(a_2^3/\rho_2^3)$ which corresponds to a force quadrupole term and contributes to $S(\lambda)$ an $O(\lambda)$ term, while the contributions of the higher order singularities are of smaller order and thus negligible. In turn, the strength of this force quadrupole at the center of the small bubble can be found using the intermediate results of §3.3 for identical bubbles. [2] Thus, on applying Faxen's law, the velocity of the large bubble is found to be

$$\mathbf{U}_1 = \mathbf{U}_2^{(0)}\left\{-\frac{3}{4}\lambda^3 + \lambda^3\sum_{n=3}^{\infty}\frac{E_n}{\bar{l}^n} + O(\lambda^4)\right\} \quad \bar{l}\sim O(1),\ \lambda\longrightarrow 0, \quad (1.81)$$

with $E_3 = -\frac{3}{8}, E_4 = E_5 = 0, E_6 = -\frac{3}{16}, E_7 = 0, E_8 = -\frac{3}{4}, \ldots$

The second term in the temperature expansion (1.80) corresponds to a quadratic temperature distribution. The leading term of the velocity field induced by this singularity at the center of the small bubble is an $O(\lambda a_2^2/\rho_2^2)$ stresslet term, while all the other terms are of smaller order and can be neglected. However, this term does not contribute to $\mathbf{U}_1$ which here is perpendicular to $\mathbf{r}$, since a stresslet only induces a velocity in the radial direction

[2] In this case, although from (1.13) the velocities of the bubbles are the same as if they were isolated, the strength of the force quadrupole depends on the distance between the two bubbles.

from its position. Therefore, we conclude that the effect of the second term on $\mathbf{U}_1$ is smaller than $O(\lambda^3)$, so that its contribution to $S(\lambda)$ is negligible. Therefore,

$$B_{12} = -\frac{3}{4}\lambda^3 + \lambda^3 \sum_{n=3}^{\infty} \frac{E_n}{\bar{l}^n} + O(\lambda^4) \quad \bar{l} \sim O(1), \ \lambda \longrightarrow 0. \tag{1.82}$$

Now, as in §5.1 we use the inner and outer expansions for A_{12} and B_{12}, (1.76), (1.77), (1.79) and (1.82) to evaluate the integral in (1.65) and obtain the asymptotic expression for $S(\lambda)$. First, we divide the interval of integration into an inner region $1+\lambda \leq R \leq 1+R_1$ and an outer region $1+R_1 \leq R \leq \infty$ with $R_1 \sim O(1)$, but note that the integral in each region will depend on the value of R_1. This difficulty can be circumvented by constructing a uniformly valid expression for the integrand (Van Dyke, 1975) or equivalently rewriting (1.65) as:

$$\int_{1+\lambda}^{\infty} f_{out}(R)dR + \int_{1+\lambda}^{R_1} [f_{in}(R) - f_{out}(R)]\, dR, \quad \lambda \longrightarrow 0,$$

and letting $R_1 \longrightarrow \infty$, where $f_{in}(R)$ and $f_{out}(R)$ refer to the integrand in (1.65) evaluated using, respectively, the inner and outer expansions for A_{12} and B_{12}. Upon evaluating the sum by the same method as that used in arriving at (1.75), we find that

$$S(\lambda) = 1 - 0.57\lambda + O(\lambda^2), \quad \lambda \longrightarrow 0. \tag{1.83}$$

This result for $S(\lambda)$ can be interpreted in terms of the effective continuum approach (Acrivos & Chang, 1986) by noting that the suspension of small

bubbles of vanishing size acts as an effective continuum with effective viscosity $\mu^* = \mu(1 + c_2)$ and effective conductivity $k^* = k(1 - \frac{3}{2}c_2)$, with k being the conductivity of the pure fluid. But a large bubble immersed in such an effective continuum will move, according to (1.9), with velocity $(1 - c_2)\mathbf{U}_1^{(0)}$, in agreement with the first term in (1.83), which therefore reflects the effect of the increase in the viscosity of the surrounding fluid , due to the presence of the small bubbles, on the velocity of the large bubble.

As noted earlier, the function $S(\lambda)$ is seen plotted in figure 1 together with its two asymptotic expressions as obtained for (1.83) and (1.75) for, respectively, $\lambda \longrightarrow 0$ and $\lambda \longrightarrow \infty$.

Chapter 2

The Transverse Shear-induced Liquid and Particle Tracer Diffusivities of a Dilute Suspension of Spheres Undergoing a Simple Shear Flow

abstract

We study the shear-induced self-diffusion of both a liquid tracer and a tagged spherical particle along the directions perpendicular to the ambient flow in a dilute suspension of neutrally buoyant spheres undergoing a simple shearing motion in the absence of inertia and Brownian motion effects. The calculation of the liquid diffusivity requires the velocity of a fluid point under the

influence of two spheres, which was determined via Lamb's series expansion; conversely, the calculation of the particle diffusivity involves the trajectories of three spheres, which were determined using far field and near field asymptotic expressions. The displacements of the liquid tracer and of the tagged sphere were then computed analytically when the spheres and the tracer are all far apart, and numerically for close encounters. After summing over all possible encounters, the leading terms of the lateral liquid diffusion coefficients, both within and normal to the plane of shear, were thereby found to be $0.12\gamma a^2c^2$ and $0.004\gamma a^2c^2$, respectively, where γ is the applied shear rate, a the radius of the spheres and c their volume fraction. The analogous coefficients of the lateral particle diffusivity were found to be $0.11\gamma a^2c^2$ and $0.005\gamma a^2c^2$, respectively. Also, liquid and particle diffusivities in a monolayer, with the liquid tracer and all the particle centers lying on the same plane of shear, were found to be $0.067\gamma a^2\bar{c}^2$ and $0.032\gamma a^2\bar{c}^2$, respectively, with $\bar{c}$ denoting the areal fraction occupied by the spheres on the plane.

1. Introduction

The non-Brownian particle migration in suspensions involving only deterministic hydrodynamic interactions can often be represented in terms of a self-diffusion process owing to the random nature of the collisions among the suspended particles. Such a shear-induced particle diffusion has been shown to play an important role in a variety of phenomena involving concentrated suspensions which affect certain of their properties in a profound way. Shear-induced diffusion was first studied experimentally by Eckstein, Bailey & Shapiro (1977), who monitored the motion of a tagged particle within a suspension being sheared in a Couette device, and then was examined in more detail by Leighton & Acrivos (1987a,b) who reported experimental values for the lateral diffusion coefficients both within and normal to the plane of shear. Two dimensional numerical simulations by Bossis & Brady (1987) and by Chang & Powell(1994) for the monolayer diffusivity were found to agree qualitatively with these results. Recently, by considering only two particle interactions, Acrivos, Batchelor, Hinch, Koch & Mauri (1992) derived an analytic expression for the coefficient of shear-induced self-diffusion in the direction of the fluid motion for a dilute suspension of spheres undergoing a simple shearing motion, while Da Cunha & Hinch (1996) studied the effect of surface roughness on the interaction of two particles and calculated the coefficients of the self- and gradient-diffusivity in the lateral directions. Here,

we shall extend the analysis of Acrivos *et al.* (1992) and present expressions for the self-diffusivity of both a tracer fluid particle and a test sphere in the two directions perpendicular to the fluid velocity.

This chapter proceeds as follows. After formulating the problem in §2, we derive in §3 and 4 the expressions for the velocities of the fluid tracer plus those of the test sphere as well as the other two spheres in a simple shear flow, which are then used in §5 to compute the displacement of a liquid tracer and of a test sphere following their encounter with the other two particles. Finally, in §6, we determine the coefficients of self-diffusion in the directions perpendicular to the fluid velocity, both within and normal to the plane of shear.

2. Statement of the problem

Consider a dilute monodisperse suspension of rigid spheres of radius a immersed in a viscous liquid. The spheres are supposed to be neutrally buoyant and torque-free, and their radius a is taken to be sufficiently large that the effects of Brownian motion and interparticle potentials can be neglected. Furthermore, the particle Reynolds number is assumed to be vanishingly small, so that all inertia effects can be ignored. Now, let the suspension undergo a simple shearing motion, the undisturbed velocity of which is given by

$$\mathbf{U} = x_2 \mathbf{e}_1, \tag{2.1}$$

where (x_1, x_2, x_3) is the position vector relative to a fixed triad of unit vectors $\mathbf{e}_1$, $\mathbf{e}_2$ and $\mathbf{e}_3$ which forms a right-hand system. All lengths, time and velocities are regarded as having been nondimensionalized with a, $1/\gamma$ and γa respectively, where γ is the shear rate.

First, consider a fluid point A* and let $\mathbf{X}$ denote its position, where $\mathbf{X} = 0$ initially. In the absence of the suspended spheres, A* would simply remain at the origin. However, when a sphere B, with its center located at $\mathbf{Y}$, approaches from far away, A* will be displaced at first from the origin, but, will return to its initial streamline at the end of the encounter, as a consequence of the reversibility of the creeping flow equations and the symmetry of the problem. Hence, the interaction of a fluid tracer with a single sphere will not lead to its being permanently displaced in the lateral direction, and therefore, to create such a displacement, it is necessary that A* and B interact with at least another sphere C located at $\mathbf{Z}$ (see Fig.2.1).

Since the probability of finding two spheres within an $O(1)$-distance from the tracer is $O(c^2)$, where c is the particle volume fraction, we expect the rate of encounters of a fluid tracer with two spheres to be of $O(c^2)$. In addition, as the rate of encounters involving more spheres is of $o(c^2)$, we need to consider only the interactions of the tracer with two spheres in order to calculate the leading-order term of the lateral diffusivities of the fluid tracer.

As a result of its encounters with the other two spheres, the fluid tracer in a statistically homogeneous suspension suffers a series of random displace-

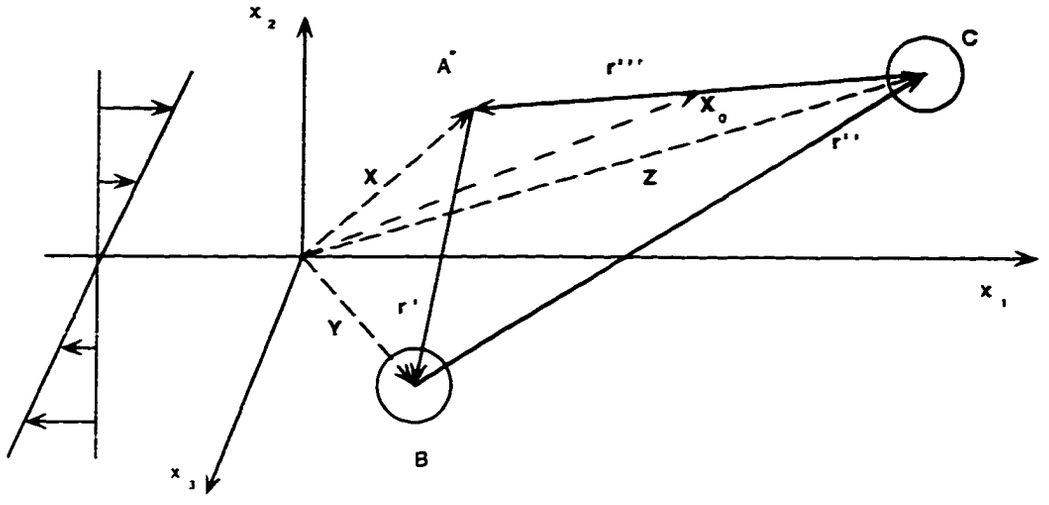

Figure 2.1: Coordinates used in chapter 2.

ment with zero mean. In a dilute suspension, these encounters can be regarded as statistically independent and thus the displacements of the fluid tracer in the lateral direction can be treated as a self-diffusive process with the diffusion coefficients D_2^* and D_3^* being defined as

$$D_j^* \equiv \lim_{T\to\infty} \frac{1}{2T} \sum_{k=1}^{N} \left(\Delta X_j^{(k)}\right)^2, \tag{2.2}$$

where $\Delta X_j^{(k)}$ refers to the displacement of the fluid tracer in the j-direction ($j = 2, 3$) resulting from its kth encounter with two spheres and N is the total number of such encounters within the time interval T.

Obviously, both the values of $\Delta X_j^{(k)}$ and the rate of encounters are determined by the initial positions of the two spheres, once the probability distribution of the initial configurations is known. Thus, as shown below, for statistically homogeneous suspensions at steady state, the expression for D_j^* given above can be reduced to an integral of the contributions over all the possible initial positions of the two spheres, which is more convenient to evaluate than the summation in (2.2).

Before analyzing the different types of possible initial configurations of the spheres, we note that, in order for an encounter to create a significant permanent lateral displacement $\Delta X_j^{(k)}$, the fluid tracer and the two spheres must all be reasonably close to each other during a certain period of time. Otherwise, the fluid tracer will interact separately with the two spheres and therefore will not suffer a permanent lateral displacement. Thus, we consider only those initial configurations where, at some time during their encounter, the spheres and the fluid tracer happen to lie within a cubic 'collision box' of dimensions $(2l)^3$. Later on, we shall show that the contribution to D_j^* in Eq. (2.2) due to the encounters which take place outside of the collision box (i.e. such that the fluid tracer and the two spheres are never present within the collision box at the same time) tends to zero as $l \longrightarrow \infty$. Therefore, the integration over the initial configurations tends to a constant value that can be determined numerically, without the need of introducing a renormalization as often happens with other calculations involving the effective properties of

suspensions.

Now, prior to the encounter, the initial positions of spheres B and C will belong to one of the following three categories:

i) both spheres B and C are far away from the fluid tracer;

ii) the fluid tracer A* orbits around one of the spheres as long as the other sphere is far away;

iii) the fluid tracer A* together with the spheres B and C form a permanent triplet.

First, consider case *i*), where initially the fluid tracer A* is located at the origin while spheres B and C can be either on the left or on the right side of the collision box. But, by virtue of the symmetry of the particle distribution about the origin, we only need to consider the case where the sphere B, chosen as the sphere which first crosses the boundary of the box, enters from the left side at $t = 0$.

Now, when we calculate the contribution of this case to the diffusion coefficient in (2.2), we consider all possible initial positions of spheres B and C, such that A*, B and C find themselves inside the collision box at some stage during the course of their encounter. The loci of these initial positions of B and C form two domains W^B and W^C, which can be determined by first neglecting the interactions among the spheres, so that B and C can be assumed to move with the velocity of the ambient flow. Then, obviously, $\mathbf{Y}^{(0)}$, which refers to the initial position of B, can only lie on the upper

half of the left surface of the box. We denote this domain by W_0^B: $\{-l \leq Y_3^{(0)} \leq l, \quad 0 \leq Y_2^{(0)} \leq l\}$. Accordingly, since B stays inside the box from $t = 0$ to $t = 2l/Y_2^{(0)}$, the possible initial position of C, $\mathbf{Z}^{(0)}$, must lie within that part of the fluid which flows into the box during that period of time. This domain W_0^C has the shape of two wedges, one of which is given by $\{-l \leq Z_3^{(0)} \leq l, \quad 0 \leq Z_2^{(0)} \leq l, \quad -l - 2lZ_2^{(0)}/Y_2^{(0)} \leq Z_1^{(0)} \leq -l\}$ while the other is that generated by rotating the wedge depicted above about the axis x_3 by an angle π (see Fig.2.2).

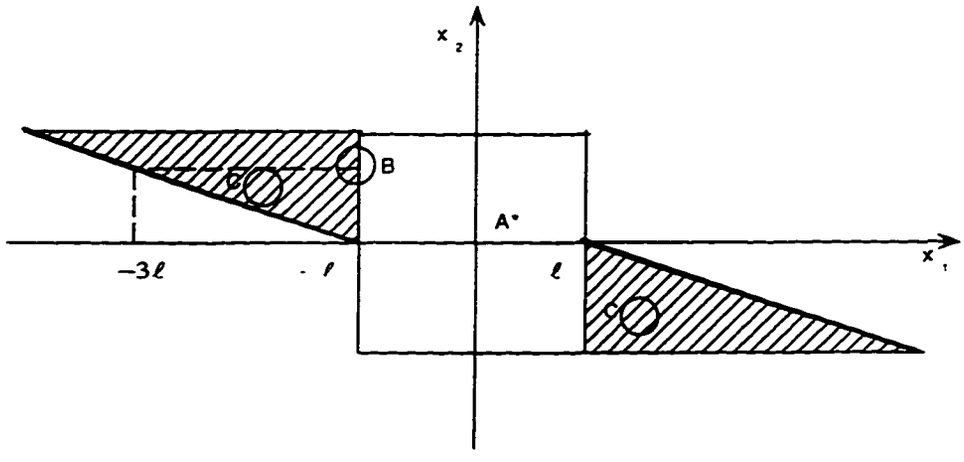

Figure 2.2: The integration domains W_0^B and W_0^C, within the plane $x_3 = 0$.

In arriving at the above estimate, all hydrodynamic interactions among

the spheres and the fluid tracer were neglected, but obviously these interactions will alter the domains only slightly. First of all, the time needed for sphere B to pass through the collision box will be slightly different from that estimated above by an amount that can be evaluated exactly through a direct numerical calculation of its trajectory. Secondly, when the interactions between B and C are considered, one needs to take into account the possibility that, initially, B could be located on the lower half of the left surface of the collision box, i.e., even when $Y_2^{(0)} < 0$, B could still end up moving from left to right in certain cases. This happens for example, when B and C form a permanent doublet when left alone in the ambient flow, provided that the midpoint between B and C lies above the plane $x_2 = 0$. The real domain W^B is therefore slightly larger than the estimate W_0^B and its exact shape can be determined via the solution of the pair sphere trajectories (Batchelor & Green, 1972a). These considerations can be extended to W^C.

Next, we consider the rate at which a pair of spheres B and C enters the collision box, with B initially lying in the surface element $dY_2^{(0)}dY_3^{(0)}$ and C within the volume element $dZ_1^{(0)}dZ_2^{(0)}dZ_3^{(0)}$. Now, the rate at which B enters the box is given by $nV_1^B dY_2^{(0)}dY_3^{(0)}|_{Y_1^{(0)}=-l}$, with n denoting the number of spheres per unit volume and V_1^B the velocity of B along the $\mathbf{e}_1$-direction, while the probability of finding C within the volume element $dZ_1^{(0)}dZ_2^{(0)}dZ_3^{(0)}$ inside the domain W^C is $np(\mathbf{r}_{BC})dZ_1^{(0)}dZ_2^{(0)}dZ_3^{(0)}$, where $p(\mathbf{r}_{BC})$ is the pair distribution function. When only two-sphere interactions are considered, $p(\mathbf{r})$

equals the function $q(r)$ of Batchelor & Green (1972b) if $\mathbf{r}$ lies outside the region of closed trajectories, and is indeterminate when it lies inside. In §6, we shall show that our final results are very insensitive to the specific form of $p(\mathbf{r})$ which is assumed to apply in the region of closed trajectories.

Finally, the contribution of case *i*) to the sum in (2.2) is given by

$$D_j^{*\prime} = n^2 \int_{W^B} \int_{W^C} p(\mathbf{r}_{BC})(\Delta X_j^*)^2 V_1^{(B)} dY_2^{(0)} dY_3^{(0)} dZ_1^{(0)} dZ_2^{(0)} dZ_3^{(0)}, \qquad (2.3)$$

where ΔX_j^* is the net displacement of A* resulting from its encounter with B and C initially lying within the elements $dY_2^{(0)}dY_3^{(0)}$ and $dZ_1^{(0)}dZ_2^{(0)}dZ_3^{(0)}$, respectively.

For case *ii*), we label as C the sphere around which, A* would orbit indefinitely in the absence of another particle. Now, in most cases C will be close to A*, so that, for large enough l, we can take $p(\mathbf{r}_{BC}) = 1$. The contribution of case *ii*) to the sum (2.2) is then given by

$$D_j^{*\prime\prime} = n^2 \int_{W_0^B} \int_{A^*,C \text{ bound}} (\Delta X_j^*)^2 V_1^{(B)} dY_2^{(0)} dY_3^{(0)} dZ_1^{(0)} dZ_2^{(0)} dZ_3^{(0)}. \qquad (2.4)$$

Here though, before the encounter, X_j changes periodically with time and its average value equals that of the position of the center of C. Moreover, since for dilute suspensions, B is located initially very far from the pair, the net displacement of A* occurs on a time scale much larger than that required for the pair to complete one revolution. In addition, we note that the periodic motion of the tracer particle A* around C does not, by itself, contribute to the diffusion process. Hence, to be consistent with (2.2), and given that

the initial location of B is also random, we take this average value of A* orbiting about C before the encounter as the initial position of A*. After the encounter, the initially-bound A* can either continue orbiting around C or be displaced out of the region of closed trajectories. In the former case, we take the average value of X_j, which is the same as the position of the center of the sphere around which it orbits, as the final position of A*. Now, as any two-sphere interactions do not lead to a permanent lateral displacement of the spheres, the net displacement of A* in this case will be zero. So, the only possible contribution to $D_j^{*''}$ comes from those cases for which A* is displaced out of the region of closed trajectories around C.

Finally, for case *iii*), where A*, B and C form a permanent triplet, the net lateral displacement of A* is zero as a consequence of the reversibility of the creeping flow equations and the symmetry of the ambient flow. Therefore this case does not contribute to the sum (2.2), so that we obtain

$$D_j^* = D_j^{*'} + D_j^{*''}. \tag{2.5}$$

In the same way, we can also define a monolayer diffusivity by assuming that the fluid tracer together with the centers of the other two spheres are confined on the same plane of shear. Obviously, all the trajectories of the fluid tracer and the particle centers will remain on that plane, due to symmetry. In this case, the diffusivity of the tracer is given by

$$\bar{D}_2^* = \bar{D}_2^{*'} + \bar{D}_2^{*''}. \tag{2.6}$$

with

$$\bar{D}_2^{*\prime} = \bar{n}^2 \int_{\bar{W}^B} \int_{\bar{W}^C} \bar{p}(\mathbf{r}_{BC})(\Delta\bar{X}_2)^2 V_1^{(B)} dZ_1^{(0)} dZ_2^{(0)} dY_2^{(0)} \tag{2.7}$$

and

$$\bar{D}_2^{*\prime\prime} = \bar{n}^2 \int_{\bar{W}^B} \int_{A^*,C \text{ bound}} (\Delta\bar{X}_2)^2 V_1^{(B)} dZ_1^{(0)} dZ_2^{(0)} dY_2^{(0)}. \tag{2.8}$$

Here $\bar{n}$ denotes the number of spheres per unit area on the plane, and

$$\bar{p}(r) = \frac{1}{1-A} exp \int_r^\infty \frac{2(B-A)}{r(1-A)} dr$$

is the probability density for a monolayer of particles, as obtained by adopting to the two-dimensional case Batchelor & Green's (1972b) analysis for $p(r)$, with the functions $A(r)$ and $B(r)$ given by Batchelor & Green (1972a).

Similar expressions for the self-diffusivity D_j and the monolayer self-diffusivity $\bar{D}_2$ of a test sphere A can be written, with the fluid tracer A* replaced by the test sphere A. It should be noted though that, in computing the contribution to D_j'' for bound pairs, c.f. (2.4), account should be taken of the fact that, as a result of its interaction with particle B, the doublet A-C will now suffer a net lateral displacement in contrast to the case when A is replaced by the fluid point A*.

3. The velocity of a fluid tracer in the presence of two spheres

Since the liquid tracer diffusivity depends on the lateral displacement of the fluid tracer for any given initial positions of the spheres B and C at

time $t = 0$ [see eq.(2.2)], we need to obtain the fluid velocity field in the vicinity of two spheres undergoing a simple shear flow, together with the velocities of the two spheres themselves. Now, while the latter are given in Batchelor & Green (1972), the fluid velocity can be determined through a far field expansion when the fluid point and the spheres are all far apart, and by Lamb's series expansion when they are close.

The far field expression of the fluid velocity was determined using the method of reflections, which we carried out up to and including terms of $O(1/\bar{r}^7)$, with $\bar{r}$ denoting the typical distance between the two spheres or that between the liquid tracer and one of the spheres. Therefore, the velocity of A* can be written as

$$\mathbf{V}^{(A^*)} = \mathbf{U}(\mathbf{X}) + \mathbf{V}_{B\to A^*} + \mathbf{V}_{C\to A^*} + \mathbf{V}_{B\to C\to A^*} + \mathbf{V}_{C\to B\to A^*} + O(\frac{1}{\bar{r}^8}), \quad (2.9)$$

where the subscripts denote the sequences of reflections. A direct calculation yields the following explicit expression:

$$\begin{aligned}
\mathbf{V}^{(A^*)} = \mathbf{U}(\mathbf{X}) &+ \mathbf{r}' \cdot \mathbf{E} \cdot [A^*(r')\frac{\mathbf{r}'\mathbf{r}'}{r'^2} + B^*(r')(\mathbf{I} - \frac{\mathbf{r}'\mathbf{r}'}{r'^2})] \\
&- \mathbf{r}''' \cdot \mathbf{E} \cdot [A^*(r''')\frac{\mathbf{r}'''\mathbf{r}'''}{r'''^2} + B^*(r''')(\mathbf{I} - \frac{\mathbf{r}'''\mathbf{r}'''}{r'''^2})] \\
&+ \frac{1}{2}\mathbf{F}(\mathbf{r}''') : \{\nabla\mathbf{F}(\mathbf{r}'') : \mathbf{E} + [\nabla\mathbf{F}(\mathbf{r}'') : \mathbf{E}]^T\} \\
&+ \frac{1}{20}\mathbf{F}(\mathbf{r}''') : \nabla^2\{\nabla\mathbf{F}(\mathbf{r}'') : \mathbf{E} + [\nabla\mathbf{F}(\mathbf{r}'') : \mathbf{E}]^T\} \\
&+ \frac{7}{24}(\mathbf{r}'''\nabla\nabla\nabla(\frac{1}{r'''})) \vdots \mathbf{G}(\mathbf{r}'') - \frac{1}{8}\nabla\nabla(\frac{1}{r'''}) : \mathbf{G}(\mathbf{r}'') \\
&+ \frac{5}{12}\mathbf{G}(\mathbf{r}'') : (\nabla\nabla(\frac{1}{r'''})) - \frac{1}{12}(\nabla\nabla(\frac{1}{r'''})) \cdot [\mathbf{I} : \mathbf{G}(\mathbf{r}'')]
\end{aligned}$$

$$-\frac{1}{2}\mathbf{F}(\mathbf{r}') : \{\nabla\mathbf{F}(\mathbf{r}'') : \mathbf{E} + [\nabla\mathbf{F}(\mathbf{r}'') : \mathbf{E}]^T\}$$
$$-\frac{1}{20}\mathbf{F}(\mathbf{r}') : \nabla^2\{\nabla\mathbf{F}(\mathbf{r}'') : \mathbf{E} + [\nabla\mathbf{F}(\mathbf{r}'') : \mathbf{E}]^T\}$$
$$-\frac{7}{24}(\mathbf{r}'\nabla\nabla\nabla(\frac{1}{r'})) : \mathbf{G}(\mathbf{r}'') + \frac{1}{8}\nabla\nabla(\frac{1}{r'}) : \mathbf{G}(\mathbf{r}'')$$
$$-\frac{5}{12}\mathbf{G}(\mathbf{r}'') : (\nabla\nabla(\frac{1}{r'})) + \frac{1}{12}(\nabla\nabla(\frac{1}{r'})) \cdot [\mathbf{I} : \mathbf{G}(\mathbf{r}'')] + O(\frac{1}{r^8}), \tag{2.10}$$

where $\mathbf{r}' = \mathbf{Y} - \mathbf{X}$, $\mathbf{r}'' = \mathbf{Z} - \mathbf{Y}$ and $\mathbf{r}''' = \mathbf{X} - \mathbf{Z}$ are the particle relative position vectors, $\mathbf{E} = (\mathbf{e}_1\mathbf{e}_2 + \mathbf{e}_2\mathbf{e}_1)/2$ is the rate-of-strain tensor of the ambient flow, while $A^*(r)$ and $B^*(r)$ are the scalar functions:

$$A^*(r) = \frac{5}{2r^3} - \frac{3}{2r^5}, \quad B^*(r) = \frac{1}{r^5}, \tag{2.11}$$

and the functions $\mathbf{F}(\mathbf{r})$ and $\mathbf{G}(\mathbf{r})$ are the third order tensors:

$$\mathbf{F}(\mathbf{r}) = -\frac{5}{6}\mathbf{r}\nabla\nabla\frac{1}{r} - \frac{1}{6}\nabla\nabla\nabla\frac{1}{r}, \quad \mathbf{G}(\mathbf{r}) = \frac{1}{2}\nabla\nabla\mathbf{F}(\mathbf{r}) : \mathbf{E}. \tag{2.12}$$

When A*, B and C are not all far apart, we used Lamb's series expansion to determine the velocity of the liquid tracer together with the results of Yoon & Kim (1987), who determined the strengths of the singularities (i.e. the coefficients in Lamb's expression) at the center of two spheres moving in pure straining fluid flows. From these coefficients we constructed a general expression for the fluid velocity, noting that the motion of a fluid point near two arbitrarily oriented spheres in a simple shear flow can be decomposed into a uniform translation, a rigid body rotation and a pure straining flow with rate of strain tensor $\mathbf{E} = (\mathbf{e}_1\mathbf{e}_2 + \mathbf{e}_2\mathbf{e}_1)/2$. Now, the contributions from

the first two parts are obvious and that from the third part is determined by transforming the old reference frame into a new one, say O', in such a way that the centers of B and C lie on the $\mathbf{e}'_3$-axis and are symmetric with respect to the new origin, with $\mathbf{e}'_2 = \mathbf{e}_3 \times \mathbf{e}'_3/|\mathbf{e}_3 \times \mathbf{e}'_3|$, and $\mathbf{e}'_1 = \mathbf{e}'_2 \times \mathbf{e}'_3$.

But, as pointed out by Kim & Karrila (1991), the rate of strain tensor $\mathbf{E}$, in the new coordinate frame, can be expressed as a linear combination of $\mathbf{E}^{(1)'} = \frac{1}{2}\mathbf{e}'_1\mathbf{e}'_1 + \frac{1}{2}\mathbf{e}'_2\mathbf{e}'_2 - \mathbf{e}'_3\mathbf{e}'_3$, $\mathbf{E}^{(2)'} = \mathbf{e}'_2\mathbf{e}'_3 + \mathbf{e}'_3\mathbf{e}'_2$, $\mathbf{E}^{(3)'} = \mathbf{e}'_1\mathbf{e}'_2 + \mathbf{e}'_2\mathbf{e}'_1$, $\mathbf{E}^{(4)'} = \mathbf{e}'_1\mathbf{e}'_3 + \mathbf{e}'_3\mathbf{e}'_1$, and $\mathbf{E}^{(5)'} = \mathbf{e}'_1\mathbf{e}'_1 - \mathbf{e}'_2\mathbf{e}'_2$ [1]. So, our problem reduces to that of determining the fluid velocity $\mathbf{v}^{(k)'}$ due to the presence of two spheres in an unperturbed flow field having constant shear rates $\mathbf{E}^{(k)'}$, with $k = 1$ to 5. Now, the cases $k = 1$, 2 and 3 are exactly the same as the three subproblems solved by Yoon & Kim (1987), while the last two cases can be easily reduced to the second and third, respectively, by appropriate coordinate transformations, namely, $\mathbf{v}^{(4)'}(x'_1, x'_2, x'_3) = \mathbf{v}^{(2)'}(-x'_2, x'_1, x'_3)$, and $\mathbf{v}^{(5)'}(x'_1, x'_2, x'_3) = \mathbf{v}^{(3)'}(\frac{1}{\sqrt{2}}(x'_1 - x'_2), \frac{1}{\sqrt{2}}(x'_1 + x'_2), x'_3)$.

Thus, by combining all these contributions, we found a series expression for the velocity of the liquid tracer for any given position of the fluid tracer and of the spheres B and C. Unfortunately, this series expansion converges very slowly when the spheres are close to each other ($r_{BC} - 2 < 0.01$) and the fluid tracer is close to the surface of one of the spheres or to both of them. Therefore, since during their motion the two spheres can get very close to

[1] This decomposition is consistent with the fact that any traceless rate of strain tensor has five independent components.

each other, special care must be taken for these cases.

First, we noted that in order to keep the computation time within reasonable limits, we had to truncate Lamb's expansion after 100 terms. In this case, the truncated series begins to lose its accuracy at distances smaller than 0.01 from the particle surface. Moreover, when the fluid point was placed on the particle surface, its velocity relative to that of the surface, as computed by the series solution, was found to be non-negligible, unless many more terms in Lamb's expansion were retained. This is an important point not only because a small error in the determination of the fluid velocity field could change significantly the final lateral position of the liquid tracer, but also because it could cause the liquid tracer to penetrate the solid sphere, thereby terminating the computation. But, when the liquid tracer is close to only one of the spheres, the leading term of its tangential and normal velocities relative to those of the surface of the sphere are obviously linear and quadratic in the distance from the surface, respectively. We then determined the corresponding local proportionality coefficients in the expressions for the tangential and normal velocity components referred to above, from the accurate velocity field at a distance 0.01 radii away from the surface, which was calculated via the 100-term Lamb's expansion and the known velocity of the surface of the sphere (Yoon & Kim, 1987). Thus, the velocity of any fluid point in this small region could be easily computed accurately to leading order.

Conversely, when the liquid tracer lies in the gap between two almost-touching spheres, we used the lubrication approximation to determine its velocity for the three subproblems corresponding to $\mathbf{E}^{(1)}$, $\mathbf{E}^{(2)}$ and $\mathbf{E}^{(3)}$ defined above. In the first subproblem the two spheres move along their centerline with known opposite velocities and thus the velocity of the fluid point in the gap is the same as that between two squeezing spheres in a fluid which is at rest at infinity. In the second subproblem, the spheres move normal to their centerline with known translational and angular velocities, which can be treated separately. The velocity of the fluid point in the gap in these cases can be determined using the velocity expressions in the lubrication approximation. In the third subproblem, the spheres remain stationary and the velocity of the fluid point is negligible, at least to the same order of approximation as in the above two cases. Thus combining the results of the three subproblems, we were able to determine accurately, to leading order in the gap distance, the velocity of the fluid point within the gap separating the two spheres.

In both cases, our approximate fluid velocities were found to differ by less than 0.2% from the results that were obtained using the truncated series expression with more terms retained.

4. The interaction of three spheres

For any set of initial positions of spheres B and C, the lateral displacement ΔX_j of the test sphere A was determined by following the trajectories of A, B and C. This required the evaluation of the velocities of the spheres at a very large number of points, which forced us to use a method that is somewhat simpler than those employed by previous investigators (Van Saarloos & Mazur, 1982, 1983, Kim, 1987, Hassonjee et al., 1991, and Cichocki et al., 1994), specifically the method of reflections when all the spheres are far apart from each other, and an asymptotic expression when two of the spheres are close to each other.

In the first case, the reflections were carried out up to and including terms of $O(1/\bar{r}^7)$, with $\bar{r}$ denoting the typical distance between any two spheres. Therefore, the velocity of A can be written as

$$\begin{aligned}\mathbf{V}^{(A)} = \mathbf{U}(\mathbf{X}) + \mathbf{V}_{B\to A} + \mathbf{V}_{C\to A} + \mathbf{V}_{A\to C\to A} + \mathbf{V}_{A\to B\to A} \\ + \mathbf{V}_{B\to C\to A} + \mathbf{V}_{C\to B\to A} + O(\frac{1}{\bar{r}^8}).\end{aligned} \tag{2.13}$$

The velocities of B and C can be obtained from (2.13) by just shifting the labels. A direct calculation yields the following explicit expression:

$$\begin{aligned}\mathbf{V}^{(A)} = \mathbf{U}(\mathbf{X}) + \frac{1}{2}\mathbf{r}' \cdot \mathbf{E} \cdot [A(r')\frac{\mathbf{r}'\mathbf{r}'}{r'^2} + B(r')(\mathbf{I} - \frac{\mathbf{r}'\mathbf{r}'}{r'^2})] \\ -\frac{1}{2}\mathbf{r}''' \cdot \mathbf{E} \cdot [A(r''')\frac{\mathbf{r}'''\mathbf{r}'''}{r'''^2} + B(r''')(\mathbf{I} - \frac{\mathbf{r}'''\mathbf{r}'''}{r'''^2})] \\ +\frac{1}{2}[\mathbf{F}(\mathbf{r}''') + \frac{1}{6}\nabla^2\mathbf{F}(\mathbf{r}''')] : \{\nabla\mathbf{F}(\mathbf{r}'') : \mathbf{E} + [\nabla\mathbf{F}(\mathbf{r}'') : \mathbf{E}]^T\}\end{aligned}$$

$$
\begin{aligned}
&+\frac{1}{20}\mathbf{F}(\mathbf{r}''') : \nabla^2\{\nabla\mathbf{F}(\mathbf{r}'') : \mathbf{E} + [\nabla\mathbf{F}(\mathbf{r}'') : \mathbf{E}]^T\} \\
&+\frac{7}{24}(\mathbf{r}'''\nabla\nabla\nabla(\frac{1}{r'''})) \vdots \mathbf{G}(\mathbf{r}'') - \frac{1}{8}\nabla\nabla(\frac{1}{r'''}) : \mathbf{G}(\mathbf{r}'') \\
&+\frac{5}{12}\mathbf{G}(\mathbf{r}'') : (\nabla\nabla(\frac{1}{r'''})) - \frac{1}{12}(\nabla\nabla(\frac{1}{r'''})) \cdot [\mathbf{I} : \mathbf{G}(\mathbf{r}'')] \\
&-\frac{1}{2}[\mathbf{F}(\mathbf{r}') + \frac{1}{6}\nabla^2\mathbf{F}(\mathbf{r}')] : \{\nabla\mathbf{F}(\mathbf{r}'') : \mathbf{E} + [\nabla\mathbf{F}(\mathbf{r}'') : \mathbf{E}]^T\} \\
&-\frac{1}{20}\mathbf{F}(\mathbf{r}') : \nabla^2\{\nabla\mathbf{F}(\mathbf{r}'') : \mathbf{E} + [\nabla\mathbf{F}(\mathbf{r}'') : \mathbf{E}]^T\} \\
&-\frac{7}{24}(\mathbf{r}'\nabla\nabla\nabla(\frac{1}{r'})) \vdots \mathbf{G}(\mathbf{r}'') + \frac{1}{8}\nabla\nabla(\frac{1}{r'}) : \mathbf{G}(\mathbf{r}'') \\
&-\frac{5}{12}\mathbf{G}(\mathbf{r}'') : (\nabla\nabla(\frac{1}{r'})) + \frac{1}{12}(\nabla\nabla(\frac{1}{r'})) \cdot [\mathbf{I} : \mathbf{G}(\mathbf{r}'')] + O(\frac{1}{r^8}),
\end{aligned}
\tag{2.14}
$$

where the tensors $\mathbf{F}$ and $\mathbf{G}$ are given by (2.12) and

$$
A(r) = \frac{5}{r^3} - \frac{8}{r^5} + \frac{25}{r^6} - \frac{35}{r^8} + O(\frac{1}{r^9}), \quad B(r) = \frac{16}{3r^5} + \frac{10}{3r^8} + O(\frac{1}{r^9}), \tag{2.15}
$$

from Da Cunha & Hinch (1996).

By applying equations (2.14) and (2.15) to the case $\mathbf{X} = (0, 0, 0)$, $\mathbf{Y} = (2\sqrt{3}, 0, 2)$ and $\mathbf{Z} = (2\sqrt{3}, 2, 0)$, we found that the sphere velocities thereby obtained differed from those of the full numerical solution of Hassonjee et al.(1991) by less than 0.4% relative to their respective speeds.

In the second case, when two of the spheres, say A and C, are close to each other while the third one, say B, is far away, we first expressed the disturbance of the fluid velocity field $\mathbf{u}$ at a point $\mathbf{x}$ due to the presence of B as

$$
\mathbf{u} = \mathbf{F}(\mathbf{r}) : \mathbf{E}, \tag{2.16}
$$

where $\mathbf{r} = \mathbf{x} - \mathbf{Y}$. The above was then expanded about the midpoint of A and C as

$$\mathbf{u}(\mathbf{x}) = \mathbf{u}(\mathbf{x}_0) + \mathbf{E}' \cdot (\mathbf{x} - \mathbf{x}_0) + \frac{1}{2}\mathbf{\Omega}' \times (\mathbf{x} - \mathbf{x}_0) + ..., \qquad (2.17)$$

where $\mathbf{x}_0 = (\mathbf{X} + \mathbf{Z})/2$, (see Fig.2.1), while

$$\mathbf{\Omega}' = \frac{1}{2}\nabla \times \mathbf{u}|_{\mathbf{x}_0}, \quad \mathbf{E}' = \frac{1}{2}[\nabla \mathbf{u} + (\nabla \mathbf{u})^T]|_{\mathbf{x}_0}. \qquad (2.18)$$

Accordingly, up to and including terms of $O(1/r^3)$, A and C can be viewed as being immersed in a linear flow field with rate-of-strain tensor $\mathbf{E} + \mathbf{E}'$ and angular velocity of solid-body rotation $\mathbf{\Omega} + \mathbf{\Omega}'$, so that the velocities of A and C are given by

$$\mathbf{V}^{(A)} = \mathbf{U}(\mathbf{x}_0) + \mathbf{u}(\mathbf{x}_0 - \mathbf{Y}) - \frac{1}{2}\mathbf{r}''' \cdot (\mathbf{E} + \mathbf{E}') \cdot [A(r''')\frac{\mathbf{r}'''\mathbf{r}'''}{r'''^2} + B(r''')(\mathbf{I} - \frac{\mathbf{r}'''\mathbf{r}'''}{r'''^2})] + \frac{1}{2}(\mathbf{\Omega} + \mathbf{\Omega}') \times \mathbf{r}''' \qquad (2.19)$$

and

$$\mathbf{V}^{(C)} = \mathbf{U}(\mathbf{x}_0) + \mathbf{u}(\mathbf{x}_0 - \mathbf{Y}) + \frac{1}{2}\mathbf{r}''' \cdot (\mathbf{E} + \mathbf{E}') \cdot [A(r''')\frac{\mathbf{r}'''\mathbf{r}'''}{r'''^2} + B(r''')(\mathbf{I} - \frac{\mathbf{r}'''\mathbf{r}'''}{r'''^2})] - \frac{1}{2}(\mathbf{\Omega} + \mathbf{\Omega}') \times \mathbf{r}''' \qquad (2.20)$$

where the fuctions $A(r)$ and $B(r)$ are given by Batchelor and Green (1972a). The accuracy of Eqs.(2.19) and (2.20) is discussed in the next section.

Finally, the velocity of B can be evaluated by assuming pairwise additivity, i.e. by neglecting the effect on B of the reflections between A and C.

An important property of equations (2.19) and (2.20) is that, by providing the correct expression for the relative velocities of spheres A and C when they are close to each other, we prevent these two particles from ever overlapping during the course of the numerical calculation of their trajectories.

Finally, when all the three spheres are close together, pairwise additivity was used to determine the velocities of the spheres. Despite of its being a crude approximation, this assumption did not affect the final result of our computation by more than 2%, as discussed in the next Section.

5. The lateral displacement resulting from an encounter

The lateral displacement of a fluid point resulting from its encounter with two incoming spheres can be obtained by integrating the equations for the trajectories

$$\frac{d\mathbf{X}}{dt} = \mathbf{V}^{(A^*)}, \quad \frac{d\mathbf{Y}}{dt} = \mathbf{V}^{(B)}, \quad \frac{d\mathbf{Z}}{dt} = \mathbf{V}^{(C)}, \tag{2.21}$$

together with the initial positions of the spheres at time $t = 0$.

Let us start by considering the case when the three objects do not get too close to one another during their encounter, so that the reflection result (2.14) can be used to determine their trajectories. In this case, an asymptotic expression for ΔX_j is obtained by the method of successive approximations

as

$$\Delta X_j = \int V_j^{(A^*)}(\xi)dt \tag{2.22}$$

with $\xi = (\mathbf{X}, \mathbf{Y}, \mathbf{Z})$ given by

$$\xi = \int \mathbf{V}dt \tag{2.23}$$

and $\mathbf{V} = (\mathbf{V}^{(A^*)}, \mathbf{V}^{(B)}, \mathbf{V}^{(C)})$, where $\mathbf{V}$ and ξ are expanded as $\mathbf{V} = \mathbf{V}^{(0)} + \mathbf{V}^{(1)} + \mathbf{V}^{(2)} + ...$ and $\xi = \xi^{(0)} + \xi^{(1)} + \xi^{(2)} + ...$ with $\mathbf{V}^{(0)}, \mathbf{V}^{(1)}$ etc. denoting the successive terms of different order in $1/\bar{r}$ in (2.14). At zeroth order, all interactions between the spheres and the fluid particle are neglected, i.e. $\mathbf{V}^{(0)} = \mathbf{U}$, so that the trajectories are just the unperturbed streamlines, with no lateral displacement. Next, considering that $\mathbf{V}^{(1)} \sim O(1/\bar{r}^2)$ and $\mathbf{V}^{(2)} \sim O(1/\bar{r}^4)$, where $\bar{r}$ is the typical distance between the spheres during their encounter, we find that again $\Delta X_j = 0$ due to left-right symmetry of $\mathbf{V}^{(1)}(\xi^{(0)})$ and $\mathbf{V}^{(2)}(\xi^{(0)})$.

Therefore, the leading term in the lateral displacement ΔX_j is $O(1/\bar{r}^5)$ and is due to both $\mathbf{V}^{(1)}(\xi^{(0)} + \xi^{(1)})$ and $\mathbf{V}^{(3)}(\xi^{(0)})$.

Comparison of the $O(1/\bar{r}^5)$ leading term of the lateral displacement ΔX_j, as obtained from this asymptotic analysis, with the results of direct numerical integration showed excellent agreement for all initial configurations of the spheres as long as the distances between any two spheres and those between the fluid particle and the spheres were $O(1)$ or larger.

For the case where the three objects are not always far apart from one another, equations (2.21) were integrated numerically using a fourth-order

Runge-Kutta scheme.

A similar approach was used to determine the lateral displacement of a test sphere. In particular, the method of successive approximations can also be used to determine the lateral displacement of the test sphere with the result that the leading term in the far field asymptotic form is found to be also of order $O(1/\bar{r}^5)$. As an example, we plot, in Fig.2.3, the displacement of A due to an encounter such that the trajectories of A, B and C pass through the points $(0,0,0)$, $(0,3d,4d)$ and $(2d,2d,2d)$ respectively, where $d \geq 1$. It is seen that the agreement between the two sets of calculations is excellent even when the distances between the three objects during their encounter are of $O(1)$.

The numerical results for the displacement ΔX_j using the far field expansion (2.13) for the velocity of the particles and those obtained by truncating the expansion to order $O(1/r^5)$ were also compared and were found to differ by less than 5%. The difference could be positive or negative depending on the initial configurations. Specifically, for the trajectory passing through the configuration A(0,0,0), B(-3,1.5,0) and C(-6,2,0), ΔX_2 was to increase by 4% if the expansion (2.13) was truncated at $O(1/r^5)$.

At this point, a brief discussion is in order about the time step used to determine the particle trajectories. First of all, in addition to using a base time step, we also used a smaller one (i.e. one fifth of the base time step) when the three objects were close ($\bar{r} < 3$) and a larger one (i.e. four times

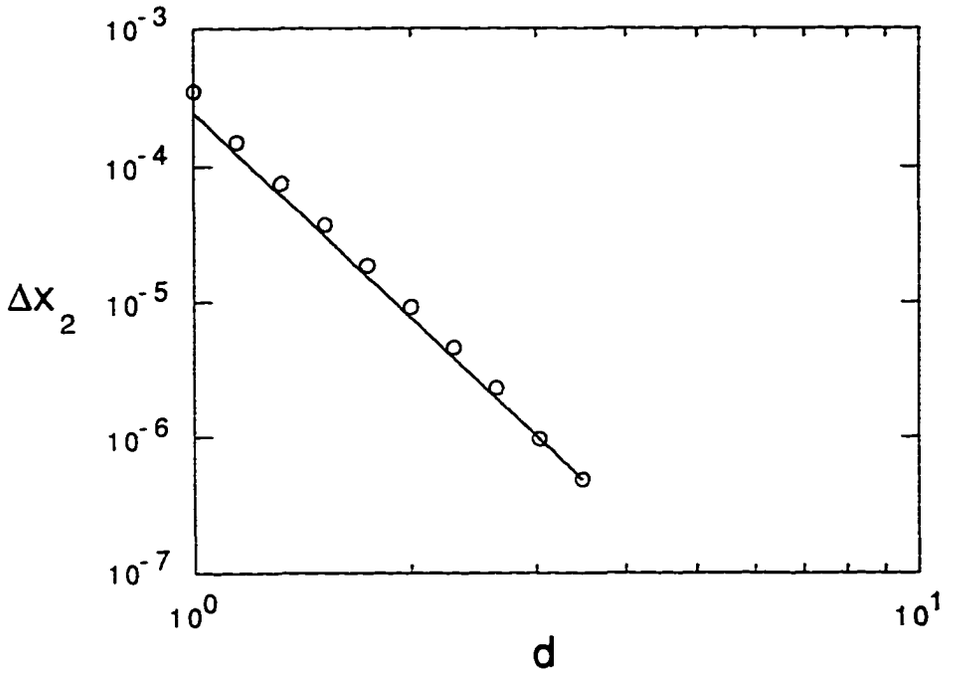

Figure 2.3: Displacement ΔX_2 of the test sphere due to encounters, when spheres A, B and C pass through the points (0, 0, 0), (0, 3d, 4d) and (2d, 2d, 2d), respectively, as a function of d. o numerical results; — asymptotic results using the far field expansion as described following Equation (2.15).

the base time step) when they were far apart ($\bar{r} > 20$). In addition, in order to determine the value of the base time step, we studied the trajectories of a closed pair of spheres and showed that when the base time step equaled 0.2, the spheres returned to their initial positions to within a 10^{-2} approximation after completing 10 revolutions. Therefore, as the times involved in our collision were always shorter than that of this example, we concluded that 0.2 is a safe choice for our base time step.

In the computation of the net transverse displacement, ΔX_j, of the tracer particle for each given initial configuration of the spheres B and C, we must

also calculate the forward and backward particle trajectories, from $t = 0$ to $t = +\infty$ and from $t = 0$ to $t = -\infty$, respectively. Therefore, in our numerical integrations, we defined a cut-off distance L such that, whenever the distance between the tracer and either B or C became larger than L, the effect of this far away sphere could be neglected, while that of the other sphere could easily be accounted for in terms of two-body interactions. But, since ΔX_j is the difference between the forward and backward displacements and is usually much smaller in magnitude than either of them, L must be large enough, such that the cutoff error is small not only compared to the forward and backward displacements, but also compared to the net displacement ΔX_j. In fact, L can be estimated in terms of the error ϵ, say, in the net displacement due to interactions that take place outside the cutoff region. Thus, by considering that the transverse velocity component of the test sphere is of $O(1/r^3)$ and then integrating outside the cutoff region, we found that $L \sim O(1/\sqrt{\epsilon})$. This point will be discussed further in detail in §6.2.

A few typical trajectories are plotted in Fig.2.4, where the centers of all the three spheres remain within the plane $x_3 = 0$. In particular, we wish to note that a bound pair of spheres was found to break up as a result of its interaction with a third sphere only very rarely, which is consistent with the fact that this can happen only when the relative positions of the spheres comprising the doublet are displaced out of the region of closed trajectories. Also, we observed that even in the most extreme cases, no particle overlap-

ping occurred during the computation of the particle trajectories, thereby confirming that Equations (2.19) and (2.20) indeed account for the correct lubrication force among the spheres.

To better illustrate the salient features of these encounters, $(\Delta X_2)^2$ is plotted as a function of Y_2 in Fig.2.5 for the initial configuration $\mathbf{X} = (0, 0, 0)$, $\mathbf{Y} = (-3, Y_2, 0)$ and $\mathbf{Z} = (-6, 2, 0)$. The existence of several peaks and zeroes in this curve is a general feature of the integrand in the expressions for the diffusion coefficients, which greatly increased the difficulty in obtaining accurate numerical values for the corresponding integrals. The zeros correspond to these initial configurations, for which the trajectories of A, B and C are symmetric with respect to a plane perpendicular to the $\mathbf{e}_1$-axis. For example, in the case where A, B and C happen to lie on the same plane perpendicular to the $\mathbf{e}_1$-axis at a certain instant of time, the trajectories of A, B and C are then symmetric with respect to that plane, due to the reversibility of the Stokes equations, and hence such encounters do not lead to a net lateral displacement of A. As another example, when B and C happen to lie on the same line parallel to the $\mathbf{e}_1$-axis while A lies on the plane passing through the midpoint of B and C and perpendicular to the $\mathbf{e}_1$-axis, then the trajectories are again symmetric with a zero lateral net displacement for A.

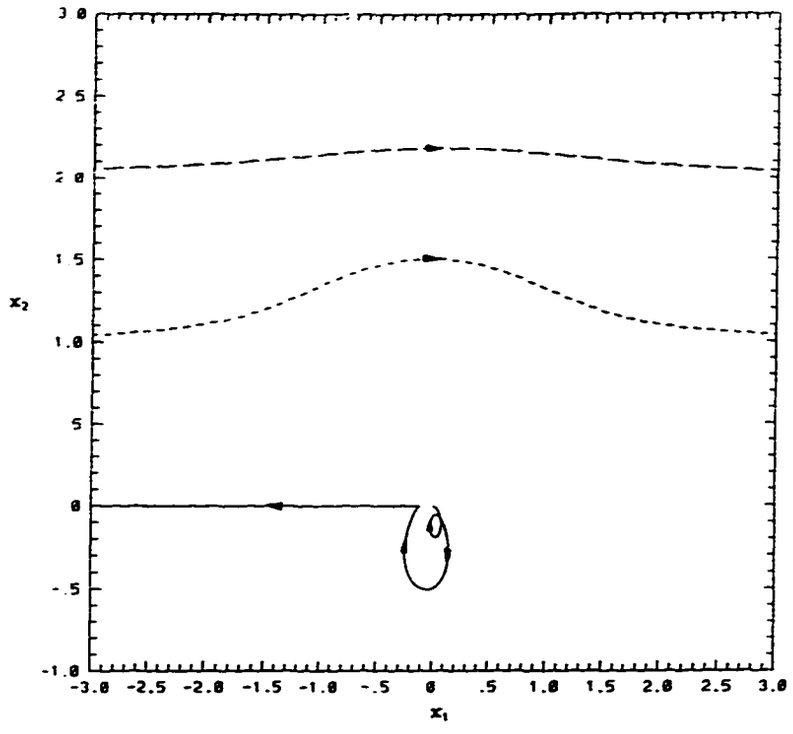

Fig.2.4a

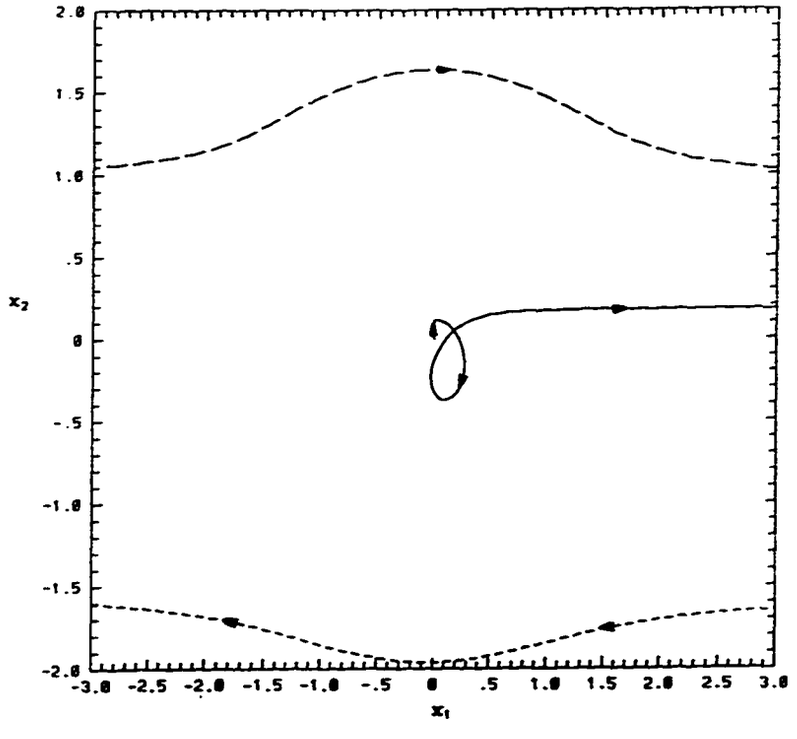

Fig.2.4b

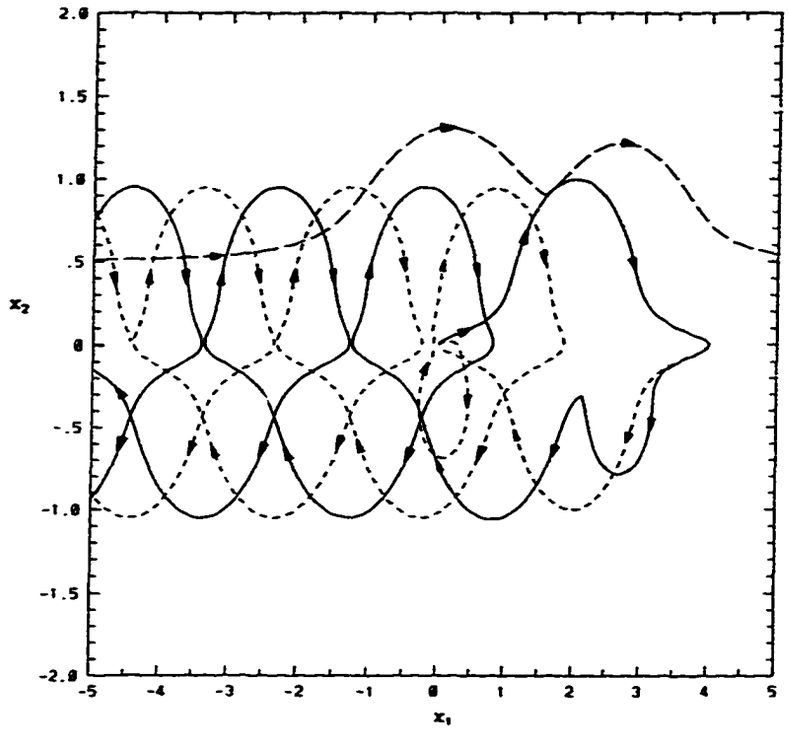

Fig.2.4c

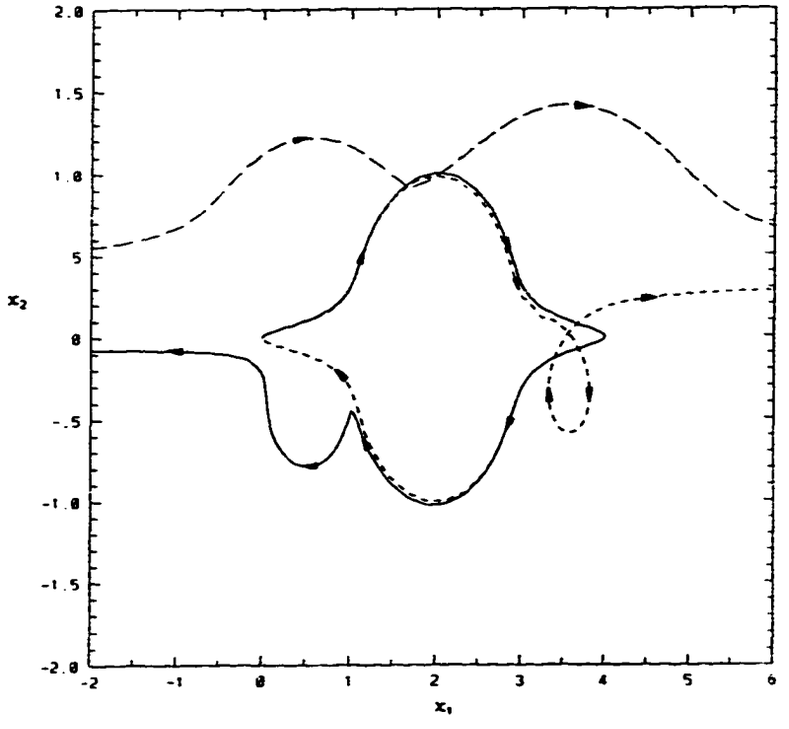

Fig.2.4d

Figure 2.4: Typical trajectories of spheres A (—), B (— — —) and C (- - - - - -), when their centers remain along the plane $x_3 = 0$. a) B and C come from infinity on the same side and interact with A, when $\mathbf{X}^{(0)} = (0, 0, 0)$, $\mathbf{Y}^{(0)} = (-30, 2, 0)$ and $\mathbf{Z}^{(0)} = (-20, 1, 0)$; b) B and C come from infinity on the different sides and interact with A; when $\mathbf{X}^{(0)} = (0, 0, 0)$, $\mathbf{Y}^{(0)} = (-30, -1.6, 0)$ and $\mathbf{Z}^{(0)} = (-20, 1, 0)$; c) A and C orbit around each other initially and remain bound after interacting with B, when $\mathbf{X}^{(0)} = (0, 0, 0)$, $\mathbf{Y}^{(0)} = (-28, 0.5, 0)$ and $\mathbf{Z}^{(0)} = (4, 0, 0)$; d) A and C orbit around each other initially and break up after interacting with B, when $\mathbf{X}^{(0)} = (0, 0, 0)$, $\mathbf{Y}^{(0)} = (-33, 0.5, 0)$ and $\mathbf{Z}^{(0)} = (4, 0, 0)$.

6. The determination of the diffusion coefficients

Finally, we turn to the task of calculating the integrals (2.3), (2.4), (2.7), (2.8) and their counterparts for the particle diffusivities, and thereby determine all the diffusion coefficients defined in §2. Before doing this, we wish to show, however, that the integrals converge as the size of the collision box $l \longrightarrow \infty$, so that they can be evaluated using a large but finite collision box without having to resort to a renormalization.

6.1. The convergency of the integrals

First, let us consider the integral (2.3) when all the variables Y_2, Y_3, Z_1, Z_2 and Z_3 together with r_{BC} are of $O(\bar{r})$, where $\bar{r} \gg 1$. In this case, we have seen (see §4) that ΔX_j is of $O(1/\bar{r}^5)$, so that the integral in (2.3) converges as the size of the collision box $l \longrightarrow \infty$, and the error, i.e. the neglected contribution from encounters that take place outside the collision box, is of

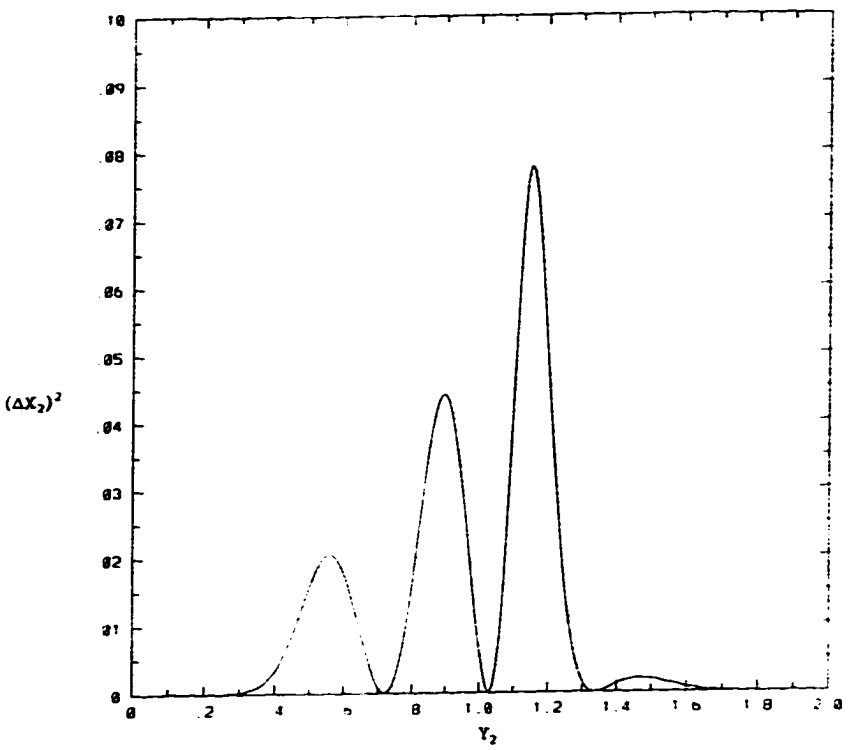

Figure 2.5: An illustration of the dependence of $(\Delta X_2)^2$ on Y_2, assuming that the initial configuration of A*, B and C is $\mathbf{X}^{(0)} = (0, 0.0)$, $\mathbf{Y}^{(0)} = (-3, Y_2, 0)$ and $\mathbf{Z}^{(0)} = (-6, 2, 0)$, respectively.

$O(1/l^4)$. Another contribution to the integral in (2.3) comes from the case where Y_2 and Y_3 are of $O(1)$, while the variables Z_1, Z_2 and Z_3 are of $O(\bar{r})$, with $\bar{r} \gg 1$. Here, since B is moving slowly near the x_1-axis, the leading-order effect of C on $\mathbf{V}^{(A^*)}$ is the $O(1/\bar{r}^2)$-term disturbance in the far field expansion, which, however, does not contribute directly to the lateral displacement of A*, due to its left-right symmetry. But, this disturbance is reflected by B to A* and contributes an $O(1/\bar{r}^3)$-term to ΔX_j. So, this contribution to the

integrand of (2.3) is of $O(1/\bar{r}^6)$ and its integral converges as the size of the collision box $l \longrightarrow \infty$, with the error vanishing as $1/l^3$. A similar result is obtained when Y_2 and Y_3 are of $O(\bar{r})$, while $r_{BC} \sim O(1)$, that is when B and C are close to each other and far from the $\mathbf{e}_1$-axis.

The integral (2.4) can be considered in the same way. Here, since Z_1, Z_2 and Z_3 are of $O(1)$, while Y_1 and Y_2 are of $O(\bar{r})$, the displacement ΔX_j is of $O(1/\bar{r}^3)$, the integrand in (2.4) is of $O(1/\bar{r}^5)$ and the integral converges as $l \longrightarrow \infty$, with the error vanishing as $1/l^3$.

Since, obviously, the integrals (2.7) and (2.8) converge even faster than (2.3) and (2.4), respectively, we can safely conclude that the fluid transverse diffusivities are determined via a series of integrals that converge as the dimension of the collision box $l \longrightarrow \infty$. The same arguments can be applied to the corresponding expressions for the particle diffusivities.

Finally, as described below, all the integrals were evaluated numerically over the domains discussed in §2 by applying a Gaussian-type scheme in order to minimize the number of trajectories that had to be computed.

6.2. The monolayer fluid and particle diffusivities

We started by computing the integral (2.7) for the monolayer diffusivity of the fluid tracer A*, which requires less computational time, so that we could easily study the consequences of the various changes of the computational parameters such as the number of mesh points needed in evaluating the integrals, the time step for the trajectory integration, the size of the box l

and the cut-off distance L.

As was described in §2, the integral (2.7) was evaluated fold by fold with respect to, in sequence, Z_1, Z_2 and Y_2. The first fold integration, i.e. that with respect to Z_1, was performed for different fixed values of Z_2 at a given Y_2 and with different numbers of mesh points, using a 6-point Gaussian quadrature and taking into account that the integrand has several peaks and zeroes, as mentioned in the last Section (see fig.5). In order to quantify the sensitivity of the integral to the number of mesh points, we compared the values of the integral as obtained using 24 and 48 mesh points, and found that the difference between the two sets was within 1% in this typical case.

As concerns the integration with respect to Z_2, it turned out, again, that the difference between using 24 mesh points and 48 mesh points was within 1%. In addition, it appeared that most of the contribution to the final fold of integration, i.e. that with respect to Y_2, comes from the interval $0 < Y_2 < 1.5$ and that the integrand has only one peak with respect to Y_2. Therefore, we integrated with respect to Y_2 by distributing 12 mesh points in the interval $0 < Y_2 < 1.5$ and 6 in the interval $1.5 < Y_2 < 4$, and then verified that the results of the integration were within 1% of those obtained using twice as many mesh points.

Now, we turn to the values of l and L. The size of the box l was set equal to 4; a decrease from 4 to 3.5 was found to alter the final result by only 0.3%. As for the cut-off distance L, we used $L = 2000$, and verified

that the results of the integration were within 1% of those obtained using $L = 1000$. On the other hand, when $L < 100$, the results strongly depend on L. A simple estimate can help explaining why L must be so large. Since the error in the diffusion coefficient resulting from a small uncertainty ϵ, say, in the net lateral displacement of the tracer is $O(\epsilon l^4)$, by requiring that this error must be less than 1%, we find that $\epsilon \sim O(10^{-6})$. Therefore since L is proportional to $1/\sqrt{\epsilon}$ (see §5), we find that $L \sim O(10^3)$, in agreement with our numerical estimate.

Similarly, we evaluated the integral (2.8) and obtained for the monolayer diffusivity of a fluid tracer $\bar{D}_2^* = 0.067\bar{c}^2$.

As a further check of the above result, we doubled all the number of mesh points used in the three folds of our integrations and found that the first two significant digits in the coefficient of diffusivity remained unchanged. In addition, an increase of the basic time step from 0.2 to 0.4 was found to alter the final result by less than 0.1%.

In the computations referred above, we assumed that the expression for $\bar{p}(\mathbf{r})$ is valid both outside and inside the region of closed trajectories, corresponding to the case where a well mixed suspension is first sheared in a pure straining flow and then is subjected to a simple shear flow. On comparing this value of $\bar{D}_2^*$ with that obtained by letting $\bar{p}(\mathbf{r}) = 1$ (i.e. a well-mixed suspension) within the region of closed streamlines, we found that the two results were only 0.2% apart, thereby showing that the value of $\bar{D}_2^*$ is insensi-

tive to the choice of the pair distribution function within the region of closed trajectories.

We now turn to the monolayer diffusivity of a test sphere. As we discussed in §4, this case is fundamentally different from that of the fluid diffusivity since, unlike the fluid velocity, which is known exactly, the velocity of a test sphere in the vicinity of two other spheres is known only approximately. First, let us examine the case when either B or C are close to A, while the other sphere is far. Here, the sphere velocity can be determined approximately using Eq.(2.19) together with the conditions of pairwise additivity applied to the far away particles. In order to test the accuracy of this approximation, we derived similar equations for the velocity of a fluid particle in the vicinity of two spheres and compared the values of the fluid diffusivity $\bar{D}_2^*$, as obtained using this approximate expression, with that using Lamb's 100 term series expansion, finding that the two results were within 1% from each other. Hence, we concluded that Eq.(2.19) can be safely used to determine the lateral displacement of the test particle in the vicinity of one of the other spheres.

Next, let us consider the case where, at some time during their encounter, the three spheres are in close proximity with each other. Here, a simple estimate shows that the contribution to the particle diffusivity due to those initial configurations which lead to such close encounters, is of $O[\epsilon^{0.6}(\Delta X_j)^2]$, where ϵ is the gap between any two close particles while ΔX_j is the typical net

lateral displacement resulting from such close encounters [2]. Therefore, since both ϵ and ΔX_j are of $O(10^{-1})$, we conclude that the error in the diffusion coefficient is less than 1%, even when the tracer velocity is evaluated to an accuracy of $\pm 20\%$, which grossly over-estimates the error introduced by using Eq.(2.19) for such close encounters. As a double check, we also computed numerically the contribution to the diffusivity of the close encounters, finding that it is about 5%, thereby confirming the above estimate.

Finally, we computed the particle monolayer diffusivity for a test sphere using the same number of mesh points, box length, cut-off distance and base time step as for the computation of the liquid monolayer diffusivity and found that $\bar{D}_2 = 0.032\bar{c}^2$.

Particle monolayer diffusivities, as obtained by direct numerical simulations, have been reported by Bossis & Brady (1987) for $\bar{c} = 0.453$ and by Chang & Powell(1994) for $0.12 \leq \bar{c} \leq 0.60$. Although these values of $\bar{c}$ are of course quite outside the range of our analysis, Chang & Powell (1994) reported that, for $\bar{c} \leq 0.25$, $\bar{D}_2$, was found to scale as $\bar{c}^2$ with the constant of proportionality being approximately 0.2, i.e. six times greater than the value 0.032 that resulted from our analysis. One possible reason for this discrepancy may be due the the fact that, in the direct simulations of Chang & Powell (1994) using periodic boundary conditions, all interactions between a particle located at the center of a unit cell and the particles outside the

[2]Here, we have assumed that the pair conditional probability diverges as $\epsilon^{-0.8}$ (Batchelor & Green, 1972b).

periodic cell were neglected, with the distance between the center of the cell and its outer edge being approximately 15. But, when we recomputed $\bar{D}_2$ using our analysis by deliberately neglecting all interactions between any two particles whenever their separation exceeded 15, the coefficient was found to increase by a factor of 4. Thus, it would appear that, at least for vey dilute systems, the cutoff distance used for far field interactions, and therefore the size of the periodic box in numerical simulations, must be quite large. This point, though, deserves further study.

6.3. The fluid and particle diffusivities

The evaluation of (2.3) and (2.4) is almost the same as that of (2.7) and (2.8), except that it is more computationally intensive because of the additional two fold integrations which need to be performed. The plot of the integrand in (2.3) for the last two folds integrations is shown in Fig.2.6 as a function of Y_3 for fixed $Z_3 = 0$. The curve appears to be smooth, decreasing monotonically with respect to Y_3 and the major contribution to the integral comes from the region $Y_3 < 2$. Using 12 mesh points for the last two fold of integrations, we found for the liquid diffusivities $D_2^* = 0.12c^2$ and $D_3^* = 0.004c^2$.

Finally, the diffusivity a test sphere was computed in the same way, finding $D_2 = 0.11c^2$ and $D_3 = 0.005c^2$.

It is surprising that for both liquid and particle diffusivities, the diffusion coefficient in the vorticity or $\mathbf{e}_3$-direction is smaller than that in the direction of the plane of shear, or $\mathbf{e}_2$ direction, by a factor of about 20. This is

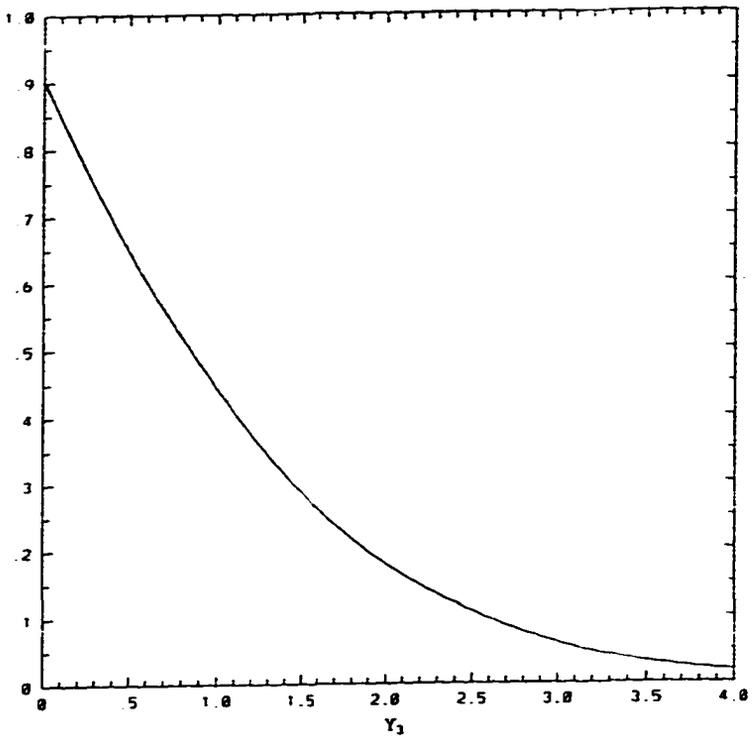

Figure 2.6: An illustration of the dependence of the integrand on Y_3 after the first three fold integrations with respect to Z_1, Z_2 and Y_2 have been performed and keeping $Z_3 = 0$.

consistent with the corresponding results of Da Cunha & Hinch (1996) for the self-diffusivities due to particles roughness, who obtained a corresponding ratio of about 10. Both these results, however, are limited to very dilute suspensions. In contrast, when $0.30 < c < 0.55$, this ratio for the particle diffusivities equals approximately 2/3, as found experimentally by Phan & Leighton (1996).

Recently, Biemfohr, Looby, Biemfohr & Leighton (1995) measured exper-

imentally the effective shear-induced coefficient of self-diffusion in a suspension of monodisperse spheres, finding that, in the dilute limit , the leading order term is of $O(c)$. Clearly, this result cannot apply to perfect spheres and can only be attributed to the non-sphericity and/or roughness of the particles that were employed. As for the coefficient of the next, $O(c^2)$, term, their measurements indicated that it is very small, consistent with our findings.

Chapter 3

The Longitudinal Shear-Induced Gradient Diffusivity of a Monodisperse Dilute Suspension of Spheres

abstract

We present the calculation of the particle volumetric flux of a dilute, neutrally buoyant suspension of spheres in the longituddinal direction under the action of shear when inertia and Brownian effects are negligible, resulting from the effect of an imposed concentration gradient. Using a renormalization technique first employed by Batchelor (1972), we found that the particle volumetric flux is proportional to the concentration gradient through a shear-induced gradient diffusivity, $D_{12} = \alpha c a^2 \gamma$. where a is the radius of the spheres and γ is the bulk shear rate, while $\alpha = -1.20$ for a simple shear flow.

1. Introduction

The shear-induced diffusion of non-Brownian, neutrally buoyant particles has received much attention in recent years, as it is responsible, among other phenomena, for the viscous resuspension of heavy particles under the influence of shear (Leighton & Acrivos, 1986, Acrivos, Mauri & Fan, 1993). The mechanism that is responsible for shear-induced diffusion is well known: particles suspended in a viscous fluid under conditions in which the flow is laminar and the particle Reynolds number is vanishingly small tend to move from high collision rate regions to low. When the shear is constant, a test particle appears to undergo a random walk as it interacts with its neighboring particles, so that the process can be described through a diffusivity proportional to the shear rate γ and the square of the particle radius a. Now, two different diffusion coefficients can be defined, namely self-diffusivity and gradient diffusivity. The former is defined as the temporal growth of the mean square displacement of a randomly chosen tagged particle in a uniform concentration field, while the latter diffusivity is the ratio between mass flux and concentration gradient. These two diffusivities are generally different from each other whenever the suspended particles interact hydrodynamically. For example, self- and gradient diffusivities of Brownian particles in a quiescent dilute suspension are equal to $D_o(1 - 1.83c)$ and $D_o(1 + 1.45c)$, respectively (Batchelor, 1976), where D_o is the particle molecular diffusivity and c is the particle volume fraction.

Shear-induced diffusion was first observed experimentally by Eckstein *et al.* (1977). Later, quantitative measurements were performed by Leighton & Acrivos (1987a,b), who obtained values for the shear-induced self-diffusivity which are in qualitative agreement with the numerical results for monolayer suspensions obtained by Brady and Bossis (1988). Analytically, shear-induced self-diffusion was studied in the dilute limit by Acrivos *et al.* (1992) and by Wang *et al.* (1996), who determined the diffusion coefficient in the direction of the fluid velocity and in that perpendicular to it, respectively.

Despite its obvious importance in practical applications, the phenomenon of shear-induced gradient diffusion appears to have been studied only experimentally, cf. Leighton and Acrivos (1987) or Phillips *et al.* (1992), with the result that no analytical expressions currently exist for the corresponding gradient diffusivity, which have been determined either from fundamental analysis or from *ab initio* computations.

In this chapter, we derived an expression for the shear-induced gradient diffusivity *in the direction of the fluid velocity* in a simple shear flow and for low values of the particle volume fraction c. We studied this, so called, longitudinal diffusivity, because it is much more easily determinable than the transverse diffusivity, which will be considered in chapter 4, as its calculation involves only pairwise particle interactions. To be sure, this coefficient is not very important from a practical standpoint, as any lateral diffusion would lead to differential convection in the streamwise direction which seems likely

to dominate longitudinal diffusion. Nevertheless, as we learned from the case of the self-diffusivity which we considered earlier (Acrivos *et al.*, 1992), solving the longitudinal case can provide us with the theoretical framework for allowing us to determine the subsequent more important coefficient of transverse gradient diffusivity.

2. The basic approach

Consider a dilute, monodisperse suspension of force-free and couple-free spherical particles immersed in a fluid with a concentration gradient along the $\hat{\mathbf{e}}_2$-direction. That means that the probability of finding a particle at location $\mathbf{r} = (x_1, x_2, x_3)$ is equal to $n_o P(\mathbf{r})$, with:

$$P(\mathbf{r}) = 1 + \frac{1}{c_o}\left\langle \frac{\partial c_o}{\partial x_2} \right\rangle x_2. \tag{3.1}$$

Here n is the number density, $\langle \partial c/\partial x_2 \rangle$ is the imposed mean gradient in the $\hat{\mathbf{e}}_2$-direction of the particle volume fraction $c = \frac{4}{3}\pi a^3 n$, and the subscript "o" refers to the value of n and c at the origin. In addition, we assume that the spheres have a radius a small enough that inertia effects can be neglected, while the fluid is incompressible, has viscosity μ, and undergoes a uniform shear flow with velocity $\mathbf{v}(\mathbf{r}) = \gamma x_2 \hat{\mathbf{e}}_1$ along the $\hat{\mathbf{e}}_1$-direction. Clearly, in writing Eq. (3.1) we have supposed that the particle concentration varies over distances which are large relative to a, or, conversely, that $x_2 << l = c_o \langle \partial c/\partial x_2 \rangle^{-1}$.

The goal of this calculation is to find the mean volumetric flux **J** of the suspended particles in terms of the concentration gradient. Now, since the self-diffusion does not contribute to the flux, **J** at the origin is the product of the local concentration c_o times $\langle \mathbf{U} \rangle$, the instantaneous mean velocity of a test sphere at the origin. In turn, $\langle \mathbf{U} \rangle$ is given by:

$$\langle \mathbf{U} \rangle = n_o \int \mathbf{U}(\mathbf{0}|\mathbf{r})\, P(\mathbf{r}|\mathbf{0})\, d^3\mathbf{r} + O(n_o^2), \tag{3.2}$$

where $\mathbf{U}(\mathbf{0}|\mathbf{r})$ is the instantaneous velocity of the test sphere at the origin in the presence of a second sphere at position $\mathbf{r}$, and $P(\mathbf{r}|\mathbf{0})$ denotes the normalized conditional probability density of finding the second sphere at $\mathbf{r}$, provided that the test sphere is located at the origin.

As shown by Batchelor and Green (1972a), the velocity $\mathbf{U}(\mathbf{0}|\mathbf{r})$ may be written as:

$$U_i(\mathbf{0}|\mathbf{r}) = \frac{1}{2} E_{jk} x_k \left[A(r) \frac{x_i x_j}{r^2} + B(r) \left(\delta_{ij} - \frac{x_i x_j}{r^2} \right) \right], \tag{3.3}$$

where $r = |\mathbf{r}|$, $E_{jk} = \frac{1}{2}\gamma(\delta_{j1}\delta_{k2} + \delta_{j2}\delta_{k1})$ is the uniform rate of strain tensor, while $A(r)$ and $B(r)$ are known scalar functions of r, decaying as r^{-3} and r^{-5} as $r \to \infty$, respectively.

Now, the conditional probability $P(\mathbf{r}|\mathbf{0})$ is not known *a priori*, as it is the solution of a two-particle convection problem, and can be determined following the method of Batchelor and Green (1972b). However, we prefer to defer this calculation to the next section, and here focus on describing the general method to solve the integral in (3.2). Accordingly, we assume that

$P(\mathbf{r}|\mathbf{0})$ is a known quantity, referred to as the "unperturbed" conditional probability, $P_\infty(\mathbf{r}|\mathbf{0})$, which is given by:

$$P_\infty(\mathbf{r}|\mathbf{0}) = \left[1 + \frac{1}{c_o}\left\langle\frac{\partial c}{\partial x_2}\right\rangle x_2\right] H(r-2a). \tag{3.4}$$

Substituting Eqs. (3.4) and (3.3) into (3.2) we obtain:

$$\langle U_2\rangle_\infty = \langle U_3\rangle_\infty = O(n_o^2), \tag{3.5}$$

and

$$\langle U_1\rangle_\infty = \alpha\gamma a^2\left\langle\frac{\partial c}{\partial x_2}\right\rangle, \tag{3.6}$$

with

$$\alpha = \frac{3}{16\pi}\int_{\hat{r}\geq 2}\left\{2\left[A(\hat{r}) - B(\hat{r})\right]\left(\frac{\hat{x}_1\hat{x}_2}{\hat{r}}\right)^2 + B(\hat{r})\,\hat{x}_2^2\right\} d^3\hat{\mathbf{r}}, \tag{3.7}$$

where $\hat{\mathbf{r}} = \mathbf{r}/a$, and we have applied the constraint that the average velocity of the test sphere in a uniform suspension must be zero, which is obvious from the macroscopic point of view. Thus, the constant term in $P_\infty(\mathbf{r}|\mathbf{0})$ does not contribute to $\langle U_1\rangle$. The subscript "∞" in the expressions (3.5) and (3.6) for the mean velocities refers to the fact that these are in terms of the unperturbed, and not the "exact", conditional probability distribution. Equations (3.5) indicate that, as expected, the transverse volumetric flux is an $O(c_o^3)$ quantity, and can be determined only if three-particle interactions are taken into account. But since, at this stage, we are only interested in the $O(c_o^2)$-terms of the volumetric flux only, we shall postpone the calculation of $\langle U_2\rangle$ and $\langle U_3\rangle$ to a future date, and concentrate instead in the determination

of $\langle U_1 \rangle$. The main difficulty which must be overcome, however, is that the integral in (3.7) diverges as $\int \hat{r}\, d\hat{r}$, hence we need to resolve the singularity through renormalization.

3. The renormalization procedure

In this section we apply the renormalization procedure developed by Batchelor (1972) to determine $< U_1 >$ in (3.2). First we follow Batchelor (1972) and by applying Faxen's law let

$$\mathbf{U}(\mathbf{0}|\mathbf{r}) = \mathbf{u}(\mathbf{0}|\mathbf{r}) + \left(\frac{a^2}{6}\right) \nabla^2 \mathbf{u}(\mathbf{0}|\mathbf{r}) + \mathbf{W}(\mathbf{0}|\mathbf{r}), \tag{3.8}$$

where $\mathbf{u}(\mathbf{0}|\mathbf{r})$ is the fluid velocity at the origin in the presence of a particle at position $\mathbf{r}$, and $\mathbf{W}(\mathbf{0}|\mathbf{r})$ is a remainder. Then, considering that the constant term, 1, can be subtracted out from $P_\infty(\hat{\mathbf{r}}|\mathbf{0})$ (recall that the mean velocity of the test sphere in a uniform suspension is zero from the constraint mentioned in the last section), we see on substituting (3.8) into (3.2) that $\langle U_1 \rangle_\infty$ equals the sum of three contributions, i.e. $\langle U_1 \rangle_\infty = I_{(1)} + I_{(2)} + I_{(3)}$, with

$$I_{(1)} = n_o a^3 \int_{\hat{r}>2} W_1(\mathbf{0}|\hat{\mathbf{r}})\, [P_\infty(\hat{\mathbf{r}}|\mathbf{0}) - 1]\, d^3\hat{\mathbf{r}}, \tag{3.9}$$

$$I_{(2)} = n_o a^3 \int_{\hat{r}>2} u_1(\mathbf{0}|\hat{\mathbf{r}})\, [P_\infty(\hat{\mathbf{r}}|\mathbf{0}) - 1]\, d^3\hat{\mathbf{r}}, \tag{3.10}$$

$$I_{(3)} = n_o \frac{a^5}{6\mu} \int_{\hat{r}>2} \frac{\partial p}{\partial x_1}(\mathbf{0}|\hat{\mathbf{r}})\, [P_\infty(\hat{\mathbf{r}}|\mathbf{0}) - 1]\, d^3\hat{\mathbf{r}}, \tag{3.11}$$

where in (3.11) p is the fluid pressure, and use has been made of the Stokes equation $\nabla p = \mu \nabla^2 \mathbf{u}$.

The integral in (3.9) is converging, since $W_1(\mathbf{0}|\hat{\mathbf{r}})$ decays like $\hat{r}^{-5}$ as $r \to \infty$. In fact,

$$W_1(\mathbf{0}|\hat{\mathbf{r}}) = \frac{1}{2}\gamma a\left[A'(\hat{r}) - B'(\hat{r})\right]\frac{\hat{x}_1^2\hat{x}_2}{\hat{r}^2} + \frac{1}{4}\gamma a\hat{x}_2 B'(\hat{r}), \tag{3.12}$$

where the functions $A'(\hat{r})$ and $B'(\hat{r})$ include only those terms of $A(\hat{r})$ and $B(\hat{r})$ which decay like $\hat{r}^{-6}$ or faster. Therefore, on substituting (3.12) and (3.4) into (3.9) we obtain:

$$I_{(1)} = \frac{1}{20}\gamma a^2\left\langle\frac{\partial c}{\partial x_2}\right\rangle\int_{\hat{r}>2}\left[2A'(\hat{r}) + 3B'(\hat{r})\right]\hat{r}^4\,d\hat{r}, \tag{3.13}$$

which, after numerical integration gives:

$$I_{(1)} = 1.317\gamma a^2\left\langle\frac{\partial c}{\partial x_2}\right\rangle. \tag{3.14}$$

The other integrals in (3.10) and (3.11) are non-absolutely convergent, and can be renormalized, as was done by Batchelor (1972) for the sedimentation problem, by imposing the constraints that the ensemble average velocity and pressure gradient at the origin both be zero. For a dilute suspension these conditions are equivalent to requiring that

$$\int \mathbf{u}(\mathbf{0}|\hat{\mathbf{r}})\,\left[P(\hat{\mathbf{r}}) - 1\right]\,d^3\hat{\mathbf{r}} = \mathbf{0} \tag{3.15}$$

and

$$\int \nabla p(\mathbf{0}|\hat{\mathbf{r}})\,\left[P(\hat{\mathbf{r}}) - 1\right]\,d^3\hat{\mathbf{r}} = \mathbf{0}, \tag{3.16}$$

where $\mathbf{u}(\mathbf{0}|\hat{\mathbf{r}})$ and $p(\mathbf{0}|\hat{\mathbf{r}})$ are the velocity and pressure at the origin given that a sphere is located at $\hat{\mathbf{r}}$. Note that the integrals in (3.15) and (3.16)

are evaluated over the whole space, including the region $0 \leq \hat{r} \leq 2$. Now, subtracting (3.15) from (3.10) and (3.16) from (3.11), and noting that $P(\hat{\mathbf{r}}) = P_\infty(\hat{\mathbf{r}}|\mathbf{0})$ for $\hat{r} > 2$, [cf. Eqs. (3.1) and (3.4)], we obtain:

$$I_{(2)} = -n_o a^3 \int_{\hat{r}<2} u_1(\mathbf{0}|\hat{\mathbf{r}})\ [P(\hat{\mathbf{r}}) - 1]\ d^3\hat{\mathbf{r}}, \tag{3.17}$$

and

$$I_{(3)} = -n_o \frac{a^5}{6\mu} \int_{\hat{r}<2} \frac{\partial p}{\partial x_1}(\mathbf{0}|\hat{\mathbf{r}})\ [P(\hat{\mathbf{r}}) - 1]\ d^3\hat{\mathbf{r}}. \tag{3.18}$$

First, we calculate $I_{(2)}$ by substituting the expression (3.1) for $P(\mathbf{r})$ into (3.17) and decomposing the resulting integral as the sum

$$I_{(2)} = -I'_{(2)} - I''_{(2)} = -\frac{3a}{4\pi} \left\langle \frac{\partial c}{\partial x_2} \right\rangle \left(\int_{\hat{r}<1} + \int_{1<\hat{r}<2} \right) u_1(\mathbf{0}|\hat{\mathbf{r}})\, \hat{x}_2\, d^3\hat{\mathbf{r}}. \tag{3.19}$$

Now, $I'_{(2)}$ can be easily evaluated considering that, when $\hat{r} < 1$, the origin lies within the particle located at $\hat{\mathbf{r}}$, so that, as the particle rotates with angular velocity $\boldsymbol{\Omega} = -\frac{1}{2}\gamma\hat{\mathbf{e}}_3$, we find: $\mathbf{u}(\hat{\mathbf{r}}) = \gamma a[\hat{x}_2\hat{\mathbf{e}}_1 + \frac{1}{2}\hat{\mathbf{e}}_3 \times \hat{\mathbf{r}}]$. Therefore,

$$I'_{(2)} = \frac{3}{8\pi}\gamma a^2 \left\langle \frac{\partial c}{\partial x_2} \right\rangle \int_{\hat{r}<1} \hat{x}_2^2 d^3\mathbf{r} = \frac{1}{10}\gamma a^2 \left\langle \frac{\partial c}{\partial x_2} \right\rangle. \tag{3.20}$$

The integral $I''_{(2)}$ in (3.19) can also be evaluated easily, since the velocity field at the origin due to the presence of an isolated sphere at $\hat{\mathbf{r}}$ is

$$u_1(\hat{\mathbf{r}}) = \frac{1}{2}\gamma a \left[5\hat{x}_1^2 \hat{x}_2 \left(\hat{r}^{-5} - \hat{r}^{-7} \right) + \hat{x}_2 \hat{r}^{-5} \right]. \tag{3.21}$$

Consequently, on performing the integration (3.19) we find $I''_{(2)} = \frac{3}{4}\gamma a^2 \left\langle \frac{\partial c}{\partial x_2} \right\rangle$, and summing $I'_{(2)}$ and $I''_{(2)}$ we obtain:

$$I_{(2)} = -\frac{17}{20}\gamma a^2 \left\langle \frac{\partial c}{\partial x_2} \right\rangle. \tag{3.22}$$

Finally, we turn to the evaluation of $I_{(3)}$. Substituting (3.1) into (3.18) and applying the divergence theorem we obtain:

$$I_{(3)} = -\frac{a^2}{8\pi\mu}\left\langle \frac{\partial c}{\partial x_2} \right\rangle \int_{\hat{r}=2} \hat{x}_1 \hat{x}_2 \hat{r}^{-1} p(\hat{\mathbf{r}})\, d^2\hat{\mathbf{r}}, \tag{3.23}$$

where $p(\hat{\mathbf{r}}) = -5\mu\gamma\hat{x}_1\hat{x}_2\hat{r}^{-5}$ is the fluid pressure at the origin due to the presence of an isolated sphere at location $\hat{\mathbf{r}}$. Performing the integration (3.23) we find:

$$I_{(3)} = \frac{1}{6}\gamma a^2 \left\langle \frac{\partial c}{\partial x_2} \right\rangle. \tag{3.24}$$

Now, summing (3.14), (3.22) and (3.24), and using the definition of the volumetric flux, we obtain:

$$J_{1\infty} = c_o \langle U_1 \rangle_\infty = \alpha_\infty \gamma a^2 c_o \left\langle \frac{\partial c}{\partial x_2} \right\rangle, \tag{3.25}$$

with $\alpha_\infty = 0.634$. In our calculation we have neglected the influence of the hydrodynamic interactions among three or more particles, so that in Eq. (3.25) all $O(c_o^2)$-terms have been neglected. In addition, as the domain of integration was such that $x_2 << l = c_o \langle \partial c/\partial x_2 \rangle^{-1}$, we have also neglected terms of $O\left(a^2 \langle \partial c/\partial x_2 \rangle^2\right)$.

The calculation for the ensemble average velocity of a test sphere can be easily generalized to the case where the mean concentration gradient is a vector $\langle \nabla c \rangle$ pointing at any direction, and the unperturbed fluid velocity field is a general shear flow, $v_i(\mathbf{r}) = \Gamma_{ij} x_j$. In this case, the antisymmetric part of the velocity gradient tensor, $(\Gamma_{ij} - \Gamma_{ji})/2$, corresponds to a rigid

body rotation of the suspension and does not disturb the test particle at the origin. Therefore, denoting by $E_{ij} = (\Gamma_{ij} + \Gamma_{ji})/2$ the rate of strain tensor, on account of the fact that the test particle velocity is linear in E_{ij}, we obtain

$$U_{i\infty} = 1.267 a^2 E_{ij} \left\langle \frac{\partial c}{\partial x_j} \right\rangle, \tag{3.26}$$

where, as before, terms of $O(c)$ and $O(|a\nabla c|^2)$ have been neglected.

4. The "exact" calculation

In this section we apply the basic approach described in the previous section to calculate "exactly" the longitudinal shear-induced diffusivity. To accomplish that, we need first to evaluate the conditional probability function $P(\mathbf{r}|\mathbf{0})$, which in the previous section had been assumed known *a priori* and equal to its unperturbed expression, $P_\infty(\mathbf{r}|\mathbf{0})$. In fact, the presence of the test sphere at the origin will alter the particle distribution in the vicinity of the origin, and so our assumed unperturbed conditional probability cannot be correct.

In fact, $P(\mathbf{r}|\mathbf{0})$ can be found by repeating the analysis of Batchelor and Green (1972b),

$$P(\mathbf{r}|\mathbf{0}) = q(r)\, P_\infty(\mathbf{r}|\mathbf{0}), \tag{3.27}$$

where $P_\infty(\mathbf{r}|\mathbf{0})$ is defined by (3.4), while $q(r)$, with $q(\infty) = 1$, is given in Eq. (3.9) of Batchelor & Green (1972b) as

$$q(r) = \frac{1}{1-A} \exp\left\{ \int_r^\infty \frac{3(B-A)}{r(1-A)}\, dr \right\}. \tag{3.28}$$

Consequently, $q(r)$ can be calculated explicitly. One finds that $q(r) - 1 \approx \frac{25}{2}\hat{r}^{-6}$ for $\hat{r} \geq 3$, $q(r) \approx 0.234(\hat{r}-2)^{-0.781}\log^{-0.29}(\hat{r}-2)^{-1}$ for $\hat{r} \leq 2.0025$, while for intermediate values of $\hat{r}$, $q(r)$ has been tabulated in Batchelor & Green (1972b).

In deriving Eqs. (3.27) and (3.28) we have assumed that all trajectories originate from infinity. But in the case of simple shear flow some trajectories are closed and occupy a region in space into which open trajectories cannot penetrate. In this region, particle 2 keeps orbiting around the test sphere indefinitely, following a trajectory that is symmetric with respect to the origin (Batchelor & Green, 1972b). Therefore, the mean velocity of the test sphere induced by such periodically orbiting particles is zero, which means that the volume integral in the expression (3.2) for the mean velocity $\langle \mathbf{U} \rangle$ must be evaluated for values of $\mathbf{r}$ laying outside the region of closed trajectories. The same conclusion can be reached by noting that the value of the conditional probability $P(\mathbf{r}|\mathbf{0})$ inside the region of closed trajectories can be determined only if the history of the suspension is known before the particles have begun to move. Now, for any such initial particle distribution, after a long time, as the particles keep orbiting the test sphere, the conditional probability will become symmetric with respect to the (x_1, x_3)- and (x_2, x_3)-planes. Therefore, since the region of closed trajectories is also equally symmetric, the contribution of these orbiting particles to Eq. (3.2) is identically zero.

Now, when the expression (3.27) is substituted into Eq. (3.2) and the

renormalization procedure described in the previous section is applied, finding again that, as expected, the transverse shear-induced velocities are $O(n_o^2)$-quantities,

$$\langle U_2 \rangle = \langle U_3 \rangle = O(n_o^2), \tag{3.29}$$

while the longitudinal velocity is the sum of its "unperturbed" value (3.25) plus two correction terms,

$$\langle U_1 \rangle = \langle U_1 \rangle_\infty + \langle U_1 \rangle' - \langle U_1 \rangle'', \tag{3.30}$$

with

$$\langle U_1 \rangle' = n_o \int_{\hat{r}_{out}} U_1(\mathbf{0}|\hat{\mathbf{r}}) \, [P_\infty(\hat{\mathbf{r}}|\mathbf{0}) - 1] \, [q(r) - 1] \, d^3\hat{\mathbf{r}}, \tag{3.31}$$

$$\langle U_1 \rangle'' = n_o \int_{\hat{r}_{in}} U_1(\mathbf{0}|\hat{\mathbf{r}}) \, [P_\infty(\hat{\mathbf{r}}|\mathbf{0}) - 1] \, d^3\hat{\mathbf{r}}, \tag{3.32}$$

where the integrations are over the volume exterior [Eq. (3.31)] and interior [Eq. (3.32)] to the region of closed trajectories. This region is symmetric with respect to the (x_1, x_3)-plane as well as with respect to the the x_2-axis, and is bounded by the surface (Batchelor & Green, 1972b):

$$|\hat{x}_2| = f(\hat{r}) = \left\{ \frac{1}{F(\hat{r})} \int_{\hat{r}}^{\infty} \frac{B(\hat{r}')}{1 - A(\hat{r}')} F(\hat{r}') \, \hat{r}' \, d\hat{r}' \right\}^{\frac{1}{2}}, \tag{3.33}$$

where

$$F(\hat{r}) = \exp\left\{ -2 \int_{\hat{r}}^{\infty} \frac{A(\xi) - B(\xi)}{1 - A(\xi)} \frac{d\xi}{\xi} \right\}. \tag{3.34}$$

The projection of the surface (3.33) on the (x_1, x_2)-plane represents the trajectory of a particle which, far downstream, lies on the x_1-axis. In view of

Eq. (3.33), such a trajectory has the asymptotic form $\hat{x}_2^2 = \frac{16}{9}\hat{r}^{-3}$ for $\hat{r} >> 1$. Finally, by taking advantage of the axial symmetry of the surface $\hat{x}_2 = f(\hat{r})$, the expression (3.30) becomes, when the imposed flow is a simple shear,

$$\langle U_1 \rangle = (\alpha_\infty + \alpha' - \alpha'')\gamma a^2 \left\langle \frac{\partial c}{\partial x_2} \right\rangle, \tag{3.35}$$

where:

$$\alpha' = \frac{3}{4}\int_{\hat{r}_{min}}^{\infty} \{A(\hat{r})G_{11}(g(\hat{r})) + B(\hat{r})G_{12}(g(\hat{r}))\}[q(\hat{r}) - 1]\,\hat{r}^4\,d\hat{r} \tag{3.36}$$

$$\alpha'' = \frac{3}{4}\int_{2}^{\infty} \{A(\hat{r})G_{21}(g(\hat{r})) + B(\hat{r})G_{22}(g(\hat{r}))\}\,\hat{r}^4\,d\hat{r}, \tag{3.37}$$

where $G_{11}(x) = \frac{1}{3}(1 - x^3) - \frac{1}{5}(1 - x^5)$, $G_{12}(x) = \frac{1}{5}(1 - x^5)$, $G_{21}(x) = \frac{1}{3}x^3 - \frac{1}{5}x^5$ and $G_{22} = \frac{1}{5}x^5$. Here $\hat{r}_{min} = 2 + 4.155 \cdot 10^{-5}$ is the minimum distance from the origin of the surface (3.33), such that $f(\hat{r}_{min}) = \hat{r}_{min}$, while $g(\hat{r}) = f(\hat{r})/\hat{r}$, with $f(\hat{r})$ given by (3.33). On computing the integral in (3.36) and (3.37) we find $\alpha' = 0.613 \pm 0.005$ and $\alpha'' = 0.045 \pm 0.001$, with the uncertainty due to the 1% inaccuracy of the tabulated values of $q(r)$ in Batchelor & Green (1972b). Comparing this result with Eq. (3.25) we see that the use of the exact probability distribution has changed the numerical value of the coefficient α in a significant way. On the other hand, the qualitative feature of our main result has not been altered in that the mean longitudinal velocity of the test sphere has remained proportional to the mean concentration gradient and independent of the local concentration. Finally, for the volumetric flux at the origin $\mathbf{J} = c_o \langle \mathbf{U} \rangle$, we obtain, up to terms of $O(c^2)$ and $O(|a\nabla c|^2)$ that,

in the case of a simple shear flow $\mathbf{v}(\mathbf{r}) = \gamma x_2 \hat{\mathbf{e}}_1$,

$$J_1 = -D_{12}\left\langle \frac{\partial c}{\partial x_2} \right\rangle, \tag{3.38}$$

where

$$D_{12} = \alpha\, \gamma a^2 c_o, \tag{3.39}$$

with $\alpha = -1.20 \pm 0.005$.

The ensemble average velocity of a test sphere in a general shear flow can be calculated following the procedure described in the previous section, finding:

$$\mathbf{U} = -\beta\, a^2 c_o \mathbf{E}\cdot\nabla c, \tag{3.40}$$

with $\beta = 2(\alpha_\infty + \alpha' - \alpha'')$. Now, unlike α_∞, which is a constant, α' and α'' depend on the particular shear flow considered, since this determines the region of closed trajectories constituting the domain of integration in (3.36) and (3.37). For example, as we saw, for simple shear flow, $\alpha' = .613 \pm 0.005$ and $\alpha'' = 0.045 \pm 0.001$, leading to $\beta = 2.40 \pm 0.01$. Another example is when the fluid undergoes pure rigid-body rotation, where all trajectories are closed, so that $\alpha'' = \alpha_\infty$, $\alpha' = 0$ and $\beta = 0$, as expected. Another interesting example is when the fluid undergoes pure straining flow. In this case, all the trajectories of one sphere relative to another originate from infinity and are open; hence $\alpha'' = 0$, while α' in (3.36) is evaluated with $g(\hat{r}) = 0$, with the result that, now, $\alpha' = 0.924$ and $\beta = 3.12 \pm 0.01$.

Perhaps the most important characteristics of the expression (3.39) for the longitudinal gradient diffusivity is that it depends linearly on the local volume fraction, unlike the coefficient of self diffusivity calculated in Acrivos *et al.* (1992) which is proportional to $c \log c$. The reason of this difference is that the coefficient of self-diffusion is proportional to the temporal growth of the mean square displacement of the test sphere, due to its hydrodynamic interactions with the other particles. Now, summing over the contributions of all possible interactions, led to a logarithmically diverging integral. This singularity was due to the very weak but long-lasting interactions between the test sphere and a very slowly moving second sphere, when the latter is at great distances from the origin and close to the (x_1, x_3)-plane. The diverging integral was made finite by allowing for the cut-off due to the occasional presence of another pair of particles.

On the other hand, the calculation of the gradient diffusivity consists in evaluating the *instantaneous* mean velocity of the test sphere immersed in a sheared suspension, due to the effect of an externally imposed particle concentration gradient. In this case, no singularity arises, so that the resulting diffusivity in the direction of the flow is proportional to c.

Chapter 4

Transverse Shear-Induced Gradient Diffusion in a Dilute Suspension of Spheres

abstract

We study the shear-induced gradient-diffusion of particles in an inhomogeneous dilute suspension of neutrally buoyant spherical particles undergoing a simple shearing motion, with all inertia and Brownian motion effects assumed negligible. The flux of particles due to a concentration gradient along the direction of the gradient of the ambient flow is calculated. The expression for the flux involves the average velocity of the particles, which in turn is expressed as an integral over contributions from all possible configurations. The constraints of zero total macroscopic flux is applied to renormalize the nonconvergent integral. The renormalized integral for the case of a monolayer

of particles is evaluated numerically following the scheme of Wang, Mauri & Acrivos (1996), giving for the gradient diffusion coefficient $0.077\gamma a^2 c^2$, where γ is the applied shear rate, a the radius of the spheres and c their aerial fraction.

1. Introduction

The shear-induced diffusion of non-Brownian particles has recently been found to play an important role in many physical processes involving suspensions of particles dispersed in a viscous fluid. In contrast to the Brownian diffusion of particles in a colloidal suspension, which is due to the thermal fluctuations of the interactions between the fluid and the particles, the shear-induced diffusion is due solely to the hydrodynamic interactions among the particles. Although, in principle, the process is deterministic, it can often be described as a diffusion process because of the random nature of the complicated hydrodynamic interactions. This shear induced diffusion leads to a net migration of particles from region of high concentration to region of low and from region of high shear rate to low. This has been shown to affect certain macroscopic properties of suspensions in a major way.

Shear-induced diffusion was first studied experimentally by Eckstein, Bailey & Shapiro (1977), who monitored the motion of a tagged particle within a suspension being sheared in a Couette device. Their technique was refined later by Leighton & Acrivos (1987a,b) who reported experimental values for the lateral diffusion coefficients both within and normal to the plane of shear. Two dimensional numerical simulations by Bossis & Brady (1987) and by Chang & Powell (1994) for the monolayer diffusivity were found to

agree qualitatively with these results. Recently, by considering only two particle interactions, expressions were derived for the coefficient of shear-induced self-diffusion in the direction of the fluid motion (Acrivos, Batchelor, Hinch, Koch & Mauri, 1992) by considering only two particle interactions, and in the transverse directions (Wang, Mauri &Acrivos, 1996) by considering three particle interactions, for a dilute suspension of spheres undergoing a simple shearing motion, while Da Cunha & Hinch (1996) studied the effect of surface roughness on the interaction of two spheres and calculated the coefficients of the self- and gradient-diffusivity in the lateral directions.

Most of the theoretical studies referred to above dealt with the self-diffusion of a test particle in an otherwise homogeneous suspension. Here, we shall examine the gradient diffusion in a dilute suspension of smooth spheres and determine the corresponding gradient diffusion coefficient, which is a key parameter in any constitutive equation which relate the particle flux to non-uniformities in the particle concentration profile.

In the next section, the problem is formulated from both the Eulerian and the Lagrangian points of view. But, since integrals in the corresponding expressions turn out to be divergent, they are renormalized for the monolayer of spheres as shown in §3. The renormalized integrals are then evaluated numerically based on the trajectory computation scheme in Wang et al. (1996).

2. The statement of the problem

Consider a dilute suspension of rigid smooth spheres undergoing a simple shear flow with negligible inertia and Brownian motion effects. If the suspension is inhomogeneous, the average velocity of a test sphere relative to the bulk flow is, in general, not zero. To determine this velocity to leading order in the particle concentration of the particles, we only need to consider three particle interactions. Recall that two particle interactions do not contribute to the drift velocity in the transverse direction owing to the symmetry of the geometry and the reversibility of the governing Stokes equations.

One way of defining the Eulerian average instantenuous velocity, $\mathbf{V}_p^E$, of a test sphere A is by taking the ensemble average of its velocity in the presence of two other spheres B and C, at a certain instant of time $t = t_i$,

$$\mathbf{V}_p^E \equiv \int \mathbf{V}(\mathbf{0}|\mathbf{y},\mathbf{z}) P(\mathbf{y},\mathbf{z}|\mathbf{0}) d^3\mathbf{y} d^3\mathbf{z}, \quad \mathbf{y} \equiv \mathbf{Y} - \mathbf{X}, \quad \mathbf{z} \equiv \mathbf{Z} - \mathbf{X}, \qquad (4.1)$$

where $\mathbf{X}$, $\mathbf{Y}$ and $\mathbf{Z}$ refer to the absolute positions of A, B and C, respectively. Thus, $\mathbf{y}$ and $\mathbf{z}$ are the positions of sphere B and C *relative* to A, while $P(\mathbf{y},\mathbf{z}|\mathbf{0})$ denotes the probability density of finding a second sphere B at $\mathbf{y}$ and third sphere C at $\mathbf{z}$ under the condition that there exists a test sphere at the origin.

It is obvious from conservation of probability that

$$P(\mathbf{y},\mathbf{z}|\mathbf{X}) d^3\mathbf{y} d^3\mathbf{z}|_{t_1} = P(\mathbf{y},\mathbf{z}|\mathbf{X}) d^3\mathbf{y} d^3\mathbf{z}|_{t_2} \qquad (4.2)$$

along any given three-particle trajectory for any instant of time t_1 and t_2.

The probability $P(\mathbf{y},\mathbf{z}|\mathbf{X})$ can then be determined by tracing the volume element $d^3\mathbf{y}d^3\mathbf{z}$ along a trajectory back to $t=-\infty$, where the probability density function for finding any one of the spheres is assumed to be linear in the direction of the gradient of the ambient velocity, $\mathbf{i}_2$, i.e.

$$P^{-\infty}(\mathbf{x}) = n_0 + \frac{dn}{dx_2}x_2 + ..., \tag{4.3}$$

where n_0 is the local average number density of particles. Thus, as the spheres are far apart at far upstream, the probability of the configuration is given by

$$P^{-\infty}(\mathbf{y}^{-\infty},\mathbf{z}^{-\infty}|\mathbf{X}^{-\infty}) = n_0^2[1+\frac{dn}{n_0 dx_2}(y_2^{-\infty}+z_2^{-\infty}+2X_2^{-\infty})+...], \tag{4.4}$$

with

$$X_2^{-\infty} = \int_{t_i}^{-\infty} V_2(\mathbf{X}|\mathbf{y},\mathbf{z})dt \tag{4.5}$$

being the displacement of the test sphere when the element moves along a trajectory from $t=t_i$ to its position at $t=-\infty$.

The integral in (4.1) is taken over the whole six dimensional space. But, first we consider the monolayer case where the motion of all the particles is confined to a plane perpendicular to the direction of the vorticity of the ambient flow, and compute the average velocity of A in the direction of the ambient velocity gradient, $\mathbf{i}_2$. Therefore,

$$V_p^E = \int\int V_2(\mathbf{0}|\mathbf{y},\mathbf{z})P(\mathbf{y},\mathbf{z}|\mathbf{0})dy_1dy_2dz_1dz_2. \tag{4.6}$$

For computational convenience, the above four fold integral is converted to a three fold integral by integrating along the trajectories of the spheres.

It is clear from (4.2) that although the element $dy_1 dy_2 dz_1 dz_2$ changes along a trajectory, the quantity $P(\mathbf{y},\mathbf{z}|\mathbf{X})dy_1 dy_2 dz_1 dz_2$, or because $dy_1 = v_1^B dt_i$, where v_1^B is the component of the velocity of particle B in the direction of the ambient flow, the rate $P(\mathbf{y},\mathbf{z}|\mathbf{X})v_1^B dy_2 dz_1 dz_2$ remains the same and changes only from one trajectory to another. Therefore, since $P(\mathbf{y},\mathbf{z}|\mathbf{X})$ is known at $t = -\infty$, we can convert eq.(4.6) into

$$V_p^E = \int v_1^B(-\infty) dy_2^{-\infty} dz_1^{-\infty} dz_2^{-\infty} \int V_2 P^{-\infty}(\mathbf{y}^{-\infty},\mathbf{z}^{-\infty}|\mathbf{X}^{-\infty}) dt_i$$

where the superscript $-\infty$ denotes the value of the corresponding quantity at $t = -\infty$. To avoid double counting the configurations, we denote as B the sphere which first arrives at a reference plane x_1^r =constant, and the other as C. After substituting (4.4) into the above expression and noting that the uniform distribution term drops out because it does not lead to any net particle migration, (4.6) can be written as

$$V_p^E = n_0 \frac{dn}{dx_2} \int v_1^B(-\infty) dy_2^{-\infty} dz_1^{-\infty} dz_2^{-\infty} \int_{-\infty}^{+\infty} [(y_2^{-\infty} + z_2^{-\infty})V_2 + 2X_2^{-\infty} V_2] dt.$$

Substituting $V_2 = -dX_2^{-\infty}/dt_i$ from eq.(4.5), the second term in the square bracket becomes, on integration with respect to dt_i,

$$2\int_{-\infty}^{+\infty} 2X_2^{-\infty} V_2 dt_i = -2\int_{-\infty}^{+\infty} 2X_2^{-\infty} \frac{dX_2^{-\infty}}{dt_i} = -(\Delta X_2)^2,$$

where ΔX_2, the total displacement of the test sphere due to an encounter with spheres B and C, is given by

$$\Delta X_2 = X_2^{-\infty}(t_i \longrightarrow \infty) = \int_{-\infty}^{+\infty} V_2(\mathbf{X}|\mathbf{y},\mathbf{z}) dt. \qquad (4.7)$$

Thus, the contribution of the second term is related to the self-diffusion coefficient D_p^s and hence the average velocity can be expressed as

$$V_p^E = -\frac{2}{n_0} D_p^S \frac{dn}{dx_2} + n_0 \frac{dn}{dx_2} \int \Delta X_2 (y_2^{-\infty} + z_2^{-\infty}) v_1^B(-\infty) dy_2^{-\infty} dz_1^{-\infty} dz_2^{-\infty} \quad (4.8)$$

where the particle self-diffusivity D_p^S is given by (Wang et al. 1996),

$$D_p^S = \frac{1}{2} n_0^2 \int (\Delta X_2)^2 v_1^B(-\infty) dy_2^{-\infty} dz_1^{-\infty} dz_2^{-\infty}, \quad (4.9)$$

which is of order c^2, with c being the aeral fraction occupied by particle phase. Using (4.8), we recover the expression given by Da Cunha & Hinch (1995) for the flux of particles in a slightly non-uniform dilute suspension of rough spheres which they obtained by considering only two particle interactions.

The integral in (4.7) is not absolutely convergent, as can be seen by noting that $\Delta X_2 \sim O(1/\bar{r}^5)$ for large $|\mathbf{y}|$ and $|\mathbf{z}|$ with $\bar{r}$ being a typical distance between any two of the spheres which participate in the encounter (Wang et al, 1996). This integral can be renormalized by applying the constraint of zero total areal flux in the $\mathbf{i}_2$ direction for the suspension as a whole, i.e.

$$J_p + J_f = 0, \quad (4.10)$$

where J_p and J_f are the areal fluxes for the particle phase and the fluid phase, respectively. They are given by

$$J_p = cV_p^E - D_p^S \frac{dc}{dx_2}$$

and

$$J_f = (1-c)V_f^E - D_f^S \frac{d(1-c)}{dx_2}.$$

where V_f^E and D_f^S are, respectively, the average Eulerian liquid velocity and the liquid self-diffusivity with D_f^S given by

$$D_f^S = \frac{1}{2} n_0^2 \int (\Delta X_2^*)^2 v_1^B(-\infty) dy_2^{-\infty} dz_1^{-\infty} dz_2^{-\infty}, \tag{4.11}$$

From this constraint, we find that $V_f^E \sim O(c^2 dc/dx_2)$, which is of smaller order than the velocity V_p^E given by (4.7). On the other hand, by means of a procedure similar to that used in arriving at (4.8) for V_p^E, we can obtain that

$$V_f^E = -\frac{2}{n_0} D_f^S \frac{dn}{dx_2} + n_0 \frac{dn}{dx_2} \int \Delta X_2^* (y_2^{-\infty} + z_2^{-\infty}) v_1^B(-\infty) dy_2^{-\infty} dz_1^{-\infty} dz_2^{-\infty} \tag{4.12}$$

which is of order cdc/dx_2. In the above, ΔX_2^* denotes the displacement of a fluid point due to its encounter with two spheres B and C. But, since V_f^E must vanish to $O(cdc/dx_2)$, we have that

$$V_p^E = -\frac{2}{n_0}(D_p^S - D_f^S)\frac{dn}{dx_2}$$
$$+n_0 \frac{dn}{dx_2} \int (\Delta X_2 - \Delta X_2^*)(y_2^{-\infty} + z_2^{-\infty}) v_1^B(-\infty) dy_2^{-\infty} dz_1^{-\infty} dz_2^{-\infty}$$
$$+O(c^2 \frac{dc}{dx_2}). \tag{4.13}$$

Since it can be easily shown that the difference $\Delta X_2 - \Delta X_2^*$ is of order smaller than $1/\bar{r}^5$, the integral in the above expression is convergent and can be evaluated numerically.

The expression for V_p^E given by (4.13) can also be obtained more directly starting from the particle flux expression as given by the Fokker-Planck equation

$$J_p = cV_p^L - \frac{d}{dx_2}D_p^S c = cV_p^L - c\frac{dD_p^S}{dx_2}\frac{dc}{dx_2} - D_p^S\frac{dc}{dx_2},$$

with all terms of order $c^2 dc/dx_2$, where V_p^L is the Lagragian particle velocity given by

$$V_p^L = \frac{c}{\pi^2}\frac{dc}{dx_2}\int \Delta X_2(y_2^{-\infty} + z_2^{-\infty})v_1^B dy_2^{-\infty} dz_1^{-\infty} dz_2^{-\infty}.$$

On the other hand, the Lagrangian expression for the fluid flux is

$$J_f = (1-c)V_f^L - (1-c)\frac{dD_p^S}{dc}\frac{dc}{dx_2} - D_p^S\frac{d(1-c)}{dx_2}.$$

But since the second term is $\sim cdc/dx_2$, the requirement that $J_p + J_f = 0$ gives that, to order cdc/dx_2,

$$V_f^L = \frac{c}{\pi^2}\frac{dc}{dx_2}\int \Delta X_2^*(y_2^{-\infty} + z_2^{-\infty})v_1^B dy_2^{-\infty} dz_1^{-\infty} dz_2^{-\infty} = \frac{dD_f^S}{dc}\frac{dc}{dx_2}.$$

Therefore,

$$V_p^E = V_p^L - \frac{dD_p^S}{dc}\frac{dc}{dx_2} = -[\frac{d}{dc}(D_p^S - D_f^S)]\frac{dc}{dx_2}$$

$$+\frac{c}{\pi^2}\frac{dc}{dx_2}\int(\Delta X_2 - \Delta X_2^*)V_1^B(y_2^{-\infty} + z_2^{-\infty})dy_2^{-\infty} dz_1^{-\infty} dz_2^{-\infty},$$

which is the same as (4.13) obtained by the Eulerian description.

3. Numerical results for a monolayer

We can use the same numerical scheme as in chapter 4 to compute the average velocity of a sphere in a monolayer by evaluating the integral in (4.13). However, in view of the fact that the term $\Delta X_2 - \Delta X_2^*$ in the integrand is numerically much smaller than either ΔX_2 or ΔX_2 terms, special care must be taken in evaluating the integral because even a small residue error in either ΔX_2 or ΔX_2^* will lead to a significant numerical uncertainty. After evaluating the integral and using the expressions given by (4.9) and (4.11), for D_p^s and D_p^s, respectively, we find

$$V_p^E = -0.045\gamma a^2 c\frac{dc}{dy},$$

$$V_f^L = \frac{dD_f}{dc}\frac{dc}{dy} = 0.134\gamma a^2 c\frac{dc}{dy},$$

while

$$V_p^L = V_p^E + \frac{dD_p}{dc}\frac{dc}{dy} = +0.019\gamma a^2 c\frac{dc}{dy}.$$

The reason why V_p^L, the Lagrangian average particle velocity is positive, which is counter intuitive, is still not clear.

Finally, we obtain the particle gradient diffusion coefficient for a monolayer of particles

$$D_p^G = 0.077a^2\gamma c^2,$$

which is defined by

$$J_p = cV_p^E - D_p^S\frac{dc}{dx_2} \equiv -D_p^G\frac{dc}{dx_2}. \tag{4.14}$$

Appendices

Appendix A

Sedimentation in a dilute suspension of spheres, renormalization of divergent integrals

In a dilute suspension of identical rigid spheres of radius a, without loss of generality set equal to unity, the particles fall through the liquid due to gravity. Under the assumption of negligible inertia and Brownian motion effects, the average velocity of the particles in a well mixed suspension can be expressed, to leading order in the particle number density n_0, as (Batchelor, 1972),

$$\bar{\mathbf{U}} = \mathbf{U}_0 + n_0 \int_{r \geq 2} [\mathbf{U}(\mathbf{x_0}|\mathbf{x_0} + \mathbf{r}) - \mathbf{U}_0] d^3\mathbf{r}, \qquad \text{(A.1)}$$

where $\mathbf{U}_0$ is the Stokes terminal velocity of an isolated sphere and $\mathbf{U}(\mathbf{x_0}|\mathbf{x_0} + \mathbf{r})$ is the velocity of a test sphere A located at $\mathbf{x_0}$ in an unbounded fluid when

another sphere B is located at $\mathbf{x_0} + \mathbf{r}$.

As is well known, the integral in the expression given above is divergent since $\mathbf{U} - \mathbf{U_0}$ decays as $1/r$ as $r \longrightarrow \infty$. On the other hand, physically, the average sedimentation velocity is obviously finite. Thus, a proper renormalization of the integral is required. Such a renormalization was given by Batchelor (1972). Here a slightly different derivation is presented which, perhaps, might be of interest in a wider context.

The velocity of sphere A in the presence of another sphere B can be written, by Faxen's law, as

$$\mathbf{U} = \mathbf{U_0} + \mathbf{u}(\mathbf{x_0}|\mathbf{x_0} + \mathbf{r}) + \frac{1}{6}\nabla^2\mathbf{u}(\mathbf{x_0}|\mathbf{x_0} + \mathbf{r}) + \mathbf{w}(\mathbf{x_0}|\mathbf{x_0} + \mathbf{r}), \qquad (A.2)$$

where $\mathbf{u}(\mathbf{x_0}|\mathbf{x_0} + \mathbf{r})$ is the velocity disturbance at $\mathbf{x_0}$ due to the motion of a single sphere at $\mathbf{x_0} + \mathbf{r}$, given by

$$\mathbf{u}(\mathbf{x_0}|\mathbf{x_0} + \mathbf{r}) = \mathbf{U_0}(\frac{3}{4r} + \frac{1}{4r^3}) + \mathbf{r}\frac{\mathbf{r}\cdot\mathbf{U_0}}{r^2}(\frac{3}{4r} - \frac{3}{4r^3}).$$

Substituting (A.2) into (A.1) yields

$$\bar{\mathbf{U}} = \mathbf{U_0} + \mathbf{I_1} + \mathbf{I_2} + \mathbf{I_3}, \qquad (A.3)$$

where

$$\mathbf{I_1} = n_0 \int_{r\geq 2} \mathbf{u}(\mathbf{x_0}|\mathbf{x_0} + \mathbf{r}) d^3\mathbf{r}, \qquad (A.4)$$

$$\mathbf{I_2} = n_0 \int_{r\geq 2} \frac{1}{6}\nabla^2\mathbf{u}(\mathbf{x_0}|\mathbf{x_0} + \mathbf{r}) d^3\mathbf{r}, \qquad (A.5)$$

and

$$\mathbf{I_3} = n_0 \int_{r=2}^{\infty} \mathbf{w}(\mathbf{x_0}|\mathbf{x_0} + \mathbf{r}) d^3\mathbf{r}. \qquad (A.6)$$

Since $\mathbf{u}$ is of order $1/r$ and $\nabla^2\mathbf{u}$ is of order $1/r^3$, the integral $\mathbf{I}_1$ and $\mathbf{I}_2$ are divergent, while $\mathbf{I}_3$ is convergent since $\mathbf{w}$ decays as $1/r^4$.

Clearly, in a dilute suspension, $\mathbf{I}_1$ equals the average velocity of the fluid point when the position of sphere B ranges over the infinite domain $r \geq 2$ outside the exclusion region. Hence, $\bar{\mathbf{V}}_f$, the average fluid velocity within the suspension, is given by

$$\bar{\mathbf{V}}_f = \mathbf{I}_1 + n_0 \int_{1\leq r\leq 2} \mathbf{u}(\mathbf{x_0}|\mathbf{x_0}+\mathbf{r}) d^3\mathbf{r} = \mathbf{I}_1 + \frac{9}{2} c\mathbf{U}_c, \tag{A.7}$$

with $c \equiv \frac{4\pi}{3} n_0$ being the volume fraction occupied by the spheres in the suspension.

Thus, the divergent integral $\mathbf{I}_1$ represents physically the average velocity of the fluid outside the exclusion regions around the spheres in a very dilute suspension and is related to the average fluid velocity within the suspension by (A.7). Naturally, this leads to consideration on the volumetric flux balance of the suspension as a whole. On the other hand, we know that the bulk velocity of the suspension on a macroscopic scale is zero relative to the container,

$$(1-c)\bar{\mathbf{V}}_f + c\bar{\mathbf{V}}_p = \mathbf{0}, \tag{A.8}$$

where $\bar{\mathbf{V}}_p$ is the average velocity of the particles. To order c, (A.8) gives

$$\bar{\mathbf{V}}_f = -c\mathbf{U}_0 + O(c^2). \tag{A.9}$$

Thus, the divergent integral $\mathbf{I}_1$ must be renormalized such that the above

constraint is satisfied. Therefore, by (A.7) and (A.9),

$$\mathbf{I}_1 = -\frac{11}{2}c\mathbf{U}_0. \tag{A.10}$$

This is identical to Batchelor's eq.(5.3) and in fact the whole derivation parallels his.

The integral $\mathbf{I}_2$, can be renormalized in a similar way by noting that, in the fluid phase, this term is related to the dynamic pressure disturbance p due to a single sphere by the Stokes equation $\nabla^2\mathbf{u} = \frac{1}{\mu}\nabla p$ (By definition, the dynamic pressure is the difference between the total pressure and the static pressure of the pure fluid). Therefore, aside from the factor $1/6\mu$, $\mathbf{I}_2$ equals the average pressure gradient of the fluid at the point $\mathbf{x}_0$ in the infinite domain $r \geq 2$, outside the exclusion region. Consequently, $\bar{\nabla p}_f$, the average pressure gradient over the whole domain occupied by the fluid phase in the dilute suspension, is given by

$$\bar{\nabla p}_f = 6\mu\mathbf{I}_2 + n_0 \int_{1\leq r\leq 2} \nabla p(\mathbf{x}_0|\mathbf{x}_0 + \mathbf{r}) d^3\mathbf{r} = 6\mu\mathbf{I}_2, \tag{A.11}$$

where the integral is evaluated using

$$p(\mathbf{x}_0 + \mathbf{r}|\mathbf{x}_0) = 3\mu\frac{\mathbf{r}\cdot\mathbf{U}_0}{2r^4}. \tag{A.12}$$

Thus, the integral $\mathbf{I}_2$ is closely related to the average pressure gradient in the fluid phase, which naturally leads to the examination of the bulk pressure gradient in the suspension. On a macroscopic scale, however, the suspension as a whole is akin to a static effective fluid with total pressure gradient

$[\rho_f + c(\rho_p - \rho_f)]\mathbf{g}$, in addition to that of the stagnant pure fluid, where ρ_p and ρ_f are the mass densities of the particles and of the fluid, respectively, and $\mathbf{g}$ is the gravitational acceleration. Thus, we have the constraint

$$(1-c)\bar{\nabla}p_f + c\bar{\nabla}p_p = c(\rho_p - \rho_f)\mathbf{g} = \frac{9}{2}c\mu\mathbf{U}_0, \tag{A.13}$$

where $\bar{\nabla}p_p$ is the average pressure gradient inside the spheres,

$$\bar{\nabla}p_p \equiv \frac{1}{\frac{4}{3}\pi}\int_{r\leq 1} \nabla p(\mathbf{x}_0|\mathbf{x}_0 + \mathbf{r})d^3\mathbf{r}. \tag{A.14}$$

The above can be converted into an integral over the volume inside a fixed sphere. Noting that $\nabla p(\mathbf{x}_0|\mathbf{x}_0 + \mathbf{r})$ depends only on the position of the sphere relative to that of the sample point and is independent of their absolute positions, we obtain

$$\int_{r\leq 1} \nabla p(\mathbf{x}_0|\mathbf{x}_0 + \mathbf{r})d^3\mathbf{r} = \int_{r\leq 1} \nabla p(\mathbf{x}_0 - \mathbf{r}|\mathbf{x}_0)d^3\mathbf{r}, = \int_{r\leq 1} \nabla p(\mathbf{x}_0 + \mathbf{r}|\mathbf{x}_0)d^3\mathbf{r},$$

where account has been taken of the symmetry of the domain of integration.

To evaluate the last integral, which refers to the integral over the position of the sample point $\mathbf{x}_0 + \mathbf{r}$ within the sphere located at $\mathbf{x}_0$, we make use of the divergence theorem and the fact that, on the surface of an isolated sphere translating with velocity $\mathbf{U}_0$, the fluid pressure is given by (A.12). Hence,

$$\int_{r\leq 1} \nabla \mathbf{p}(\mathbf{x}_0|\mathbf{x}_0 + \mathbf{r})d^3\mathbf{r} = 2\pi\mu\mathbf{U}_0, \tag{A.15}$$

and therefore,

$$\bar{\nabla}p_p = \frac{3}{2}\mu\mathbf{U}_0. \tag{A.16}$$

From (A.13) and (A.16), we obtain the constraint

$$\bar{\nabla} p_f = 3c\mu \mathbf{U}_0 + O(c^2), \tag{A.17}$$

so that, on account of (A.11),

$$\mathbf{I}_2 = \frac{1}{2} c\mathbf{U}_0. \tag{A.18}$$

Although this is identical to Batchelor's eq.(5.4), its derivation is somewhat different than his.

Finally, by substituting (A.6), (A.10) and (A.18) into (A.3), we obtain the convergent expression for $\bar{\mathbf{U}}$,

$$\bar{\mathbf{U}} = \mathbf{U}_0 - 5c\mathbf{U}_0 + n_0 \int_{r=2}^{\infty} \mathbf{w}(\mathbf{x}_0|\mathbf{x}_0 + \mathbf{r}) d^3\mathbf{r}. \tag{A.19}$$

In conclusion, by means of the volumetric flux constraint and the pressure gradient constraint given by (A.8) and (A.13), respectively, we were able to renormalize the expression for the average velocity expression (A.1), which yields exactly the same result as given by Batchelor (1972) in his expression (3.14) together with (5.3) and (5.4). The approach, given here, however, might be helpful in finding the relevant constraints for some other renormalization problems.

Appendix B

Renormalization of the transverse gradient diffusivity expression for the three dimensional distribution of spheres

In chapter 4, we were able to renormalize the expression for the average velocity of a test sphere in a monolayer of spheres using the zero bulk flux constraint. For the case of three dimensional distribution of spheres, however, this constraint is not sufficient to yield a convergent expression for the average velocity. Specifically, after applying this constraint to the three dimensional case, the Euler average velocity becomes

$$V_p^E = -\frac{2}{n_0}(D_p^S - D_f^S)\frac{dn}{dx_2}$$

$$+n_0\frac{dn}{dx_2}\int(\Delta X_2 - \Delta X_2^*)(y_2^{-\infty} + z_2^{-\infty})v_1^B(-\infty)dy_2^{-\infty}dy_3^{-\infty}dz_1^{-\infty}dz_2^{-\infty}dz_3^{-\infty}$$

$$+O(c^2\frac{dc}{dx_2}). \tag{B.1}$$

But, since the difference $\Delta X_2 - \Delta X_2^*$ is of order $O(1/\bar{r}^7)$ for large $\bar{r}$, the above expression is still not convergent and an additional renormalization is required. In this appendix, the integral is renormalized by applying the constraint of zero bulk pressure gradient in the suspension.

The $O(1/\bar{r}^7)$ term in $\Delta X_2 - \Delta X_2^*$ for large $\bar{r}$ is due to the difference between the hydrodynamic interaction of a test sphere and that of a fluid tracer with the other two spheres. Specifically, following the reflection method, the velocity disturbance due to an isolated sphere, say B, will be reflected by another sphere C, producing a velocity disturbance $\mathbf{u}'$. This disturbance influences velocity of a test particles, which can be either a test sphere or a fluid tracer. However, the response velocity of a test sphere differs from that of a fluid tracer, according to Faxen's law, by $\frac{1}{6}\nabla^2\mathbf{u}'$. It is the summation of this response velocity difference to the reflected disturbance arising from all the sphere pairs in the suspension that renders the integral in (B.1) divergent. However, this summation is related to the average pressure gradient in the suspension in view of the fact that the difference $\frac{1}{6}\nabla^2\mathbf{u}'$ in the response

velocity is related to the corresponding pressure gradient disturbance by the usual Stokes equation $\mu\nabla^2\mathbf{u}' = \nabla p'$. On the other hand, from a macroscopic point of view, the bulk pressure gradient in the transverse direction must be zero at steady state even with the presence of a concentration gradient in this direction. Now, it is clear that the constraint of zero bulk pressure gradient can be used to remove the non-convergence in the average velocity expression by subtracting the corresponding divergent parts and evaluating the remaining convergent parts (Batchelor, 1972).

The constraint of zero bulk pressure gradient in the velocity gradient direction can be expressed as an ensemble average

$$< \nabla p >_2 = \mathbf{i}_2 \cdot \int \nabla p(\mathbf{Y}, \mathbf{Z}) P(\mathbf{Y}, \mathbf{Z}) d^3\mathbf{Y} d^3\mathbf{Z} = 0, \qquad \text{(B.2)}$$

where ∇p is the pressure gradient at a test point $\mathbf{X}^t$ located at the origin for the configuration of two spheres B and C at $\mathbf{Y}$ and $\mathbf{Z}$ respectively, while $P(\mathbf{Y}, \mathbf{Z})$ denotes the probability density of the configuration. Note that the above integral is taken over all possible configurations as long as the spheres B and C do not overlap, including the configuration where the sample point lies in one of the spheres.

The probability density function P($\mathbf{Y}$,$\mathbf{Z}$) is given by

$$P(\mathbf{Y}, \mathbf{Z}) = P^{-\infty}(\mathbf{Y}^{-\infty}, \mathbf{Z}^{-\infty}) q(|\mathbf{Y} - \mathbf{Z}|) \qquad \text{(B.3)}$$

by noting that the midpoint of the centerline of B and C does not move in the $\mathbf{i}_2$ direction with $q(|\mathbf{Y} - \mathbf{Z}|)$ being the probability factor given by Batchelor

& Green (1972).

Thus, the domain of the above integral can be divided into two parts: one in which the sample point lies outside of the spheres and the other where the sample point lies inside, i.e.

$$< \nabla p >_2 = \mathbf{i}_2 \cdot [\int_{outside} + 2 \int_{inside\ one\ of\ the\ spheres}] \tag{B.4}$$

The first integral

$$I_1 = \mathbf{i}_2 \cdot \int_{outside} \nabla p(\mathbf{Y}, \mathbf{Z}) P(\mathbf{Y}, \mathbf{Z}) d^3\mathbf{Y} d^3\mathbf{Z}, \tag{B.5}$$

is related to the divergent part in the expression (B.1) as mentioned above. It is convenient to use $\mathbf{r} \equiv \mathbf{X}^t - \mathbf{Y}$ and $\mathbf{z} \equiv \mathbf{Z} - \mathbf{Y}$ as variables in the second integral, yielding

$$I_2 = 2\mathbf{i}_2 \cdot \int_{1<r} \nabla p(\mathbf{r}, \mathbf{z}) P(\mathbf{r}, \mathbf{z}) d^3\mathbf{r} d^3\mathbf{z} \tag{B.6}$$

and

$$P(\mathbf{r}, \mathbf{z}) = n_0^2 [1 + \frac{1}{2n_0} \frac{dn}{dx_2} (z_2 - 2r_2) + ...] q(z). \tag{B.7}$$

The integral I_2, which is over the domain inside one of the spheres, say B, can be determined by converting the volume integral into an surface integral by Gauss's theorem, as done for similar problems (Batchelor & Green, 1972).

Substituting (B.7) into the expression for I_2 yields

$$I_2 = n_0 \frac{dn}{dx_2} \mathbf{i}_2 \cdot \int_{z>2} q(z) d^3\mathbf{z} \int_{r<1} (z_2 - 2r_2) \nabla p d^3\mathbf{r}. \tag{B.8}$$

Applying Gauss's theorem to the integral with respect to $d^3\mathbf{r}$ gives

$$I_2 = n_0 \frac{dn}{dx_2} \int_{z>2} q(z) d^3\mathbf{z} [\mathbf{i}_2 \cdot \int_{r=1} (z_2 - 2r_2) p\mathbf{n} dS + 2 \int_{r<1} p d^3\mathbf{r}]. \qquad \text{(B.9)}$$

Obviously, I_2 is independent of the nature of the material inside the sphere B as long as its surface is rigid. So we can use any constitutive relation to determine the volume integral inside B. One convenient choice is to assume that the sphere is made of an infinitely viscous fluid with no surface tension on the interface. For this choice, the pressure field p is a harmonic function without any singularity inside the sphere. Therefore its average over the volume inside the sphere equals the average on the surface of the sphere

$$\frac{1}{\frac{4}{3}\pi} \int_{r\leq 1} p d^3\mathbf{r} = \frac{1}{4\pi} \int_{r=1} p dS. \qquad \text{(B.10)}$$

Thus,

$$I_2 = n_0 \frac{dn}{dx_2} \mathbf{i}_2 \cdot \int_{z>2} q(z) d^3\mathbf{z} \int_{r=1} (\frac{2}{3} + z_2 r_2 - 2r_2^2) p dS \qquad \text{(B.11)}$$

For large z, the leading term for p is due to the reflection by C of the disturbance induced by the presence of B, which is of order $1/z^5$, the above integral is absolutely convergent and can be evaluated numerically.

By the same procedure used to convert (4.6) to (4.8), we can convert (B.5) into

$$I_1 = n_0 \frac{dn}{dx_2} I_{10}$$

$$+ n_0 \frac{dn}{dx_2} \int \Delta X_2' (y_2^{-\infty} + z_2^{-\infty}) v_1^B(-\infty) dy_2^{-\infty} dy_3^{-\infty} dz_1^{-\infty} dz_2^{-\infty} dz_3^{-\infty}, \qquad \text{(B.12)}$$

where

$$\Delta X_2' = \int_{-\infty}^{+\infty} \frac{1}{6}\nabla^2 V_2'(\mathbf{X}|\mathbf{y},\mathbf{z})dt, \tag{B.13}$$

and

$$I_{10} = \int \alpha(y_2^{-\infty} + z_2^{-\infty}) v_1^B(-\infty) dy_2^{-\infty} dy_3^{-\infty} dz_1^{-\infty} dz_2^{-\infty} dz_3^{-\infty}, \tag{B.14}$$

with

$$\alpha = \int_{-\infty}^{+\infty} \frac{1}{6} X_2^{-\infty} \nabla^2 V_2'(\mathbf{X}|\mathbf{y},\mathbf{z})dt. \tag{B.15}$$

$\Delta X_2'$ and α can be computed just as ΔX_2 by integrating along the trajectory for any given initial configurations. The integral in the expression for I_{10} is obviously convergent in view of the fact that $\alpha \sim O(1/\bar{r}^8)$.

The non-convergence of the integral in (B.12) has the same origin as that of the integral in (B.1). Now, we can remove the non-convergent part in (B.1) by the constraint (B.2) together with (B.12), yielding

$$\begin{aligned} V_p^E = &-\frac{2}{n_0}(D_p^S - D_f^S)\frac{dn}{dx_2} - n_0 \frac{dn}{dx_2} I_{10} - I_2/6 \\ &+ n_0 \frac{dn}{dx_2} \int (\Delta X_2 - \Delta X_2^* - \frac{1}{6}\Delta X_2')(y_2^{-\infty} + z_2^{-\infty}) v_1^B(-\infty) \\ &\qquad dy_2^{-\infty} dy_3^{-\infty} dz_1^{-\infty} dz_2^{-\infty} dz_3^{-\infty} \end{aligned} \tag{B.16}$$

The term $\Delta X_2 - \Delta X_2^* - \frac{1}{6}\Delta X_2'$ in the integrand decays faster than $1/\bar{r}^8$, thus, the integral is convergent now.

In conclusion, we can renormalize the average velocity expression by using together the constraints of zero bulk flux and zero bulk pressure gradient and obtain a convergent expression for the Eulerian average velocity which can

be evaluated numerically. This in turn can be used to determine the gradient diffusivity through (4.14). However, we shall leave the numerical evaluation of this integral to future work partially because of the computational intensity involved.

Appendix C

Some further remarks on renormalization of the thermocapillary migration problem

Consider, as in Chaper 1, a space filling bidisperse suspension of spherical bubbles undergoing thermocapillary migration and let $\mathbf{u}_\infty^f$ and ∇T_∞^f be, respectively, the velocity and the temperature gradient at the origin for a given configuration of bubbles. Let us further restrict ourselves to those configurations in which the space enclosed by a sphere of radius a_1 with its center at the origin contains only pure fluid, hence the superscript f. Next, suppose that a bubble of type 1, the so called test bubble, is inserted into the suspension with its center at the origin. In the absence of any thermal or hydrodynamic interactions between the test bubble and all the other bubbles in the suspension, $\overline{\mathbf{U}}_1$, the velocity of this test bubble, averaged over all

the configurations referred to above, will equal the sum of a thermocapillary velocity

$$\frac{a_1}{2\mu}(-\frac{d\gamma}{dT}) < \nabla T^f_\infty >$$

(cf. the comment following equation (1.9)) and $< \mathbf{u}^f_\infty >$, where the brackets denote the ensemble conditional average of the undisturbed temperature gradient at the origin and the undisturbed fluid velocity at the origin. Hence,

$$\overline{\mathbf{U}}_1 = \frac{a_1}{2\mu}(-\frac{d\gamma}{dT}) < \nabla T^f_\infty > + < \mathbf{u}^f_\infty > . \tag{C.1}$$

Similarly,

$$\overline{\mathbf{U}}_2 = \lambda\frac{a_1}{2\mu}(-\frac{d\gamma}{dT}) < \nabla T^f_\infty > + < \mathbf{u}^f_\infty > . \tag{C.2}$$

Now, one of the constraints in the space filling suspension is that

$$\mathbf{H} = (1 - c_1 - c_2) < \nabla T^f > -c_1\overline{\mathbf{S}}_1 - c_2\overline{\mathbf{S}}_2 \tag{C.3}$$

where $\mathbf{H}$ is the applied temperature gradient and $\overline{\mathbf{S}}_1$ and $\overline{\mathbf{S}}_2$ are, respectively, the average thermal dipole strengths of particles 1 and 2 (Jeffrey 1973; Acrivos et al. 1990). In addition, as shown by Jeffrey (1973)

$$c_1\overline{\mathbf{S}}_1 + c_2\overline{\mathbf{S}}_2 = (\frac{k^*}{k} - 1)\mathbf{H} \tag{C.4}$$

where, once again, k^* is the effective thermal conductivity of the suspension and k is the thermal conductivity of the fluid. Consequently,

$$< \nabla T^f_\infty >= \frac{k^*/k}{1 - c_1 - c_2}\mathbf{H} \tag{C.5}$$

where the expression for k^*/k to $O(c^2)$ was derived by Thovert and Acrivos (1989). It should be noted that, although the term $< \nabla T^f >$ in equation $(C.3)$ refers to the unconditional ensemble average of the temperature gradient at any point within the fluid, it also equals the conditional ensemble average $< \nabla T^f_\infty >$ at the origin referred to above on account of the symmetry of the problem.

Similarly, the constraint that the average velocity be zero gives

$$0 = (1 - c_1 - c_2) < \mathbf{u}^f > + c_1 \overline{\mathbf{U}}_1 + c_2 \overline{\mathbf{U}}_2 \tag{C.6}$$

hence, on combining equations $(C.1)$ - $(C.6)$, we arrive at

$$\overline{\mathbf{U}}_1 = \frac{k^*/k}{1 - c_1 - c_2}\{1 - c_1 - \lambda c_2\}\mathbf{U}_1^{(0)} \tag{C.7}$$

and

$$\overline{\mathbf{U}}_2 = \frac{k^*/k}{1 - c_1 - c_2}\{1 - \frac{1}{\lambda}c_1 - c_2\}\mathbf{U}_2^{(0)} \tag{C.8}$$

where $\mathbf{U}_1^{(0)}$ and $\mathbf{U}_2^{(0)}$ are the velocities of the corresponding single bubbles.

The expressions given above for $\overline{\mathbf{U}}_1$ and $\overline{\mathbf{U}}_2$ are, of course, incomplete because they do not take into account the hydrodynamic and thermal interactions between a given test bubble and the other bubbles in the suspension. For monodisperse suspensions ($\lambda = 1$), however, their interactions cancel each other and hence equations $(C.7)$ and $(C.8)$ reduce to the exact result given by Acrivos et al. (1990)

$$\overline{\mathbf{U}} = \frac{k^*}{k}\mathbf{U}^{(0)}. \tag{C.9}$$

In addition, for dilute suspensions,

$$\frac{k^*}{k} = 1 - \frac{3}{2}c_1 - \frac{3}{2}c_2 + O(c^2),$$

in which case equation $(C.7)$ becomes

$$\overline{\mathbf{U}}_1 = \{1 - \frac{3}{2}c_1 - (\lambda + \frac{1}{2})c_2 + ...\}\mathbf{U}_1^{(0)}.$$

The above is identical to equations (1.63) and (1.64) with $I(\lambda) = 0$. But since, as shown earlier, $I(\lambda)$ is much smaller than $(\lambda + \frac{1}{2})$ for $\lambda > \frac{1}{2}$ it seems reasonable to anticipate that the expressions $(C.7)$ and $(C.8)$, which were derived using only the constraints of renormalization, should apply with acceptable accuracy when $\lambda > \frac{1}{2}$ for the case of $\overline{\mathbf{U}}_1$, and when $\lambda < 2$ for the case of $\overline{\mathbf{U}}_2$. This point requires, however, further study.

Appendix D

A generalization and a simple proof of the Helmholtz-Smoluchowski theory

In the electrophoresis problem, charged non-conducting particles move through an electrolyte in a uniform electric field $\mathbf{E}$ at a velocity equal to that of an isolated sphere as obtained from the Helmholtz-Smoluchowski theory,

$$\mathbf{U}_s = \frac{\epsilon\epsilon_0\zeta}{\mu}\mathbf{E}, \tag{D.1}$$

as long as the double layer is thin compared with the radius of curvature of the particle surface and all inertia effects are negligible. Here ϵ is the dielectric constant of the suspending fluid, ϵ_0 is the permittivity of free space, ζ is the electrostatic potential at the surface, and μ is the viscosity of the suspending electrolyte.

The theoretical proof of the above result is available for two identical

spheres in Reed & Morrison (1976), for n identical spheres in Zukoski (1984) and Acrivos et al. (1990), and for a single particle of arbitrary shape in Morrison (1970) and Teubner(1982).

In this appendix, a slight extension of this result is presented and proved which contains the results referred to above as special cases. The extension parallels the relations given by (1.10)-(1.13) in §1.2.

Consider the motion of a group of N particles of arbitrary shapes through an electrolyte in an ambient electric field with potential ϕ_∞ and an ambient flow field $\mathbf{u}_\infty$. Assuming that the double layer is thin compared with the radius of curvature of the particle surface and that all inertia effects are negligible, the governing equation and boundary conditions for the electric field potential ϕ are given by (Acrivos et al. 1990)

$$\nabla^2\phi = 0, \tag{D.2}$$

$$\phi \longrightarrow \phi_\infty \quad \text{as} \quad |\mathbf{x}| \longrightarrow \infty, \tag{D.3}$$

$$\mathbf{n}_i \cdot \nabla\phi = 0 \quad \text{on the surface of particle } i, i = 1, N \tag{D.4}$$

where $\mathbf{n}_i$ denotes the unit vector normal to the surface of particle i. On the other hand, the velocity field $\mathbf{u}$ and pressure field p around the particles satisfy

$$\nabla^2\mathbf{u} = \frac{1}{\mu}\nabla p, \tag{D.5}$$

$$\nabla \cdot \mathbf{u} = 0, \tag{D.6}$$

$$\mathbf{u} \longrightarrow \mathbf{u}_\infty \quad \text{as} \quad |\mathbf{x}| \longrightarrow \infty, \tag{D.7}$$

$$\mathbf{n}_i \cdot \mathbf{u} = \mathbf{n}_i \cdot (\mathbf{U}_i + \boldsymbol{\Omega}_i \times \mathbf{x}_i) \quad \text{on the surface of particle } i, i = 1, N, \tag{D.8}$$

$$(\mathbf{I} - \mathbf{n}_i \mathbf{n}_i) \cdot \mathbf{u} = \alpha (\mathbf{I} - \mathbf{n}_i \mathbf{n}_i) \cdot \nabla \phi \quad \text{on the surface of particle } i, i = 1, N, \tag{D.9}$$

where $\alpha \equiv \epsilon \epsilon_0 \zeta / \mu$. Here $\mathbf{U}_i$ and $\boldsymbol{\Omega}_i$ are, respectively, the translational and angular velocity of particle i. We further require that the particles be force-free and torque-free, i.e.

$$\mathbf{F}_i = \mathbf{0} \quad \text{and} \quad \mathbf{T}_i = \mathbf{0} \quad \text{for } i = 1, N.$$

Now, if the ambient electric potential and velocity fields, ϕ_∞ and $\mathbf{u}_\infty$ respectively, satisfy the relation

$$\mathbf{u}_\infty = \alpha \nabla \phi_\infty, \tag{D.10}$$

then it can be shown that the flow field remains irrotational and is given by

$$\mathbf{u} = \alpha \nabla \phi \quad \text{with} \quad p = 0, \tag{D.11}$$

and all the particles will be stationary, i.e.

$$\mathbf{U}_i = \mathbf{0} \quad \text{and} \quad \boldsymbol{\Omega}_i = \mathbf{0} \quad \text{for } i = 1, N. \tag{D.12}$$

The relations (D.11) and (D.12) can be easily verified by a direct substitution into (D.5) - (D.9) and using (D.2) - (D.4), together with the uniqueness theorem for the above governing equations and boundary conditions.

A physical interpretation of this result can be obtained by an argument similar to that in the corresponding thermocapillary problem in §1.2.

The electrophoretic velocities of N arbitrarily shaped particles in a quiescent ambient electrolyte in a uniform electric field $\mathbf{E}$ can be easily obtained using $(D.10)$ - $(D.12)$. If we take a new reference frame which moves relative to the original reference frame with a constant velocity $\alpha\mathbf{E}$, the ambient flow in the new reference frame is then given by $\mathbf{u}_\infty = -\alpha\mathbf{E}$, which satisfies $(D.10)$. Thus, according to $(D.12)$, all particles remain stationary in the new reference frame. However, if we observe the phenomenon in the original reference frame, all the particles will move with the same constant velocity $\alpha\mathbf{E}$, in agreement with the Helmholtz-Smoluchowski theory.

In conclusion, we were able to obtain a more general relation for the electrophoretic motion of particles of arbitrary shapes, containing the earlier available results for the motion in a uniform electric field as special cases. The proof is very simple in contrast with the others. The slightly more general relation for arbitrary irrotational ambient flow might be useful in certain future studies.

REFERENCES

ACRIVOS, A., BATCHELOR, G.K., HINCH, E.J., KOCH, D.L. & MAURI, R. 1992 Longitudinal shear-induced diffusion of spheres in a dilute suspension. *J. Fluid Mech.* **240**, 651.

ACRIVOS, A & CHANG, E. 1986 The transport properties of non-dilute suspensions. Renormalization via an effective continuum method. In *Physics and Chemistry of Porous Media II* (eds. J. R. Banavar, J. Koplik & K. W. Winkler), pp. 129-142. AIP Conf. Proc. No. 154, (AIP, New York).

ACRIVOS, A., JEFFREY, D.J. & SAVILLE, D.A. 1990 Particle migration in suspensions by thermocapillary or electrophoretic motion. *J. Fluid Mech.* **212**, 95-110.

ACRIVOS, A., MAURI, R. & FAN, X.C. 1993 Shear-induced resuspension in a Couette device. *Int. J. Multiphase Flow* **19**, 797.

ANDERSON, J.L. 1985 Droplet interactions in thermocapillary motion. *Intl J. Multiphase Flow* **11**, 813-824.

BATCHELOR, G.K. 1972 Sedimentation in a dilute suspension of spheres. *J. Fluid Mech.* **52**, 245-268.

BATCHELOR, G.K. 1976 Brownian Diffusion of particles with hydrodynamic interaction *J. Fluid Mech.* **74**, 1.

BATCHELOR, G.K. & GREEN, J.T. 1972a The hydrodynamic interaction of two small freely-moving spheres in a linear flow field. *J. Fluid Mech.* **56**, 375.

BATCHELOR, G.K. & GREEN, J.T. 1972b The determination of the bulk stress in a suspension of spherical particles to order c^2. *J. Fluid Mech.* **56**, 400.

BIEMFOHR, S., LOOBY, T., BIEMFOHR, S. & LEIGHTON, D. 1995 Measurement of the shear-induced coefficient of self-diffusion in dilute suspensions. *J. Fluid Mech.* (submitted).

BOSSIS, G. & BRADY, J.F. 1987 Self-diffusion of Brownian particles in concentrated suspensions under shear. *J. Chem. Phys.* **87**, 5437.

BRADY, J.F. & BOSSIS, G. 1987 Stokesian dynamics. *Ann. Rev. Fluid Mech.* **20**, 111.

CHANG, C. AND POWELL, R.L. 1994 Self-diffusion of bimodal suspensions of hydrodynamically interacting spherical particles in shearing flow. *J. Fluid Mech.* **281**, 51.

CHANG, E. & ACRIVOS, A. 1986 Rate of heat conduction from a heated sphere to a matrix containing passive spheres of a different conductivity. *J. Appl. Phys.* **59**(10), 3375-3382.

CHANG, E. & ACRIVOS, A. 1987 Conduction of heat from a planar wall with uniform surface temperature to a monodispersed suspension of spheres. *J. Appl. Phys.* **62**(3), 771-776.

CICHOCKI, B., FELDERHOF, B.U., HINSEN, K., WAJNRYB, E. & BLAWZDZIEWICZ, J. 1994 Friction and mobility of many spheres in Stokes flow. *J. Chem. Phys.* **100**, 3780.

DA CUNHA, F.R. & HINCH, E.J. 1996 Shear-induced dispersion in a dilute suspension of rough spheres. *J. Fluid Mech.* **309**, 211.

ECKSTEIN, E.C., BAILEY, D.G. & SHAPIRO, A.H. 1977 Self-diffusion of particles in shear flow of a suspension. *J. Fluid Mech.* **79**, 191.

HAPPEL, J. & BRENNER, H. 1991 *Low Reynolds Number Hydrodynamics.* Kluwer Academic Publishers. 62-66.

HASSONJEE, Q., PFEFFER, R. & GANATOS, P. 1992 Behavior of multiple spheres in shear and Poiseuille flow fields at low Reynolds number. *Int. J. Multiphase Flow* **18**, 353.

JEFFREY, D.J. 1973 Conduction through a random suspension of spheres. *Proc. R. Soc. Lond. A* **335**, 355-367.

JEFFREY, D.J. & ONISHI, Y. 1984 Calculation of the resistance and mobility functions for two unequal rigid spheres in Low-Reynolds number flow. *J. Fluid Mech.* **139**, 261-290.

KEH, H.J. & CHEN, S.H. 1990 The axisymmetric thermocapillary motion of two fluid droplets. *Intl J. Multiphase Flow* **16**, 515-527.

KEH, H.J. & CHEN, L.S. 1992 Droplet interactions in axisymmetric thermocapillary motion. *J. Colloid Interface Sci.* **151**, 1-16.

KEH, H.J. & CHEN, L.S. 1993 Droplet interactions in thermocapillary migration. *Chem. Eng. Sci.* **48**, 3565-3582.

KIM, S. 1987 Stokes flow past three spheres: An analytic solution. *Phys. Fluids* **30**, 2309.

KIM, S. & KARRILA, S.J. 1991 *Microhydrodynamics: Principles and Selected Applications.* (Butterworth-Heinemann, 1991). 102.

LEIGHTON, D. & ACRIVOS, A. 1986 Viscous resuspension. *Chem. Engr. Sci.* **177**, 109.

LEIGHTON, D. & ACRIVOS, A. 1987a Measurement of shear-induced self-diffusion in concentrated suspensions of spheres. *J. Fluid Mech.* **177**, 109.

LEIGHTON, D. & ACRIVOS, A. 1987b The shear-induced migration of particles in concentrated suspensions. *J. Fluid Mech.* **181**, 415.

MAZUR, P. & VAN SAARLOOS, W. 1982 Many-sphere hydrodynamic interactions and mobilities in a suspension. *Physica A* **115**, 21.

MEYYAPPAN, M. & SUBRAMANIAN, R.S. 1984 The thermocapilary motion of two bubbles oriented arbirearily relative to a thermal gradient. *J. Colloid Interface Sci.* **97**, 291-294.

MEYYAPPAN, M., WILCOX, W.R. & SUBRAMANIAN, R.S. 1983 The slow axisymmetric motion of two bubbles in a thermal gradient. *J. Colloid Interface Sci.* **94**, 243-257.

MORRISON, F.A. 1970 Electrophoresis of a particle of arbitrary shape. *J. Colloid Interface Sci.* **34**, 210-214.

PHAN, S.E. & LEIGHTON, D. 1996 Measurement of the shear-induced tracer diffusivity in concentrated suspensions. *J. Fluid Mech.* (submitted).

PHILLIPS, R.J., ARMSTRONG, R.C., BROWN, R.A., GRAHAM, A.L. & ABBOTT, J.R. 1992 A constitutive equation for concentrated suspensions that accounts for shear-induced particle migration. *Phys. Fluids A* **4**, 30.

RALLISON, J. M. 1978 Note on the Faxen relations for a particle in Stokes flow. *J. Fluid Mech.* **88**, 529-533.

REED, L.D. & MORRISON, F.A. 1976 Hydrodynamic interaction in electrophoresis. *J. Colloid Interface Sci.* **54**, 117-133.

SATRAPE, J.V. 1992 Interactions and collisions of bubbles in the thermocapillary motion. *Phys. Fluids A* **4**(9), 1883-1900.

SUBRAMANIAN, R.S. 1985 The Stokes force on a droplet in an unbounded fluid medium due to capillary effects. *J. Fluid Mech.* **153**, 389-400.

TEUBNER, M. 1982 The motion of charged colloidal particles in electric fields. *J. Chem. Phys.* **76**, 5564-5573.

THOVERT, J.F. & ACRIVOS, A. 1989 The effective thermal conductivity of a random polydisperse suspension of spheres to order C^2. *Chem. Eng. Comm.* **82**, 177-191.

VAN DYKE, M. 1975 *Perturbation Methods in Fluid Mechanics.* The Parabolic Press, Stanford, California. 94-97.

VAN SAARLOOS, W. & MAZUR, P. 1983 Many-sphere hydrodynamic interactions II. Mobilities at infinite frequencies. *Physica A* **120**, 77.

WANG, Y., MAURI, R. & ACRIVOS, A 1996 Transverse shear-induced diffusion of spheres in a dilute suspension. *J. Fluid Mech.* **327**, 255.

YOON, B.J. & KIM, S. 1987 Note on the direct calculation of mobility functions for two equal-sized spheres in Stokes flow. *J. Fluid Mech.* **185**, 437.

YOUNG, N.O., GOLDSTEIN, J.S. & BLOCK, M.J. 1959 The motion of bubbles in a vertical temperature gradient. *J. Fluid Mech.* **6**, 350-356.

ZUKOSKI, C.F. 1984 Studies of electrokinetic phenomena in suspensions. Ph.D. thesis, Princeton University.